

DOKUZ EYLÜL UNIVERSITY
GRADUATE SCHOOL OF NATURAL AND APPLIED SCIENCES

**DEVELOPMENT OF OPTICAL CHEMICAL
NANOSENSORS FOR THE ANALYSIS OF
REACTIVE GASES SUCH AS NITRIC
OXIDE AND AMMONIA**

by
Cansu DOĞAN

November, 2019

İZMİR

**DEVELOPMENT OF OPTICAL CHEMICAL
NANOSENSORS FOR THE ANALYSIS OF
REACTIVE GASES SUCH AS NITRIC
OXIDE AND AMMONIA**

**A Thesis Submitted to the
Graduate School of Natural and Applied Sciences of Dokuz Eylül University
In Partial Fulfillment of the Requirements for the Degree of Master of Science
in Nanoscience and Nanoengineering Department**

**by
Cansu DOĞAN**

**November , 2019
İZMİR**

M.Sc THESIS EXAMINATION RESULT FORM

We have read the thesis entitled **DEVELOPMENT OF OPTICAL CHEMICAL NANOSENSORS FOR THE ANALYSIS OF REACTIVE GASES SUCH AS NITRIC OXIDE AND AMMONIA** completed by **CANSU DOĞAN** under supervision of **PROF. DR. ÖZLEM ÖTER** and we certify that in our opinion it is fully adequate, in scope and in quality, as a thesis for the degree of Master of Science.



Prof.Dr.Özlem ÖTER

Supervisor



(Jury Member)



Doc. Dr. Vedra Nüket TIRTOM

(Jury Member)



Prof.Dr. Kadriye ERTEKİN

Director

Graduate School of Natural and Applied Sciences

ACKNOWLEDGMENTS

I would like to express my sincere gratitude to my supervisor Prof.Dr. Özlem ÖTER for providing this fascinating subject and encouraging me to further my study and guidance during this thesis and for the great working conditions at our laboratory.

I also sincerely thank Prof.Dr. Kadriye ERTEKİN for valuable and continuous support and professors at EMUM and Faculty of Science for their assistance, understanding and encouragement.

Finally, I would like to thank to my mother SEHER DOĞAN and my family, my working effort during enhancement of this thesis and for their sustained support and understanding during all the times of my studies.

Cansu DOĞAN

DEVELOPMENT OF OPTICAL CHEMICAL NANOSENSORS FOR THE ANALYSIS OF REACTIVE GASES SUCH AS NITRIC OXIDE AND AMMONIA

ABSTRACT

Nitric oxide is one of the most important biochemical parameters taking place in numerous physical and pathological processes in biological systems. Nitrogen oxides are also one of the major pollutants in the atmosphere which cause acid rains, photochemical smog and ozone accumulation. Therefore real-time sensor development studies for nitric oxide attract great attention. This study is largely concerned with the development of optical chemical sensor for nitric oxide radical that can be applied for quantification studies in aqueous environments.

For this purpose nitric oxide sensitive molecules mesotetrakis (4-phenylethynyl) phenylporphyrin (PHACH₂), mesotetraphenylporphyrinato Zn(II) (ZnTPP), mesotetraphenylporphyrinato Pt(II) (TPPPt(II)) were studied in solvent and/or aqueous media and also embedded in polymeric matrices along with appropriate additives either in thin film or electrospun nanofiber forms. Matrix material of PVC (polyvinyl chloride) were chosen due to excellent compatibility with the indicator dyes, resistant characteristics to water and harsh conditions providing an appropriate micro environment for them.

The performances of the potential sensing agents were tested by steady state fluorescence and decay time measurements. Among them the PHACH₂ dye exhibited the highest response for radicalic nitric oxide.

Keywords: Nitric oxide, optical sensors, nanofiber, thin film, porphyrin

NİTRİK OKSİT VE AMONYAK GİBİ REAKTİF GAZLARIN ANALİZİNE YÖNELİK KİMYASAL OPTİK NANOSENSÖR GELİŞTİRİLMESİ

ÖZ

Nitrik oksit biyolojik sistemlerde sayısız fiziksel ve patolojik süreçte yer alan en önemli biyokimyasal parametrelerden biridir. Nitrik oksitler ayrıca atmosferde asit yağmurlarına, fotokimyasal sis ve ozon birikimine neden olan kirleticilerden biridir. Bu nedenle nitrik oksit için gerçek zamanlı sensör geliştirme çalışmaları büyük dikkat çekiyor. Bu çalışma büyük ölçüde sulu ortamlarda miktar tayin çalışmaları için uygulanabilecek nitrik oksit radikali için optik kimyasal sensörün geliştirilmesi ile ilgilidir.

Nitrik okside duyarlı moleküller mesotetrakis (4-phenylethynyl) phenylporphyrin (PHACH₂), mesotetraphenylporphyrinato Zn(II) (ZnTPP), mesotetraphenylporphyrinato Pt(II) (TPPPt(II)) çözücü ve /veya sulu ortamda incelenmiş ve ayrıca ince film ve elektroğirilmiş nano-fiber formlarında uygun katkı maddeleri ile birlikte polimetrik matrislere gömülmüştür. PVC'nin matris malzemesi (polivinil klorür) gösterge boyaları ile mükemmel uyumluluk, suya dayanıklılık özellikleri ve bunlar için uygun bir mikro ortam sağlayan sert koşullar nedeniyle seçildi.

Potansiyel algılayıcı maddelerin performansları durgun hal floresans ve zaman çözömlenmeli floresans ölçümleri ile test edilmiştir. Bunların arasında PHACH₂ boyası, radikalik nitrik oksit için en yüksek sensör cevabını gösterdi.

Anahtar Kelimeler: Nitrik oksit, optik sensörler, nanolif (nanofiber), ince film, porfirin

CONTENTS

	Page
M.Sc THESIS EXAMINATION RESULT FORM.....	ii
ACKNOWLEDGMENTS	iii
ABSTRACT.....	iv
ÖZ	v
LIST OF FIGURES	ix
LIST OF TABLES	xv
CHAPTER ONE - INTRODUCTION	1
1.1 Definition of a Chemical Sensor	1
1.1.1 Electrochemical Sensors	1
1.1.2 Optical Chemical Sensors	2
1.1.2.1 Advantages and Disadvantages of Optical Chemical Sensors	2
1.2 Luminescence	4
1.2.1 Mechanism of Luminescence	4
1.2.1.1 Fluorescence and Phosphorescence	4
1.2.1.2 Fluorescence.....	4
1.2.1.3 Phosphorescence	5
1.3 Stoke's Shift	6
1.4 Fluorescence Lifetime	7
1.5 Time Correlated Single Photon Counting (TCSPC) Method.....	8

CHAPTER TWO - EXPERIMENTAL METHOD AND INSTRUMENTATION
..... 10

2.1 Reagents 10

2.2 Preparation of 0.005M NaH₂PO₄/Na₂HPO₄ Buffer 10

2.3 Preparation of Sodium Dodecyl Sulphate (SDS) Micelles 10

2.4 Preparation of TEMPO Solution 11

2.5 Thin Film Fabrication..... 11

2.6 Fabrication of Electrospun Fibers13

2.6.1 Electrospinning Apparatus.....13

2.7 Instruments..... 14

2.7.1 Spectrophotometer and Spectrofluorometer Apparatus..... 14

CHAPTER THREE - PHACH₂(mesotetrakis(4-phenylethynyl)phenylporphyrin) BASED STUDIES 16

3.1 Introduction 16

3.2 Spectral Characteristics of the PHACH₂ Dye 16

3.3 Spectral Response of the PHACH₂ Dye to TEMPO Radical..... 16

3.4 Lifetime Based Measurements in THF media.....20

3.5 Spectral Characteristics of the PHACH₂ Dye in PVC Matrix.....29

3.6 Fluorescence Intensity Based Kinetic Response to Gaseous NH₃.....35

3.7 Lifetime Based Measurements of Embedded Forms.....36

CHAPTER FOUR - ZnTPP (mesotetraphenylporphyrinato Zn(II)) BASED STUDIES.....55

4.1 Introduction 55

4.2 Spectral Characteristics of the ZnTPP Dye 55

4.3 Spectral Response of the ZnTPP Dye to TEMPO Radical	57
4.4 Lifetime Based Measurements in THF Media	59
4.5 Spectral Characteristics of the ZnTPP Dye in PVC Matrix.....	66
CHAPTER FIVE - TPPPt(II) (mesotetraphenylporphyrinato Pt(II))BASED STUDIES	69
5.1 Introduction	69
5.2 Spectral Characteristics of the TPPPt(II) Dye.....	69
5.3 Spectral Response of the TPPPt(II) Dye to TEMPO Radical	71
5.4 Lifetime Based Measurements in THF media.....	73
5.5 Spectral Characteristics of the TPPPt(II) Dye in PVC Matrix.....	81
5.6 Lifetime Based Measurements of Embedded Forms.....	86
CHAPTER SIX - CONCLUSIONS.....	105
REFERENCES.....	107

LIST OF FIGURES

	Page
Figure 1.1 Spin in the ground and excited state.....	4
Figure 1.2 Jablonski diagram with the reciprocal rates of transition in [s].....	6
Figure 1.3 The main components for signal processing in TCSPC	9
Figure 2.1 Structure of the Sodium Dodecyl Sulphate	10
Figure 2.2 Structure of the TEMPO.....	11
Figure 2.3 The placement of the sensor film in the sample cuvette.....	12
Figure 2.4 The Chemical structures of PVC	12
Figure 2.5 The chemical structures of DOP.....	12
Figure 2.6 Schematic of the Electrospinning Apparatus.....	13
Figure 2.7 Time resolved fluorescence spectrometer of Edinburg Instruments of FLS920	15
Figure 3.1 Structure of the PHACH ₂ dye	16
Figure 3.2 Excitation and emission spectral characteristics for PHACH ₂ dye in THF media.....	17
Figure 3.3 Absorption spectrum for PHACH ₂ dye in THF media.....	17
Figure 3.4 Fluorescence response of PHACH ₂ to different concentrations of TEMPO in THF media.....	19
Figure 3.5 The calibration plot was drawn as I ₀ /I versus TEMPO concentrations for PHACH ₂ dye in THF solution.....	20
Figure 3.6 Decay response of PHACH ₂ in absence of TEMPO solution in THF media.....	21
Figure 3.7 Decay response of PHACH ₂ in presence of 6 μl (7.68×10 ⁻⁸ Mol L ⁻¹) TEMPO in THF media.....	22
Figure 3.8 Decay response of PHACH ₂ in presence of 12 μl (1.53×10 ⁻⁷ Mol L ⁻¹) TEMPO in THF media.....	23
Figure 3.9 Decay response of PHACH ₂ in presence of 20 μl (2.54×10 ⁻⁷ Mol L ⁻¹) TEMPO in THF media.....	24

Figure 3.10 Decay response of PHACH ₂ in presence of 90 μl (1.11×10 ⁻⁶ Mol L ⁻¹) TEMPO in THF media.....	25
Figure 3.11 Decay response of PHACH ₂ in presence of 1290 μl (1.12×10 ⁻⁵ Mol L ⁻¹) TEMPO in THF media.....	26
Figure 3.12 Variations of the lifetime ratio (τ ₀ /τ) of PHACH ₂ versus quencher TEMPO concentrations in THF media.....	27
Figure 3.13 Fluorescence intensity based response of PHACH ₂ in nanofiber form to TEMPO concentrations in pH 7.4 buffered SDS media.....	31
Figure 3.14 The calibration plot for PHACH ₂ nanofiber form in pH 7.4 buffered SDS media	33
Figure 3.15 Fluorescence response of PHACH ₂ embedded in NH ₃ media.....	35
Figure 3.16 Decay response of PHACH ₂ embedded PVC based thin film with in pH 7.4 buffer SDS media without TEMPO solution.....	37
Figure 3.17 Decay response of PHACH ₂ embedded PVC based thin film in the presence of 7 μl (8.96×10 ⁻⁸ Mol L ⁻¹) TEMPO in pH 7.4 buffer in SDS media.....	38
Figure 3.18 Decay response of PHACH ₂ embedded PVC based thin film in the presence of 25 μl (3.17×10 ⁻⁷ Mol L ⁻¹) TEMPO in pH 7.4 buffer in SDS media.....	39
Figure 3.19 Variations of the lifetime ratio (τ ₀ /τ) PHACH ₂ versus quencher (TEMPO) concentrations thin film form to pH 7.4 buffer in SDS media.....	41
Figure 3.20 Decay response of PHACH ₂ embedded PVC based nanofiber with in pH 7.4 buffer SDS media without TEMPO solution.....	43
Figure 3.21 Decay response of PHACH ₂ embedded PVC based nanofiber in the presence of 0.6 μl (7.68×10 ⁻⁹ Mol L ⁻¹) TEMPO in pH 7.4 buffer in SDS media.....	44
Figure 3.22 Decay response of PHACH ₂ embedded PVC based nanofiber in the presence of 1 μl (1.28×10 ⁻⁸ Mol L ⁻¹) TEMPO in pH 7.4 buffer in SDS media.....	45

Figure 3.23 Decay response of PHACH ₂ embedded PVC based nanofiber in the presence of 2.8 μl (3.58×10 ⁻⁸ Mol L ⁻¹) TEMPO in pH 7.4 buffer in SDS media.....	46
Figure 3.24 Variations of the lifetime ratio (τ ₀ /τ) PHACH ₂ versus quencher (TEMPO) concentrations nano-fiber form to pH 7.4 buffer in SDS media.....	48
Figure 3.25 Decay response of PHACH ₂ embedded PVC based nanofiber in the presence of without in NH ₃ media.....	50
Figure 3.26 Decay response of PHACH ₂ embedded PVC based nano fiber in presence of concentrated NH ₃ medium exposed for 30 minutes.....	51
Figure 3.27 Decay response of PHACH ₂ embedded PVC based nano fiber in presence of concentrated NH ₃ medium exposed for 60 minutes.....	52
Figure 3.28 Decay response of PHACH ₂ embedded PVC based nano fiber in presence of concentrated NH ₃ medium exposed for 120 minutes.....	53
Figure 4.1 Structure of the ZnTPP dye.....	55
Figure 4.2 Excitation and emission spectral characteristics for ZnTPP dye in THF media.....	56
Figure 4.3 Absorption spectrum for the ZnTPP dye.....	56
Figure 4.4 Fluorescence response of ZnTPP to different concentrations of TEMPO in THF media.....	58
Figure 4.5 The calibration plot was drawn as I ₀ /I versus TEMPO concentrations for ZnTPP dye in THF solution.....	59
Figure 4.6 Decay response of ZnTPP in absence of TEMPO solution in THF media.....	60
Figure 4.7 Decay response of ZnTPP in the presence of 2 μl (2.56×10 ⁻⁸ Mol L ⁻¹) TEMPO in THF media.....	61
Figure 4.8 Decay response of ZnTPP in the presence of 6 μl (7.68×10 ⁻⁸ Mol L ⁻¹) TEMPO in THF media.....	62
Figure 4.9 Decay response of ZnTPP in the presence of 12 μl (1.53×10 ⁻⁷ Mol L ⁻¹) TEMPO in THF media.....	63
Figure 4.10 Variations of the lifetime ratio (τ ₀ /τ) of ZnTPP versus quencher (TEMPO) concentrations in THF media.....	64
Figure 5.1 Structure of the TPPPt(II) dye.....	69

Figure 5.2 Excitation and emission spectral characteristics for TPPPt(II) dye in THF media.....	70
Figure 5.3 Absorption spectrum for TPPPt(II) dye in THF media.....	70
Figure 5.4 Fluorescence response of TPPPt(II) to different concentrations of TEMPO in THF media.....	72
Figure 5.5 Decay response of TPPPt(II) in absence of TEMPO solution in THF media.....	74
Figure 5.6 Decay response of TPPPt(II) in presence of 10 μ l (1.27×10^{-7} Mol L ⁻¹) TEMPO in THF media.....	75
Figure 5.7 Decay response of TPPPt(II) in presence of 20 μ l (2.54×10^{-7} Mol L ⁻¹) TEMPO in THF media.....	76
Figure 5.8 Decay response of TPPPt(II) in presence of 1000 μ l (2.56×10^{-5} Mol L ⁻¹) TEMPO in THF media.....	77
Figure 5.9 Variations of the lifetime ratio (τ_0/τ) of TPPPt(II) versus quencher (TEMPO) concentrations in THF media.....	79
Figure 5.10 Fluorescence intensity based response of TPPPt(II) in nanofiber form to TEMPO concentrations in pH 7.4 buffered SDS media.....	83
Figure 5.11 The calibration plot for TPPPt(II) nanofiber form in pH 7.4 buffered SDS media.....	84
Figure 5.12 Decay response of TPPPt(II) embedded PVC based thin film with in pH 7.4 buffer SDS media without TEMPO solution.....	87
Figure 5.13 Decay response of TPPPt(II) embedded PVC based thin film in the presence of 3 μ l (3.84×10^{-8} Mol L ⁻¹) TEMPO in pH 7.4 buffer in SDS media.....	88
Figure 5.14 Decay response of TPPPt(II) embedded PVC based thin film in the presence of 7 μ l (8.96×10^{-8} Mol L ⁻¹) TEMPO in pH 7.4 buffer in SDS media.....	89
Figure 5.15 Decay response of TPPPt(II) embedded PVC based thin film in the presence of 13 μ l (1.66×10^{-7} Mol L ⁻¹) TEMPO in pH 7.4 buffer in SDS media.....	90

Figure 5.16 Decay response of TPPPt(II) embedded PVC based thin film in the presence of 25 μl ($3.17 \times 10^{-7} \text{ Mol L}^{-1}$) TEMPO in pH 7.4 buffer in SDS media.....	91
Figure 5.17 Decay response of TPPPt(II) embedded PVC based thin film in the presence of 50 μl ($6.28 \times 10^{-7} \text{ Mol L}^{-1}$) TEMPO in pH 7.4 buffer in SDS media.....	92
Figure 5.18 Variations of the lifetime ratio (τ_0/τ) TPPPt(II) versus quencher (TEMPO) concentrations thin film form to pH 7.4 buffer in SDS media.....	94
Figure 5.19 Decay response of TPPPt(II) embedded PVC based nanofiber with in pH 7.4 buffer SDS media without TEMPO solution.....	96
Figure 5.20 Decay response of TPPPt(II) embedded PVC based nanofiber in the presence of 0.4 μl ($5.12 \times 10^{-9} \text{ Mol L}^{-1}$) TEMPO in pH 7.4 buffer in SDS media.....	97
Figure 5.21 Decay response of TPPPt(II) embedded PVC based nanofiber in the presence of 0.8 μl ($1.02 \times 10^{-8} \text{ Mol L}^{-1}$) TEMPO in pH 7.4 buffer in SDS media.....	98
Figure 5.22 Decay response of TPPPt(II) embedded PVC based nanofiber in the presence of 1.2 μl ($1.54 \times 10^{-8} \text{ Mol L}^{-1}$) TEMPO in pH 7.4 buffer in SDS media.....	99
Figure 5.23 Decay response of TPPPt(II) embedded PVC based nanofiber in the presence of 2 μl ($2.56 \times 10^{-8} \text{ Mol L}^{-1}$) TEMPO in pH 7.4 buffer in SDS media.....	100
Figure 5.24 Decay response of TPPPt(II) embedded PVC based nanofiber in the presence of 4 μl ($5.12 \times 10^{-8} \text{ Mol L}^{-1}$) TEMPO in pH 7.4 buffer in SDS media.....	101
Figure 5.25 Decay response of TPPPt(II) embedded PVC based nanofiber in the presence of 10 μl ($1.27 \times 10^{-7} \text{ Mol L}^{-1}$) TEMPO in pH 7.4 buffer in SDS media.....	102

Figure 5.26 Decay response of TPPPt(II) embedded PVC based nanofiber in the presence of 30 μl ($3.79 \times 10^{-7} \text{ Mol L}^{-1}$) TEMPO in pH 7.4 buffer in SDS media.....103



LIST OF TABLES

	Page
Table 3.1 Excitation and emission spectral characteristics of the PHACH ₂ dye.....	18
Table 3.2 The fluorescence emission based data of PHACH ₂ dye to different TEMPO concentrations.....	19
Table 3.3 The variation of the lifetime values for different TEMPO concentrations in THF.....	27
Table 3.4 Summary of the decay characteristics and chi square values of the studied composites in presence and absence of TEMPO in THF media.....	28
Table 3.5 Cocktail compositions for thin film and nano-fiber sensing probes.....	29
Table 3.6 Excitation and emission spectral characteristics of the PHACH ₂ dye.....	30
Table 3.7 The fluorescence intensities for nanofiber forms in pH 7.4 buffered SDS media at different TEMPO concentrations.....	32
Table 3.8 Excitation and emission based spectral characteristics of the PHACH ₂ dye in nano-fiber form.....	34
Table 3.9 The Stern - Volmer equations, regression coefficients and Stern - Volmer constants of all of the studied composites.....	34
Table 3.10 (τ_0/τ) values corresponding to TEMPO concentrations thin film form to pH 7.4 buffer SDS media TEMPO solution for PHACH ₂ dye.....	47
Table 3.11 Summary of the decay characteristics and chi square values of the studied composites in presence and absence of TEMPO for thin film form.....	42
Table 3.12 (τ_0/τ) values corresponding to TEMPO concentrations nanofiber form to pH 7.4 buffer SDS media TEMPO solution for PHACH ₂ dye.....	47
Table 3.13 Summary of the decay characteristics and chi square values of the studied composites in presence and absence of TEMPO for nanofiber form.....	49
Table 3.14 Summary of the decay characteristics and chi square values of the studied composites in presence and absence of nanofiber exposed to ammonia.....	54
Table 4.1 Excitation and emission spectral characteristics of the ZnTPP dye.....	57
Table 4.2 The fluorescence emission based data of ZnTPP dye to different TEMPO concentrations.....	58

Table 4.3 The variation of the lifetime values for different TEMPO concentrations in THF	64
Table 4.4 Summary of the decay characteristics and chi square values of the studied composites in presence and absence of TEMPO in THF media.....	65
Table 4.5 Cocktail compositions for thin film sensing probes.....	66
Table 4.6 Excitation and emission spectral characteristics of the ZnTPP dye.....	67
Table 4.7 The Stern-Volmer equations, regression coefficients and Stern - Volmer constants of all of the studied composites.....	68
Table 5.1 Excitation and emission spectral characteristics of the TPPPt(II) dye.....	71
Table 5.2 The variation of the lifetime values for different TEMPO concentrations in THF.....	78
Table 5.3 Summary of the decay characteristics and chi square values of the studied composites in presence and absence of TEMPO in THF media.....	80
Table 5.4 Cocktail compositions for thin film and nano-fiber sensing probes.....	81
Table 5.5 Excitation and emission spectral characteristics of the TPPPt(II) dye.....	82
Table 5.6 The fluorescence intensities for nanofiber forms in pH 7.4 buffered SDS media at different TEMPO concentrations.....	84
Table 5.7 The Stern-Volmer plots, regression coefficients and Stern-Volmer constants of all of the studied composites.....	85
Table 5.8 (τ_0/τ) values corresponding to TEMPO concentrations thin film form to pH 7.4 buffer SDS media TEMPO solution for TPPPt(II) dye.....	93

CHAPTER ONE

INTRODUCTION

1.1 Definition of a Chemical Sensor

Different sensor definitions can be found in the related literature and the discussions about the features and the requirements of the sensors is still going on. The definition given by an IUPAC commission on sensors is as follows. Chemical sensors have been intensively used in different types of applications as process and product quality controls, critical care units, safety, industrial hygiene, human comfort controls, emission monitoring, automotive, clinical diagnostics and, more recently, homeland security (Wolfbeis, 1991).

Mainly a chemical sensor has a chemical or molecular target to be measured. Sensors can be classified in many different ways. They may be classified considering the principle of operation of the transducer as “physical” and “chemical” sensors. They also can be divided into sub groups as optical, electrochemical, electrical, mass sensitive, magnetic and thermometric devices. They can also be classified as direct and indirect sensors or as reversible or non-reversible ones and respect of their applications or sizes (Wolfbeis, 1991). However in case of chemical or molecular targets, electrochemical or optical chemical sensors become prominent.

1.1.1 Electrochemical Sensors

The electrochemical sensors may be amperometric or potentiometric. The earliest example of an amperometric gas sensor is the Clark oxygen sensor used for the measurement of dissolved oxygen in the blood. The amperometric sensor produces current signal, which is related to the concentration of the analyte by Faraday’s law and the laws of mass transport (Cao, Shakin,&Sun, 1992). On the other hand a potentiometric sensor measures the electrical potential of an electrode when no voltage is present. The analytical signal arises from the potential difference between the

working and the reference electrodes. The working electrode's potential must depend on the concentration of the analyte. In case of electrochemical sensors, the reference electrode is needed to provide a defined reference potential. Ion-selective electrodes (ISEs) belong to potentiometric chemical sensor group and are most often based on the measurement of the interfacial potential at an electrode surface caused by a selective ion exchange reaction. The glass pH electrode is a well-known typical ion selective electrode (Galster, 1991). In addition to the glass electrode, Ca^{2+} , Mg^{2+} , Na^+ , K^+ , NH_4^+ , F^- , Cl^- and NO_3^- selective electrodes are currently available.

1.1.2 Optical Chemical Sensors

An optical chemical sensor consists of a chemical recognition moiety coupled with a transducer. The recognition moiety or receptor part of the optical chemical sensor selectively recognizes the analyte. On the other hand the transducer converts the optical analytical signal produced by the receptor into a measurable signal.

Optical chemical sensors can also be mentioned as probes, fiber-optic chemical sensors and/or nanofiber optic chemical sensors. Probes' are the sensors, sometimes produce irreversible responses to existence of analytes. Whereas the signal is not irreversible and discontinuous, it is named as sensor (Wolfbeis, 1991).

1.1.2.1 Advantages and Disadvantages of Optical Chemical Sensors

Upon the other kinds of sensing approaches, chemical optical sensors have plenty of advantages.

- Optical sensors do not require a reference signal as electrochemical sensor.
- The ease of miniaturization allows the development of very small, thin and flexible sensors, especially suitable for sensing in clinical chemistry, biotechnology, cell studies and medicine.

- Today's sensor technology utilizes the fiber optics as an integral part of the sensors. Optical fibers provide optical signal transmission over distances without any loss. Therefore remote sensing becomes possible to perform analyses.
- The optical chemical sensors are not subject of the electrical interferences, strong magnetic fields and surface potentials
- Analyses can be performed in real time.
- Fiber optic chemical sensing is a non-destructive analytical method.
- The materials used for manufacturing fibers are stainless, thus they have outstanding steadiness. They also show resistance to radiation.
- The sensors depending on dynamic fluorescence quenching have a beneficial dynamic range bigger than that electrochemical sensors have .
- Most of the fiber sensors can be used upon a broader temperature range than electrodes (Wolfbeis, 1991).

Besides these advantages optical sensors also have some disadvantages:

- Ambient light is a problem while studying with optical chemical sensors and can interfere with the analytical signal. Therefore optical isolation becomes necessary.
- Sometimes they exhibit limited long term stability due to the photo bleaching and washout of the sensing molecule. The signal drifts arising from these reasons can be overcome utilizing ratio metric method or time resolved measurement approach. (Wolfbeis, 1991).

In summary, optical sensors offer a variety of new aspects in sensing of many types of chemicals. In spite of several limitations, they look like very promising with respect to other sensing methods (Wolfbeis, 1991).

1.2 Luminescence

1.2.1 Mechanism of Luminescence

Luminescence is the light emission by the electronically excited molecules or atoms. Electronic excitation requires energy. Luminescence occurs when an electron returns to the electronic ground state from an excited state and loses its excess energy as a photon. The most intensively studied forms of the luminescence are fluorescence and phosphorescence.

1.2.1.1 Fluorescence and Phosphorescence

Singlet and triplet are two different states that the electronic states of the molecules that have conjugated systems may reveal. In singlet excited and triplet excited states, fluorescence and phosphorescence take place, respectively.

Singlet state: All electrons in the molecule are in opposite spin (spin-paired).

Triplet state: One set of electron spins is unpaired (See Figure 1.1).

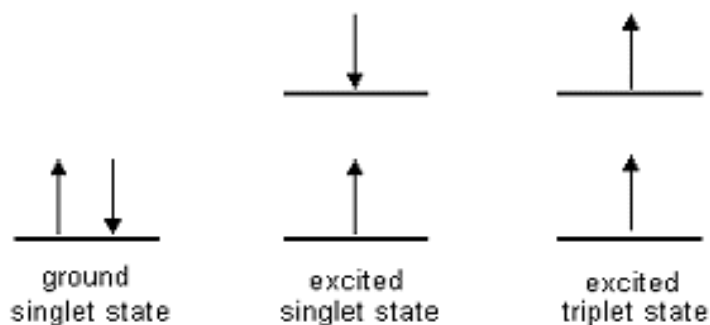


Figure 1.1 Spin in the ground and excited states (Sheffield Hallam University, n.d.)

1.2.1.2 Fluorescence

Absorption of UV or visible wavelengths by a molecule generally results with excitation from the vibrational levels of the ground state to one of the vibrational levels of the first excited singlet state. When the excitation performed with more energetic

wavelengths the excited electron occupies the second or third levels of the singlet-excited states (Frohne, 2004).

The excited electron cannot stay at the excited levels so long and quickly falls to the lowest vibrational level by losing its energy through collisions or emitting light. The molecule may also transfer the excess energy by means of vibrational or rotational movements. When the molecule returns to the ground state, from the singlet excited, by emitting of photon, this is called 'Fluorescence'. The lifetime of the excited singlet state (fluorescence) can be defined in nanoseconds. A light absorbed molecule may also lose its energy by other ways except that of radiation. All of these processes are called 'radiationless energy transfer' (Frohne, 2004).

1.2.1.3 Phosphorescence

When the molecule is in an excited *triplet* state, the spin of the excited electron can be reversed; this is called *intersystem crossing*. A molecule in the excited triplet state does not always use this way to return to the ground state. It can also lose its energy by emitting a photon. A triplet/singlet transition is much less possible than that of a singlet/singlet transition. The lifetime of the excited triplet state (phosphorescence) may extent to seconds or 100 seconds. Emission from triplet/singlet transitions can continue even after irradiation stopped. Phosphorescence is usually measured at low temperatures or alternatively in highly viscous media (Frohne, 2004).

The electronic transitions during absorption and emission of light are illustrated by Jablonski level diagram, shown in Figure 1.2.

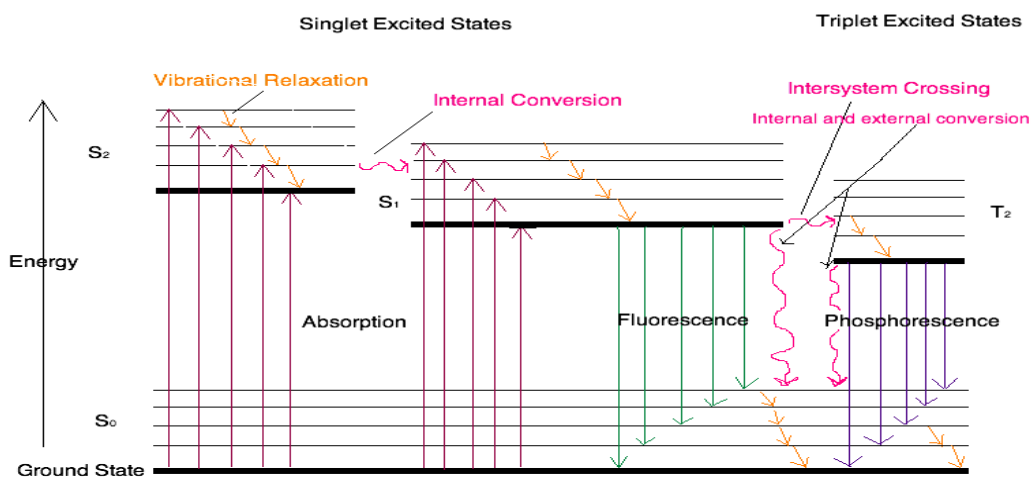


Figure 1.2 Jablonski diagram for absorption, fluorescence and phosphorescence (Chemistry Libretexts, 2017)

1.3 Stoke's Shift

The difference between the band maxima of the absorption and emission spectra of the same electronic transition concerning wavenumber or wavelength can be defined as stokes shift. This was named after Irish physicist Sir George G. Stokes (Lakowicz, 1983).

A molecule or an atom gains energy and becomes excited when it absorbs a photon. One method for the molecule or the atom is to release a photon to relax, losing its energy. Another way is to lose the energy in form of heat. This energy difference between the emitted photon and the absorbed photon is called as the Stokes Shift (Lakowicz, 1983).

1.4 Fluorescence Lifetime

Excited states fluorescence lifetime is an average time for a molecule to remain in the excited state before emitting a photon. Presenting a distinct fluorescence lifetime for a molecule is not easy. After excitation, each molecule emits randomly. Many excited molecules will fluoresce earlier than the average lifetime, whereas some fluoresce long after the average lifetime. Fluorescence lifetimes for most of the molecules generally take approximately 1-10 nanoseconds. However, they also can range from microseconds to the sub nanoseconds (Ongun, 2013).

Measurement of the fluorescence lifetime is different from measurement of steady-state fluorescence and requires specific equipment, light sources and detectors (Ongun, 2013).

Information taken by normal fluorescence spectroscopy is different than that of the information can be obtained by using time-resolved fluorescence method. Time-resolved fluorescence measurements provide information about the microenvironment of the molecule (Ongun, 2013).

Time-dependent decays of fluorescence can be measured both, time or frequency domains. In the time domain measurements, the sample emission following pulsed excitation has been recorded by using detectors with high temporal resolution (e.g. streak cameras) or time-sampling circuits (e.g. time correlated single photon counting approach; TCSPC). In the frequency domain measurements, the delay between emission phase angles has been measured.

In a single exponential decay process, the time course can be described by a single exponential decay equation 1.3;

$$Fl_{(t)} = Fl_0 e^{-t/\tau} \quad (1.3)$$

Where; Fl_0 is the fluorescence intensity at the time excitation is terminated and τ is the excited-state fluorescence lifetime. In many cases, the intensity decay cannot be accurately defined by a single exponential decay equation (Bright, & Munson, 2003).

In such cases, the observed intensity decay(See Equation 1.4) is given by a sum of exponential terms:

$$Fl_{(t)} = \sum_{i=1}^n \alpha_i e^{-\frac{t}{\tau_i}} \quad (1.4)$$

Where α_i is the pre-exponential factor indicating the contribution of the each component the total time-resolved decay.

1.5 Time Correlated Single Photon Counting (TCSPC) Method

Time Correlated Single Photon Counting is a digital photon counting technique, which is time correlated in relation to a pulsed excitation light. The main components for signal processing in TCSPC are;

1. Constant fraction discriminators (CFD) are used to extract precise timing information from the detector pulse output.
2. Electrical Delays (DEL),
3. Time-to-Amplitude Converter (TAC),
4. Amplifier (between the TAC and ADC),
5. Analogue to Digital Converter (ADC),
6. Digital Memory (Mem) (See in Fig 1.3).

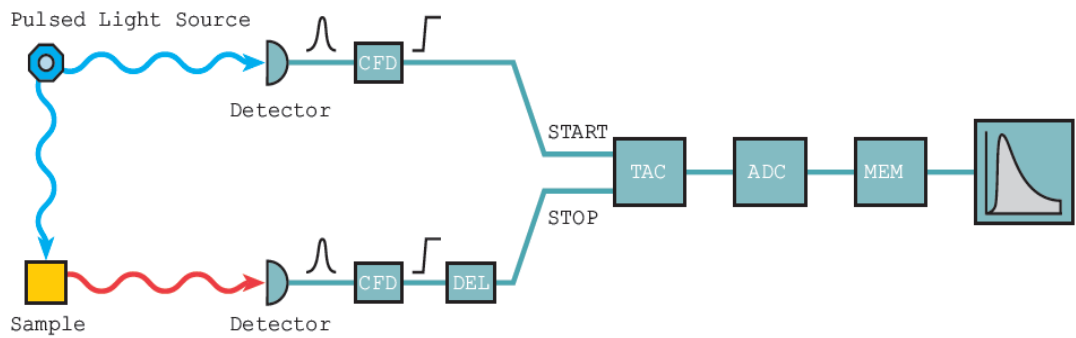


Figure 1.3 The main components for signal processing in TCSPC (FLS920 Series, 2011)

In TCSPC technique, the sample is excited many times using a pulsed light source. The acquired data forms a probability histogram correlating the time between an excitation pulse (START) and the observation of the first photon coming from fluorescence (STOP). In TCSPC technique, the time at which a photon is incident on the detector should be defined at least with a pico-second resolution to obtain a highprecision (FLS920 Series, 2011).

CHAPTER TWO

EXPERIMENTAL METHOD AND INSTRUMENTATION

2.1 Reagents

Nitric oxide sensitive fluorescent dyes, which are PhacH₂, ZnTPP, TPPPt(II) were synthesized by a working group in the laboratories of technical university of Gebze. The polymer of polyvinylchloride (PVC, high molecular weight) and the plasticizer dioctylphthalate (DOP) were obtained from Aldrich. All solvents used in this thesis were of analytical grade and purchased from Merck and Sigma. 2,2,6,6-tetramethylpiperidine-N-oxyl free radical (TEMPO, 98%) from Aldrich, the anionic surfactant sodium dodecyl sulphate (SDS) from Merck.

2.2 Preparation of 0.005M NaH₂PO₄/Na₂HPO₄ Buffer

0.156 g of NaH₂PO₄·2H₂O (MA=156.01) and 0.358 g of Na₂HPO₄·12H₂O (MA=358.14) were dissolved in 190 mL ultra-pure water. The solution was titrated to pH 7.4 at the lab temperature of 20 °C either with 0.1 M HNO₃ or 0.1 M NaOH as needed. The resulting solution was made up to 200 ml with ultra-pure water in a volumetric flask.

2.3 Preparation of Sodium Dodecyl Sulphate (SDS) Micelles

A solution of 5 mL 0.01 M SDS (see Figure 2.1) was prepared in 0.4 M NaCl containing 0.001 M pH 7.4 phosphate buffer. Then, it was sonicated for 15 minutes.

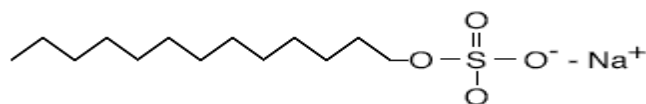


Figure 2.1 Structure of the Sodium Dodecyl Sulphate (Wikimedia, n.d.)

2.4 Preparation of TEMPO Solution

2,2,6,6-tetramethylpiperidine-1-oxyl (TEMPO) is not stable under oxygenated conditions. Therefore the dissolved oxygen should be removed prior to the preparation of the TEMPO solution. 5mL of Et-OH was deoxygenated via 1 minute bubbling with N₂ and 0.00093 g of TEMPO was added into the oxygen free Et-OH.

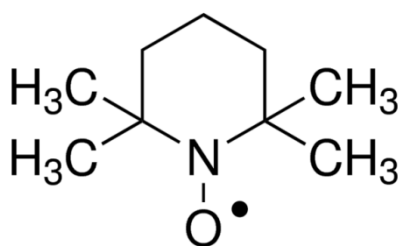


Figure 2.2 Structure of the TEMPO (Sigma-Aldrich, Tempo, 2019)

2.5 Thin Film Fabrication

We referred the sensing composites as cocktails. The cocktails were prepared in 25 mL of glass vials to contain the dye (2mg/kg polymer dye), 33% PVC (High molecular weight), 66% plasticizer (Diocetyl phthalate, DOP). The chemical structures of the utilized PVC, DOP were shown in Figure 2.4, 2.5 respectively. In the solvent of tetrahydrofuran (THF), the mixture was dissolved and it is mixed by several hours with the help of a magnetic stirrer.

The resulting cocktail was spread on a 125 μ m polyester support (Mylar from Du Pont) and dried in a desiccator which was saturated with the solvent vapour. The support material was optically fully transparent, ion impermeable and exhibited good adhesion to PVC. Acting as a mechanical support was the most significant function of the polyester because the thin films were not possible to handle. The films were kept in a desiccator in the dark. By this way, the photo stability of the membrane was ensured and the damage from the ambient air of the laboratory was avoided. For steady state fluorescence measurements each sensing film was cut to 12 mm width and 25

mm length and fixed diagonally into the sample cuvette (See Figure 2.3) and the emission spectra were recorded (Türe, 2008).

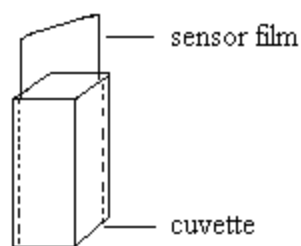


Figure 2.3 The placement of the sensor film in the sample cuvette

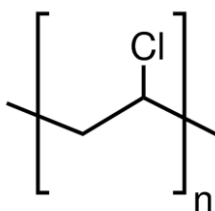


Figure 2.4 The chemical structure of PVC (Sigma-Aldrich, Poly(vinyl chloride), 2019)

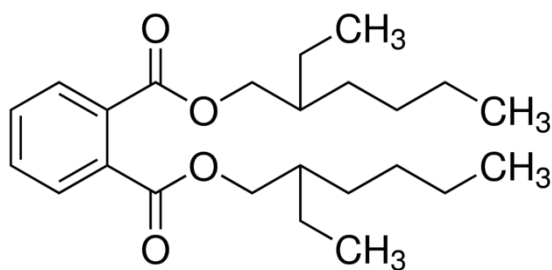


Figure 2.5 The chemical structure of DOP (Sigma-Aldrich, Dioctyl phthalate, 2019)

2.6 Fabrication of Electrospun Fibers

2.6.1 Electrospinning Apparatus

A programmable syringe pump (Top Syringe Pump Top-5300) and a high voltage power supply (Gamma High Voltage ES30) were used together for fabrication of electrospun fibers. Figure 2.6 shows components of the utilized electrospinning apparatus.

The homogeneous polyvinyl chloride solutions were placed in a 10 mL plastic syringe fitted with a metallic needle of 0.4 mm of inner diameter. The syringe is fixed vertically on the syringe pump (Top Syringe Pump Top-5300) and the electrode of the high voltage power supply (Gamma High Voltage ES30) was clamped to the metal needle tip. The feed rate of the cocktail was adjusted to 2.0 mL/h; the applied voltage was between 25-30 kV. The electrospun fibers were collected on the surface of an aluminium foil coated substrate (Kaçmaz, 2012).

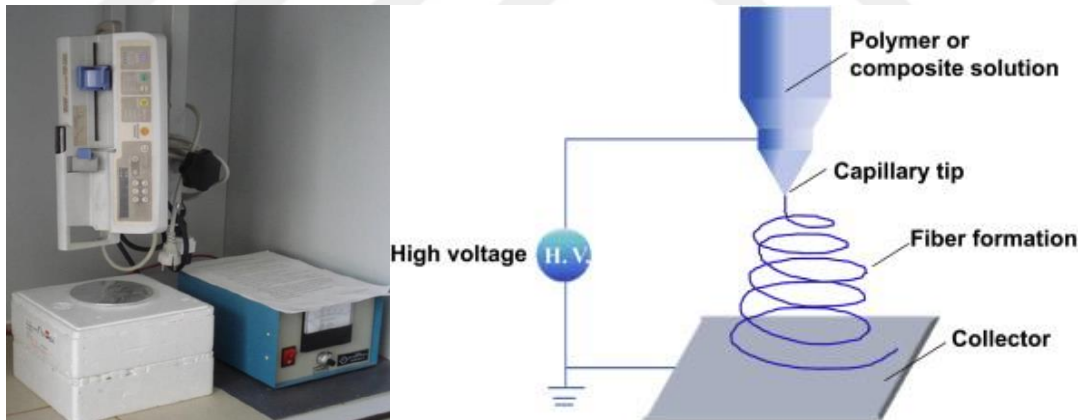


Figure 2.6 Schematic of the electrospinning apparatus (Personal archive, 2019)

2.7 Instruments

2.7.1 Spectrophotometer and Spectrofluorometer Apparatus

The steady state fluorescence measurements of the solutions, sensor films and fibers were recorded by using Varian Cary Eclipse and Edinburgh Instruments Spectrofluorometers. Fluorescence lifetimes were measured by time resolved fluorescence spectrometer of Edinburgh Instruments of FLS920 which works on the principle of time correlated single photon counting (TCSPC) principle (see Figure 2.6). During lifetime measurements the samples were excited either with laser lamp and/or a microsecond flash lamp. The excitation and emission slits were set to 5 nm. During measurements, the Instrument Response Function (IRF) was obtained from a non-fluorescing suspension of a colloidal silica (LUDOX 30%, Sigma Aldrich) in water, held in 10mm path length quartz cell and was considered to be wavelength in dependent. The lifetime parameters were recovered by iterative convolution (reconvolution) with a weighted, nonlinear least-squares method using the measured IRF and emission decay data. The reduced chi-square values and plots of weighted residuals were used to determine the “goodness of fit” between the calculated and measured decay curves. In all cases the calculated chi square values (χ^2) were less than 1.2 and in on cases the residuals trace symmetrically distributed around the zero axes.

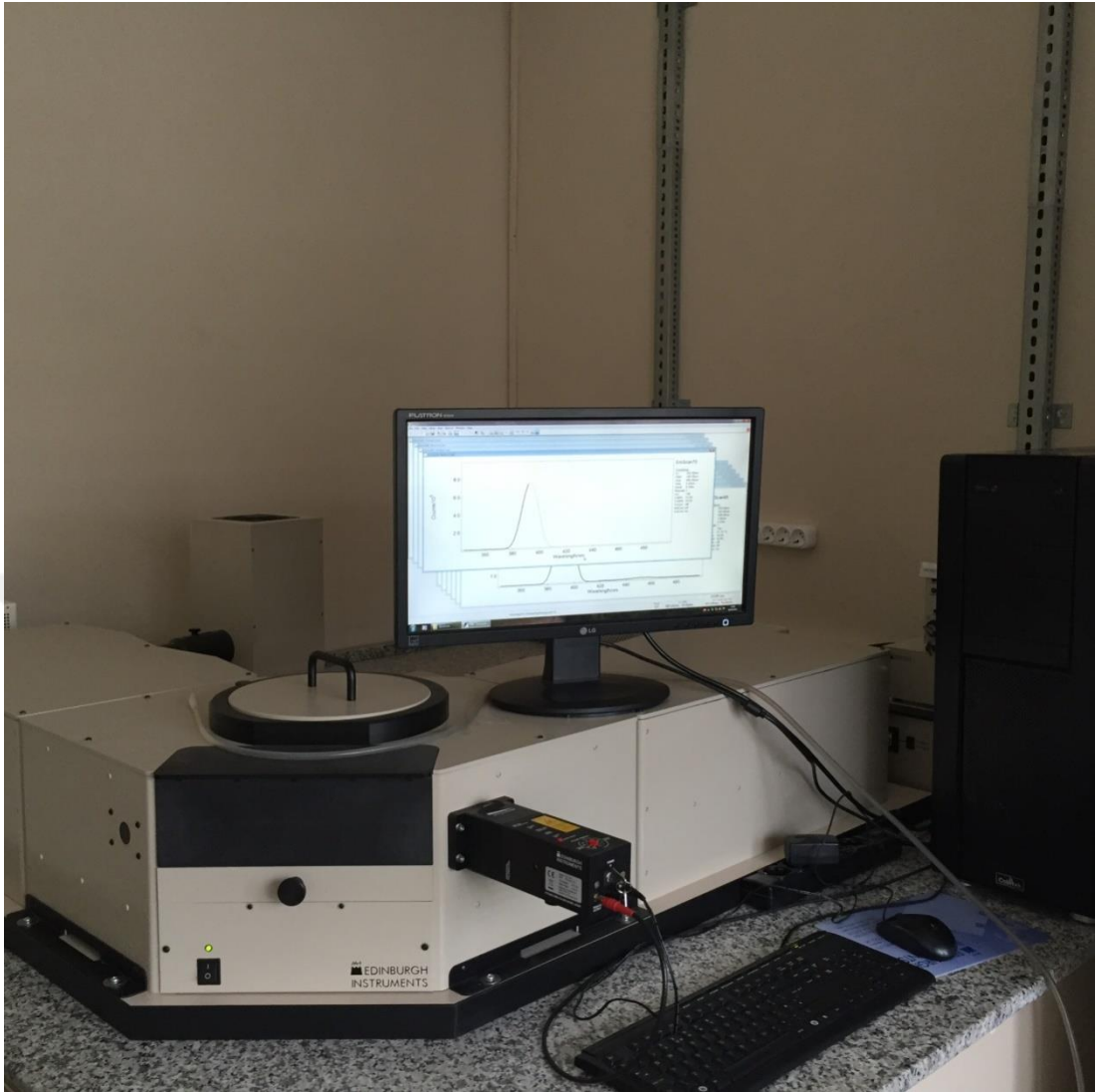


Figure 2.7 Time resolved fluorescence spectrometer of Edinburg Instruments of FLS920 (Personal archive, 2016)

CHAPTER THREE

PHACH₂ (mesotetrakis(4-phenylethynyl)phenylporphyrin) BASED STUDIES

3.1 Introduction

The well-known PHACH₂ dye along with THF has been utilized for optical chemical sensing of the nitric oxide. Structure of the PHACH₂ dye was shown in Figure 3.1.

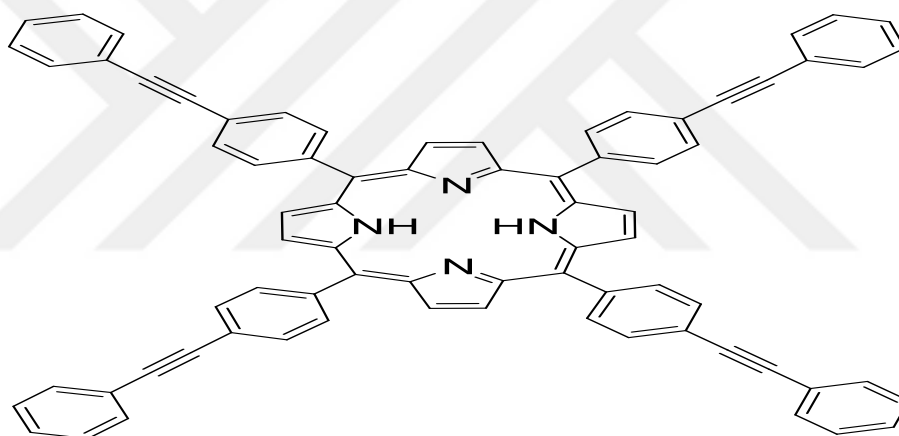


Figure 3.1 Structure of the PHACH₂ dye

3.2 Spectral Characteristics of the PHACH₂ Dye

Excitation and emission based spectral characteristics of the PHACH₂ dye were recorded in THF solution in the absence of nitric oxide. When the PHACH₂ dye was excited at 550 nm, it exhibited an emission spectrum in the wavelength range of 570-750 nm. There were seen two emission maxima at around 650 nm and 720 nm (Figure 3.2). The excitation spectrum was obtained for the emission wavelength of 550 nm. Three peak maxima were observed at 520, 550 and 590 nm. For further studies, 550 nm was chosen as excitation wavelength. The minimum. Stoke's shift value was

obtained as 60 nm. The absorption spectrum for PHACH₂ dye in THF media was shown in Figure 3.3

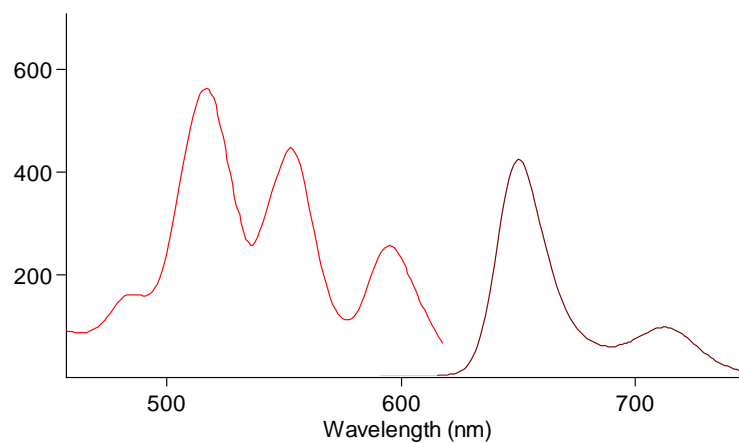


Figure 3.2 Excitation and emission spectral characteristics for PHACH₂ Dye in THF media

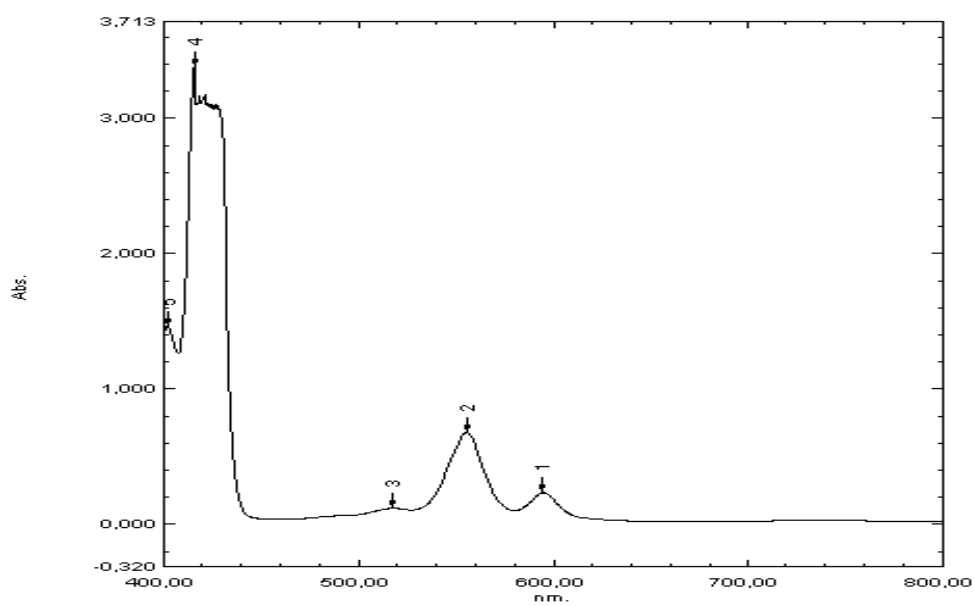


Figure 3.3 Absorption spectrum for PHACH₂ dye in THF media

3.3 Spectral Response of the PHACH₂ Dye to TEMPO Radical

Emission based spectral response of the PHACH₂ dye to TEMPO radical was investigated into detail.

Table 3.1 reveals spectral characteristics of the PHACH₂ dye in THF media in presence and in absence of TEMPO radical. According to the data, no significant response was observed by the addition of TEMPO radical. The PHACH₂ dye exhibited decreasing fluorescence intensity based response, while the concentrations of TEMPO radical was increased. The concerning data were shown in Table 3.2

Table 3.1 Excitation and emission spectral characteristics of the PHACH₂ dye

Dye	TEMPO (Mol L ⁻¹)	$\lambda_{\text{max}}^{\text{ex}}$ (nm)	$\lambda_{\text{max}}^{\text{em}}$ (nm)
PHACH ₂ in THF	-	550, 590	650, 720
PHACH ₂ in THF	1.12×10^{-5}	550, 590	648, 715

Table 3.2 The fluorescence emission based data of PHACH₂ dye to different TEMPO concentrations

Matriks: THF			
Dye: PHACH ₂			
Concentration (mol L ⁻¹)	I ₀ /I	I ₀	I
0	1	425.11	425.11
1.27×10 ⁻⁷	1.003	425.11	423.96
5.04×10 ⁻⁷	1.003	425.11	423.71
1.7×10 ⁻⁶	1.031	425.11	412.42
3.83×10 ⁻⁶	1.099	425.11	386.87
1.12×10 ⁻⁵	1.364	425.11	311.73

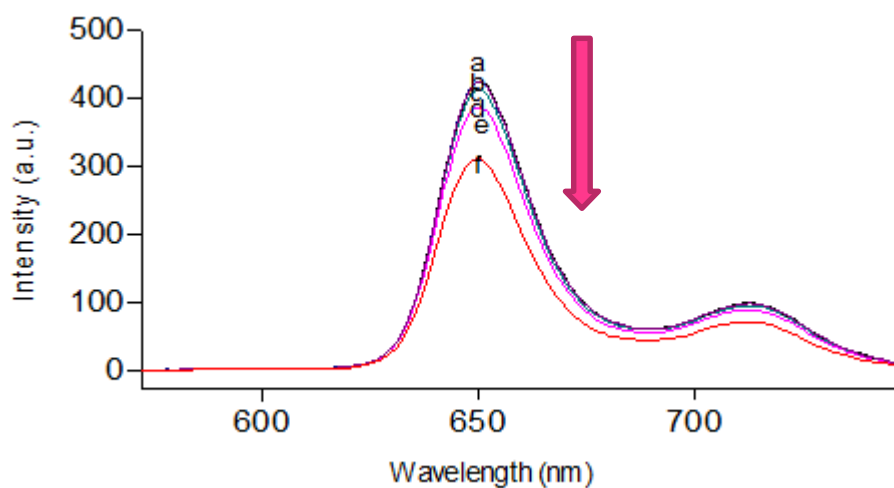


Figure 3.4 Fluorescence response of PHACH₂ to different concentrations of TEMPO in THF media
 a) 0 Mol L⁻¹ b) 1.27×10⁻⁷ Mol L⁻¹ c) 5.04×10⁻⁷ Mol L⁻¹ d) 1.7×10⁻⁶ Mol L⁻¹ e) 3.83×10⁻⁶ Mol L⁻¹
 f) 1.12×10⁻⁵ Mol L⁻¹

Figure 3.4 also shows emission based response of PHACH₂ to different concentrations of TEMPO in the range of 0-1.12×10⁻⁵ mol L⁻¹.

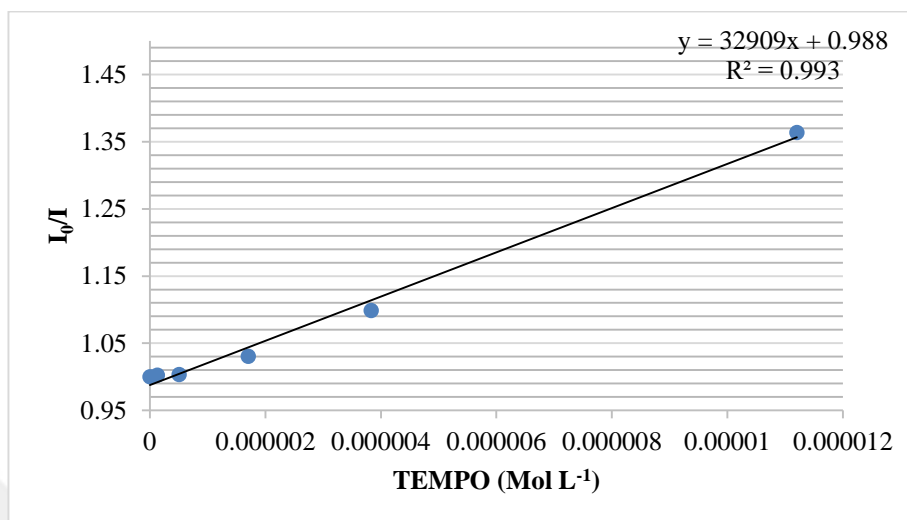
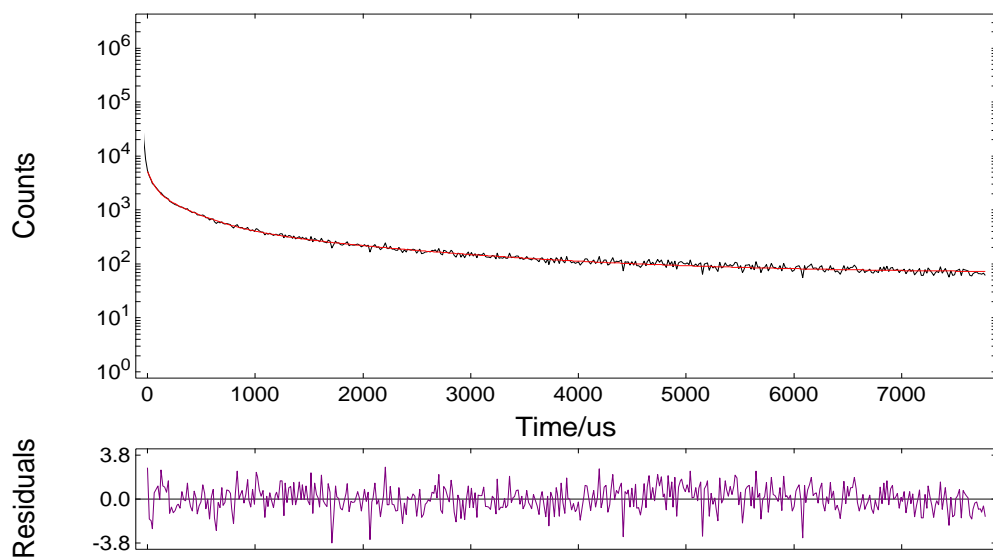


Figure 3.5 The calibration plot was drawn as I₀/I versus TEMPO concentrations for PHACH₂ dye in THF solution

Figure 3.5 reveals the calibration plot (Stern Volmer plot) which was drawn as I₀/I versus TEMPO concentrations for PHACH₂ dye in THF solution. The gathered equations of the Stern-Volmer plots(y) derived from the spectra, related regression coefficients and Stern-Volmer constants of all of the studied composites as well as THF media can be seen at Table 3.10.

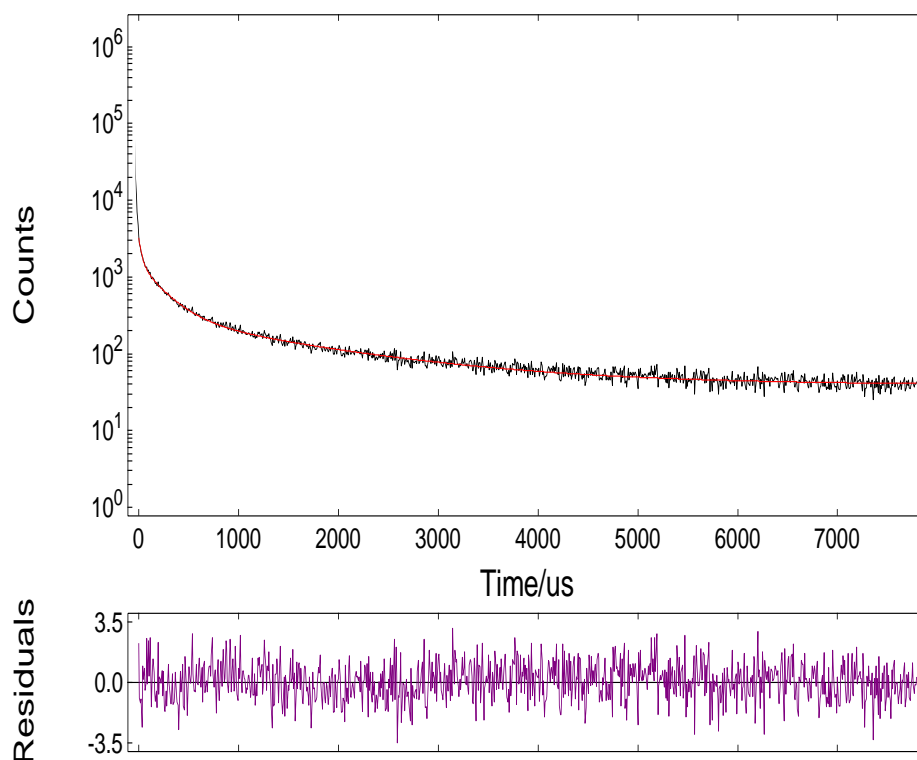
3.4 Lifetime Based Measurements in THF Media

The fluorescence lifetimes were recorded for the PHACH₂ dye in THF media in absence and presence of different concentrations of TEMPO. The dye was excited with the microsecond flash lamp of the instrument at 550 nm. The excitation and emission slits were set to 5 nm. The figures 3.6 – 3.11 show the decay characteristics of the dye. Table 3.3 shows the variation of the lifetime ratio (τ_0/τ) in THF media. Table 3.4 gives a summary of the decay characteristics and chi square values of all studied concentrations. The K_{sv} constant was found as 3.3×10⁴ μM⁻¹ and the quenching constant (k_q) was found as 33.9 M⁻¹ s⁻¹.



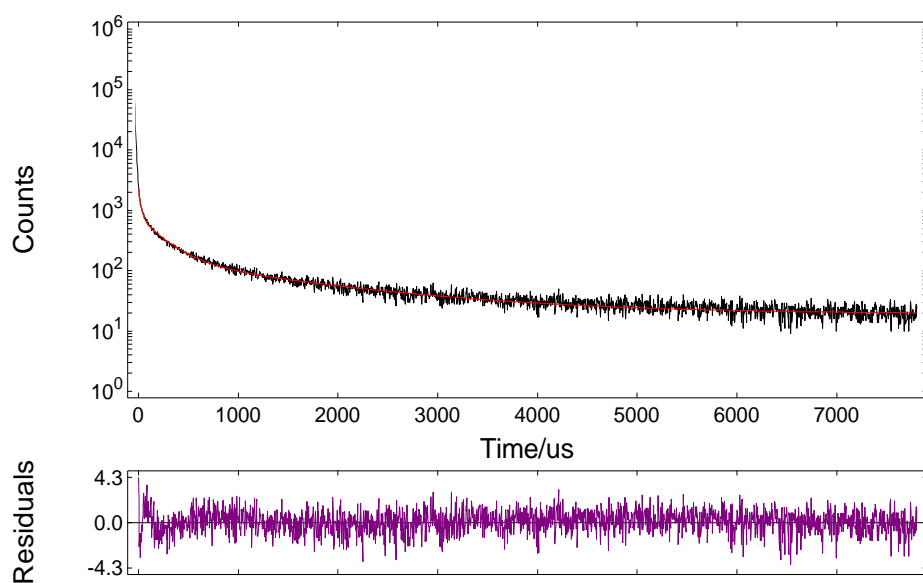
	Fix	Value / μs	Std. Dev / μs	Fix	Value	Std. Dev	Rel %
τ_1	<input type="checkbox"/>	51.4951	2.51601	B_1	<input type="checkbox"/>	3803.112	12.12
τ_2	<input type="checkbox"/>	303.6403	11.04300	B_2	<input type="checkbox"/>	1952.981	36.69
τ_3	<input type="checkbox"/>	1667.1227	53.76077	B_3	<input type="checkbox"/>	496.410	51.20
τ_4	<input type="checkbox"/>			B_4	<input type="checkbox"/>		
				A	<input checked="" type="checkbox"/>	68.144	
$\chi^2 : 1.135$							

Figure 3.6 Decay response of PHACH₂ in absence of TEMPO solution in THF media



	Fix	Value / μs	Std. Dev / μs	Fix	Value	Std. Dev	Rel %
τ_1	<input type="checkbox"/>	29.4240	1.47576	B_1	<input type="checkbox"/>	2290.146	73.4348
τ_2	<input type="checkbox"/>	226.9151	6.07630	B_2	<input type="checkbox"/>	1227.832	30.0607
τ_3	<input type="checkbox"/>	1511.3884	35.48560	B_3	<input type="checkbox"/>	279.025	7.6014
τ_4	<input type="checkbox"/>			B_4	<input type="checkbox"/>		
				A	<input type="checkbox"/>	39.324	
$\chi^2 : 1.184$							

Figure 3.7 Decay response of PHACH₂ in presence of 6 μl ($7.68 \times 10^{-8} \text{ Mol L}^{-1}$) TEMPO in THF media



	Fix	Value / μ s	Std. Dev / μ s	Fix	Value	Std. Dev	Rel %
τ_1	<input type="checkbox"/>	22.7736	0.79450	B_1	<input type="checkbox"/> 1786.843	44.0881	10.35
τ_2	<input type="checkbox"/>	227.7234	5.36977	B_2	<input type="checkbox"/> 631.025	12.2707	36.55
τ_3	<input type="checkbox"/>	1508.0104	34.64794	B_3	<input type="checkbox"/> 138.445	3.7044	53.10
τ_4	<input type="checkbox"/>			B_4	<input type="checkbox"/>		
				A	<input type="checkbox"/> 19.273		
$\chi^2 : 1.187$							

Figure 3.8 Decay response of PHACH₂ in presence of 12 μ l (1.53×10^{-7} Mol L⁻¹) TEMPO in THF media

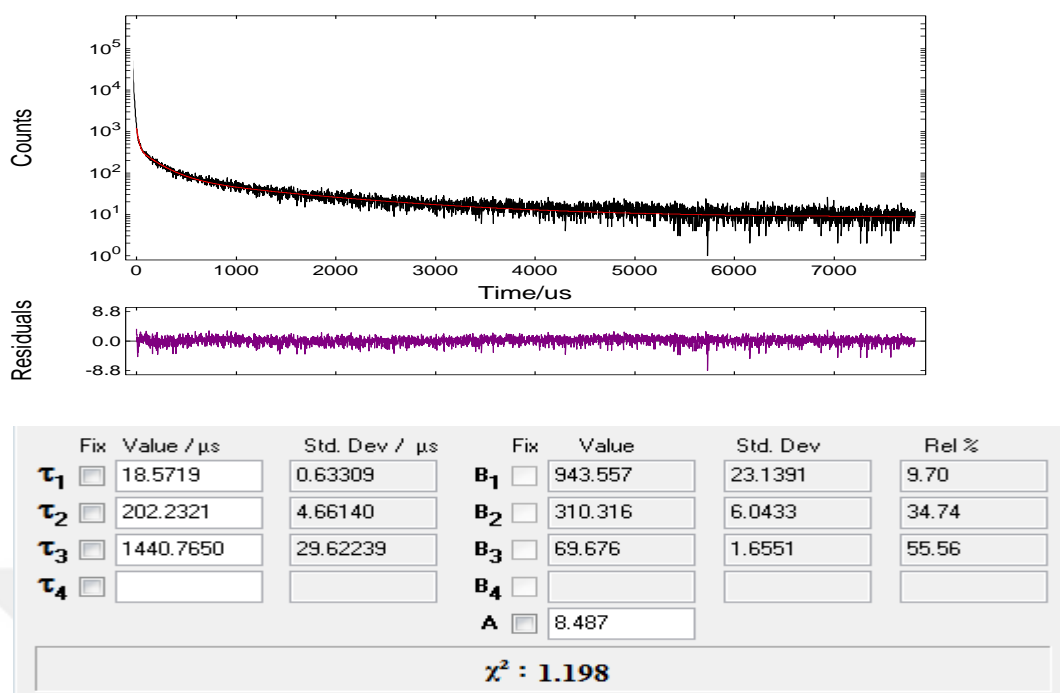
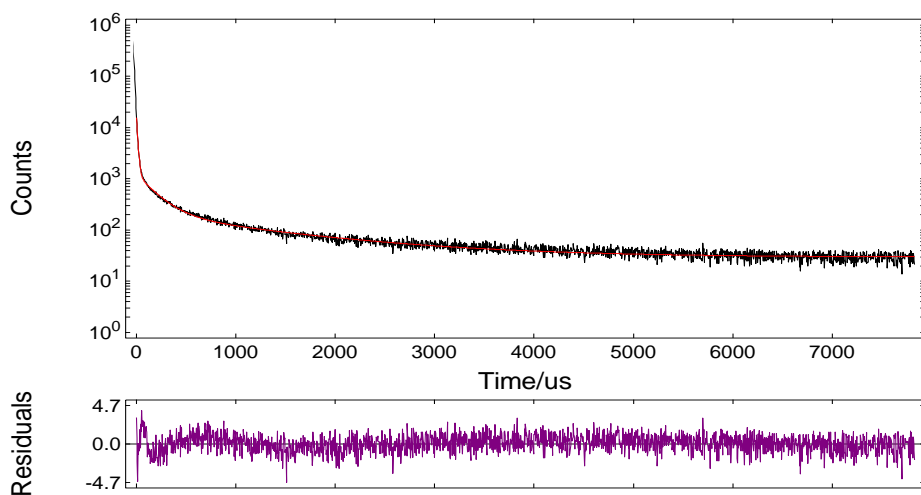


Figure 3.9 Decay response of PHACH₂ in presence of 20 μl (2.54×10^{-7} Mol L⁻¹) TEMPO in THF media



	Fix	Value / μ s	Std. Dev / μ s		Fix	Value	Std. Dev	Rel %
τ_1	<input type="checkbox"/>	12.3668	0.09664	B_1	<input type="checkbox"/>	20059.018	165.6139	36.20
τ_2	<input type="checkbox"/>	178.4960	2.97479	B_2	<input type="checkbox"/>	1050.714	14.8972	27.37
τ_3	<input type="checkbox"/>	1337.4197	24.04799	B_3	<input type="checkbox"/>	186.670	3.8623	36.43
τ_4	<input type="checkbox"/>			B_4	<input type="checkbox"/>			
				A	<input type="checkbox"/>	29.548		
$\chi^2 : 1.191$								

Figure 3.10 Decay response of PHACH₂ in presence of 90 μ l (1.11×10^{-6} Mol L⁻¹) TEMPO in THF media

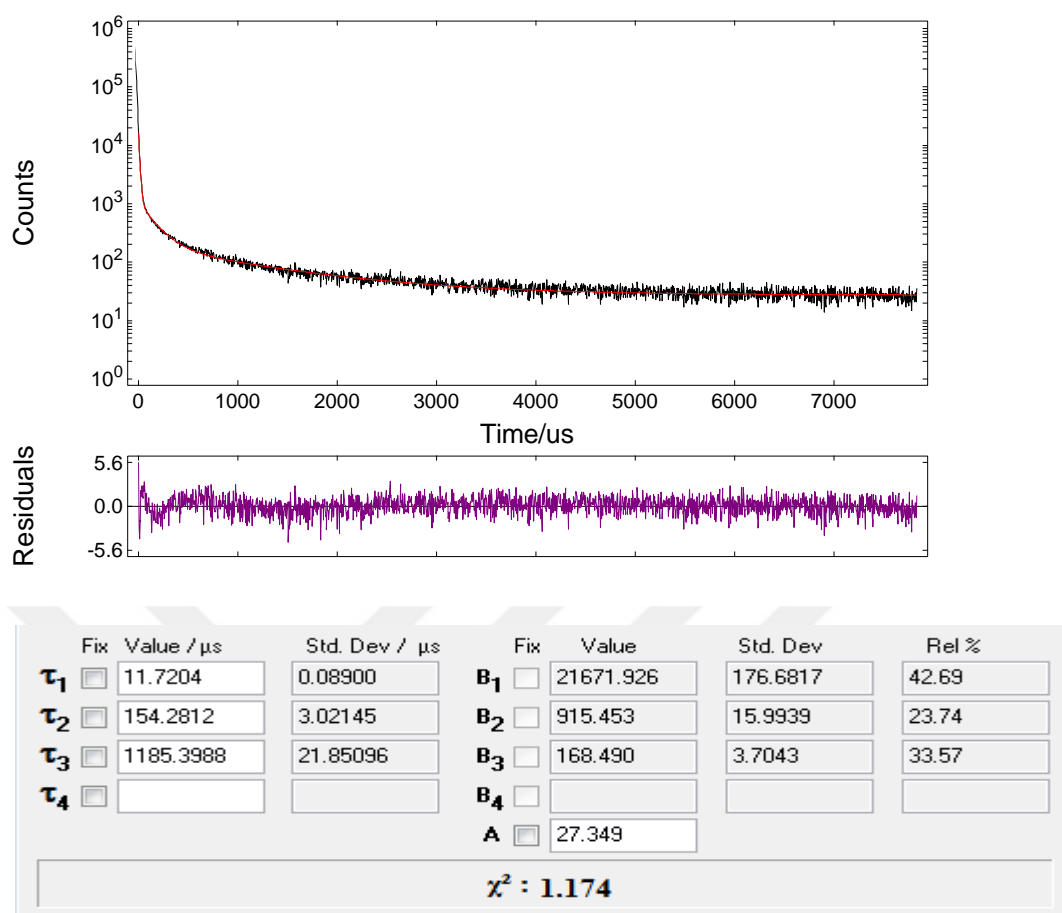


Figure 3.11 Decay response of PHACH₂ in presence of 1290 μl (1.12 × 10⁻⁵ Mol L⁻¹) TEMPO in THF media

Table 3.3 The variation of the lifetime values for different TEMPO concentrations in THF

Matrix: THF			
Dye: PHACH ₂			
Concentration (mol L ⁻¹)	τ_0/τ	τ_0	τ
0	1	971.2	971.2
7.68×10^{-8}	1.0613	971.2	915.13
1.54×10^{-7}	1.0965	971.2	885.66
2.54×10^{-7}	1.1130	971.2	872.54
1.11×10^{-6}	1.7967	971.2	540.55
K _{sv}	3.3×10^4		
K _q	33.9		

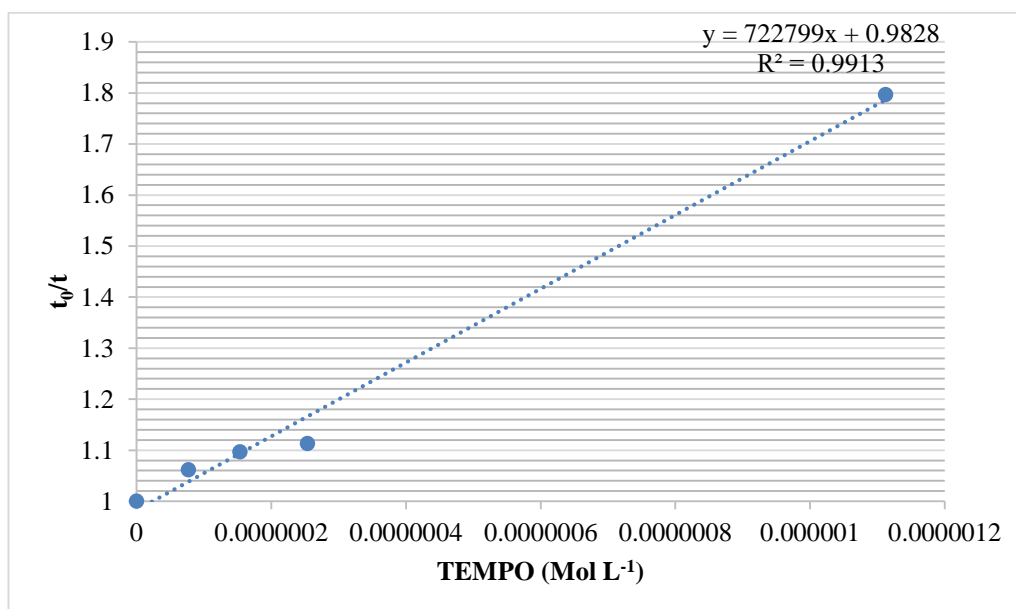


Figure 3.12 Variations of the lifetime ratio (τ_0/τ) of PHACH₂ versus quencher (TEMPO) concentrations in THF media

Figures 3.6-3.11 reveals that the PHACH₂ dye also exhibited decreasing fluorescence lifetime based response which is the sign of dynamic quenching.

Table 3.4 Summary of the decay characteristics and chi square values of the studied composites in presence and absence of TEMPO in THF media

TEMPO ($\mu\text{Mol L}^{-1}$)	τ_0 (μs)	τ_{TEMPO} (average)	χ^2	τ_0/τ	K_{sv} [TEMPO] ⁻¹ (μM^{-1})	k_q ($\text{M}^{-1}\text{s}^{-1}$)
0	51.49±2.51 (12.12 %)	971.2	1.135	1	3.3×10^4	33.9
	303.64±11.04 (36.69 %)					
	1667.12±53.76 (51.20%)					
7.68×10^{-2}	29.42±1.47 (8.78 %)	915.13	1.184	1.06	3.3×10^4	33.9
	226.91±6.07 (36.29 %)					
	1511.38±35.48 (54.93%)					
1.54×10^{-1}	22.77±0.79 (8.78 %)	885.66	1.187	1.1	3.3×10^4	33.9
	227.72±5.36 (36.29 %)					
	1508.01±34.64 (54.93%)					
2.54×10^{-1}	18.57±0.63 (9.7 %)	872.54	1.198	1.11	3.3×10^4	33.9
	202.23±4.66 (34.74 %)					
	1440.76±29.62 (55.56%)					
1.11	12.36±0.09 (36.2 %)	540.55	1.191	1.8	3.3×10^4	33.9
	178.49±2.97 (27.37 %)					
	1337.41±24.04 (36.43%)					
17.2	11.72±0.08 (42.69 %)	439.57	1.17	2.21	3.3×10^4	33.9
	154.28±3.02 (23.74 %)					
	1185.39±21.85 (33.57%)					

3.5 Spectral Characteristics of the PHACH₂ Dye in PVC matrix

The response of PVC encapsulated PHACH₂ dye either in thin film and in nano-fiber form has been studied in SDS solution prepared in phosphate buffer at pH 7.4. The prepared cocktail composition containing the indicator and the additives was shown in Table 3.5

Table 3.5 Cocktail compositions for thin film and nano-fiber sensing probes

	Matrix (PVC)	Plasticizer (DOP)	Dye Solution PHACH ₂	Ionic Liquid [BMIM ⁺] [PF ₆ ⁻]	Solvent (SDS)
Thin film / nano-fiber	120 mg	240 mg	50 μL	-	2.5 mL

In all of the test moieties the PHACH₂ dye exhibited two emission maxima around 658 and 720 nm. Table 3.6 reveals spectral characteristics of the embedded PHACH₂ dye in SDS media at pH 7.4. The excitation has been performed at 428 nm. The Stoke's shift was calculated as 230 nm. Emission based response at 658 nm decreased upon exposure to the increasing concentrations of the TEMPO. Table 3.7 contains the fluorescence intensities for nanofiber forms in pH 7.4 buffered SDS media at different TEMPO concentrations.

Table 3.6 Excitation and emission spectral characteristics of the PHACH₂ dye

Dye	Matrix	Thin Film/ Nanofiber	Solvent	$\lambda_{\max}^{\text{ex}}$ (nm)	$\lambda_{\max}^{\text{em}}$ (nm)	Stoke's Shift ($\Delta\lambda$) (nm)
PHACH ₂	PVC	+/+	pH 7.4 buffer in SDS	428	658	230

It was seen that a linear graph could not be created in Stern Volmer studies of the thin films performed in pH 7.4 buffered SDS in the studied TEMPO concentration range. This can be attributed to the inefficient diffusion of TEMPO through PVC membrane which is obtained by manual knife coating method.

In the case of nano-fibers, the dye exhibited a decrease in signal intensity at 658 nm when exposed to TEMPO. In Figure 3.13 emission based response of PHACH₂ to different concentrations of TEMPO in the range of 0- 3.58×10^{-8} Mol L⁻¹ was shown. In Figure 3.14, the calibration plot and related equation were also shown.

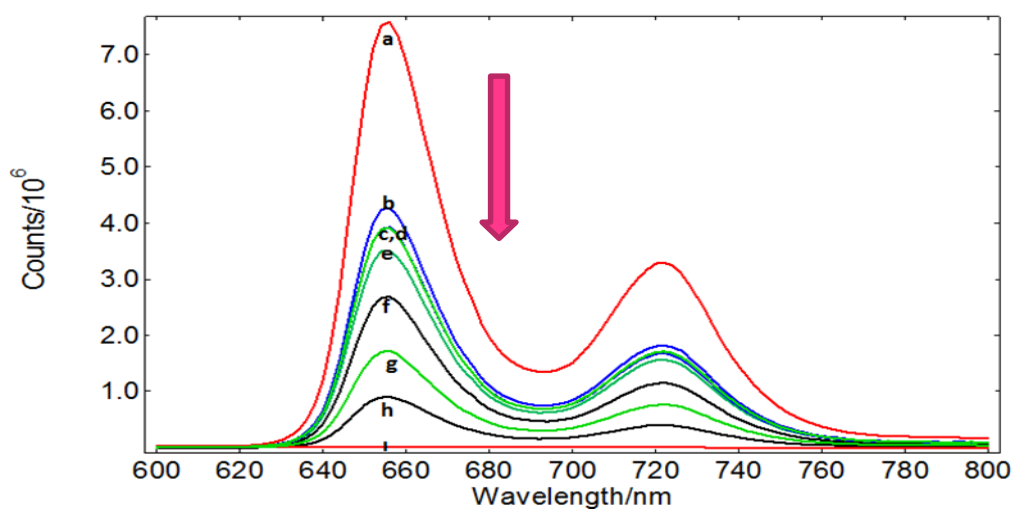


Figure 3.13 Fluorescence intensity based response of PHACH₂ in nanofiber form to TEMPO concentrations in pH 7.4 buffered SDS media. a) 0 Mol L⁻¹ b) 2.56×10⁻⁹ Mol L⁻¹ c) 5.12×10⁻⁹ Mol L⁻¹ d) 7.68×10⁻⁹ Mol L⁻¹ e) 1.28×10⁻⁸ Mol L⁻¹ f) 1.92×10⁻⁸ Mol L⁻¹ g) 2.56×10⁻⁸ Mol L⁻¹ h) 3.58×10⁻⁸ Mol L⁻¹ i) 3.84×10⁻⁸ Mol L⁻¹

Table 3.7 The fluorescence intensities for nanofiber forms in pH 7.4 buffered SDS media at different TEMPO concentrations

Matrix: PVC			
Dye: PHACH ₂			
Concentration (Mol L ⁻¹)	I ₀ /I	I ₀	I
0	1.00	7.57×10 ⁶	7.57×10 ⁶
5.12×10 ⁻⁹	1.93	7.57×10 ⁶	3.92×10 ⁶
1.92×10 ⁻⁸	2.82	7.57×10 ⁶	2.68×10 ⁶
2.56×10 ⁻⁸	4.40	7.57×10 ⁶	1.72×10 ⁶

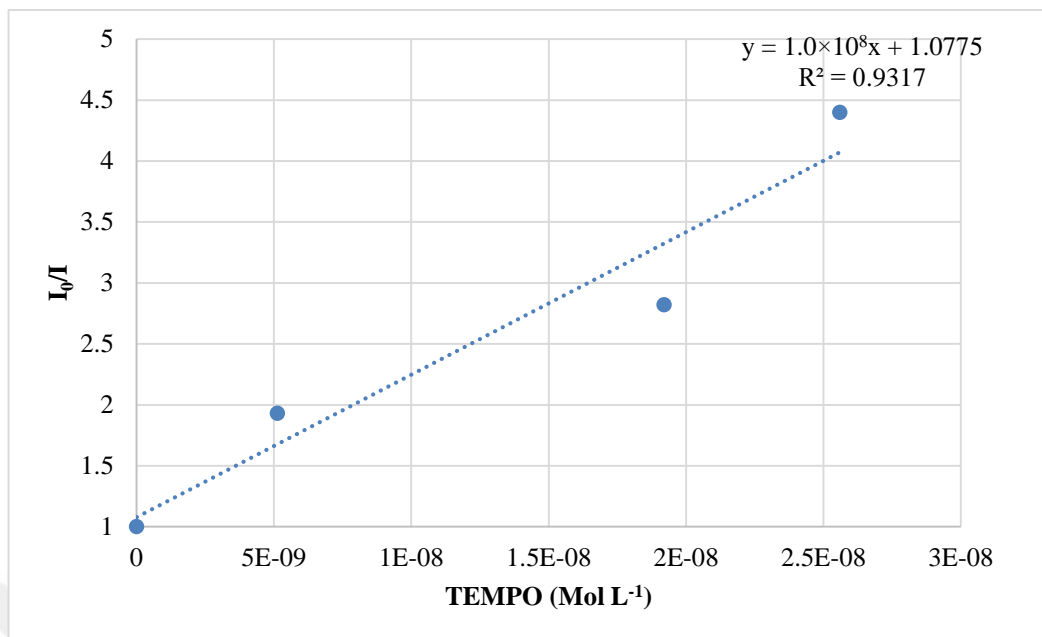


Figure 3.14 The calibration plot for PHACH₂ nanofiber form in pH 7.4 buffered SDS media

Table 3.8 Excitation and emission based spectral characteristics of the PHACH₂ dye in nano-fiber form

Dye	Matrix	Nanofiber	NH ₃	$\lambda_{\max}^{\text{ex}}$ (nm)	$\lambda_{\max}^{\text{em}}$ (nm)	Stoke's Shift ($\Delta\lambda$) (nm)
PHACH ₂	PVC	+	+	425	654	229

Table 3.8 shows the excitation and emission based spectral characteristics of the PHACH₂ dye in nano-fiber form. Table 3.9 contains the gathered data of Stern-Volmer equations, regression coefficients and Stern-Volmer constants of all of the studied composites. The best Stern-Volmer constant for TEMPO was obtained for nano-fiber composites in the buffered SDS solutions.

Table 3.9 The Stern-Volmer equations, regression coefficients and Stern-Volmer constants of all of the studied composites

Dye	Matrix	Thin Film/ Nano fiber	TEMPO	SOLVENT	Stern-Volmer plots	Regression Coefficient
PHACH ₂	THF	-	+	THF	$y = 32909x + 0.988$	0.993
PHACH ₂	PVC	Thin film	+	Ph 7.4 Buffer in SDS	-	-
PHACH ₂	PVC	Nano fiber	+	Ph 7.4 Buffer in SDS	$y = 1.0 \times 10^8 x + 1.0775$	0.932

3.6 Fluorescence Intensity Based Kinetic Response to Gaseous NH₃

In order to test the response of PHACH₂ dye to gaseous NH₃, the dye embedded in nano-fiber forms were exposed to NH₃ in a closed box containing the gas vapours for different periods of time in the range of 0-120 minutes. Figure 3.15 shows the fluorescence intensity based kinetic response. According to the figure, the emission of PHACH₂ is affected from NH₃ gas in the way of decreasing response by time. The dye has a potential for NH₃ sensing and can be tested by further studies.

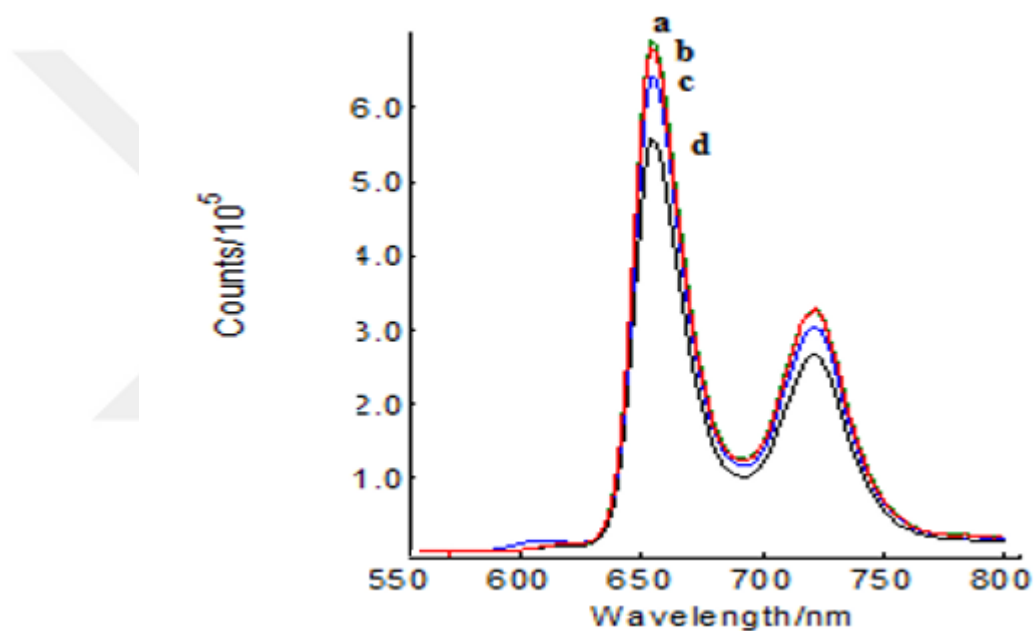
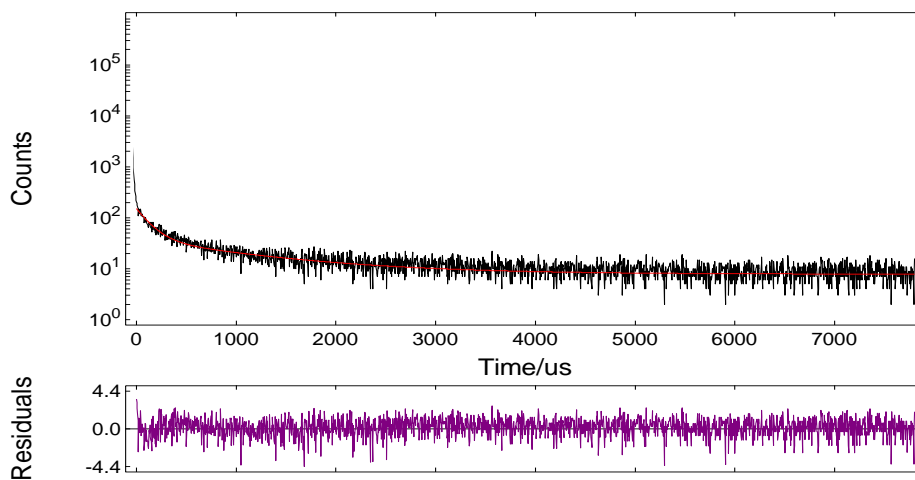


Figure 3.15 Fluorescence response of PHACH₂ embedded in NH₃ media a) 0 min. b) 30 min. c) 60 min. d) 120 min.

3.7 Lifetime Based Measurements of Embedded Forms

The fluorescence lifetimes were recorded for PVC forms of the PHACH₂ dye. The Figures between 3.16 – 3.18 show decay characteristics of the encapsulated dyes in buffered solutions in the absence and presence of the TEMPO. Table 3.10 show the variation of the lifetime ratio (τ_0/τ) of PHACH₂ versus quencher (TEMPO) concentration in pH 7.4 buffer media. Table 3.11 gives a summary of the decay characteristics and chi square values of the studied composites





	Fix	Value / μ s	Std. Dev / μ s	Fix	Value	Std. Dev	Rel %
τ_1	<input type="checkbox"/>	136.7751	6.80005	B_1	<input type="checkbox"/> 117.416	3.8718	31.26
τ_2	<input type="checkbox"/>	1160.0891	52.58471	B_2	<input type="checkbox"/> 30.436	1.4891	68.74
τ_3	<input type="checkbox"/>			B_3	<input type="checkbox"/>		
τ_4	<input type="checkbox"/>			B_4	<input type="checkbox"/>		
				A	<input type="checkbox"/> 7.808		
$\chi^2 : 1.197$							

Figure 3.16 Decay response of PHACH₂ embedded PVC based thin film with in pH 7.4 buffer SDS media without TEMPO solution

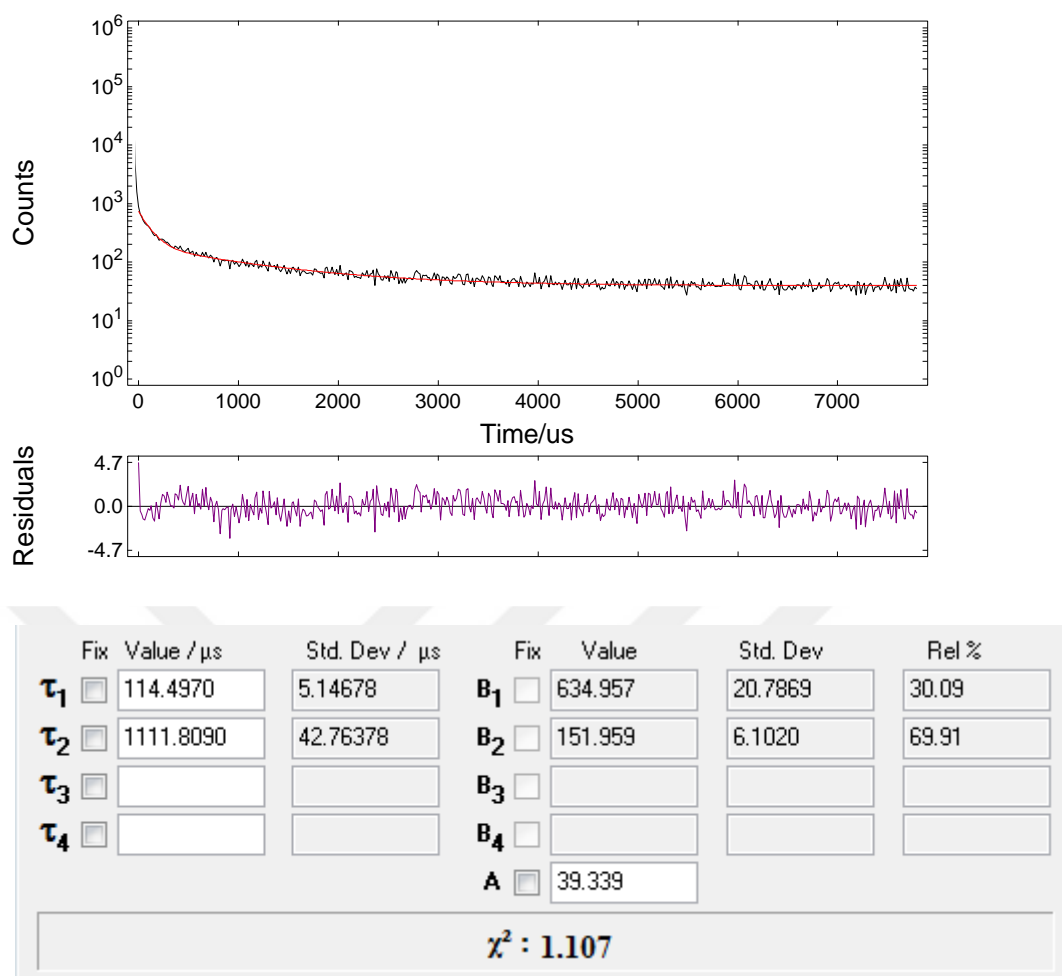
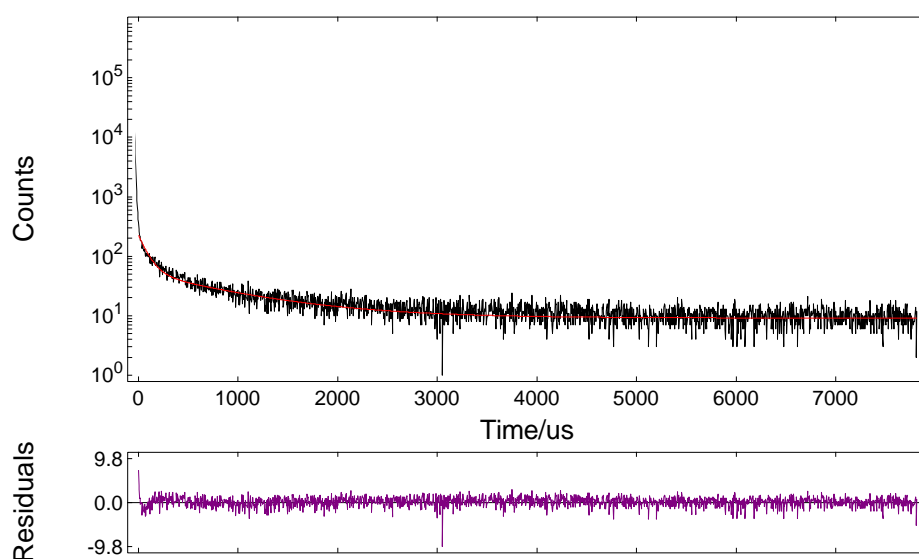


Figure 3.17 Decay response of PHACH₂ embedded PVC based thin film in the presence of 7 μl ($8.96 \times 10^{-8} \text{ Mol L}^{-1}$) TEMPO in pH 7.4 buffer in SDS media



	Fix	Value / μ s	Std. Dev / μ s	Fix	Value	Std. Dev	Rel %
τ_1	<input type="checkbox"/>	89.4701	3.90927	B_1	<input type="checkbox"/> 180.864	5.8600	27.96
τ_2	<input type="checkbox"/>	918.8806	29.83596	B_2	<input type="checkbox"/> 45.376	1.6213	72.04
τ_3	<input type="checkbox"/>			B_3	<input type="checkbox"/>		
τ_4	<input type="checkbox"/>			B_4	<input type="checkbox"/>		
				A	<input type="checkbox"/> 9.140		
$\chi^2 : 1.240$							

Figure 3.18 Decay response of PHACH₂ embedded PVC based thin film in the presence of 25 μ l (3.17×10^{-7} Mol L⁻¹) TEMPO in pH 7.4 buffer in SDS media

Table 3.10 (τ_0/τ) values corresponding to TEMPO concentrations thin film form to pH 7.4 buffer SDS media TEMPO solution for PHACH₂ dye

Matrix: SDS			
Dye: PHACH ₂			
Concentration (Mol L ⁻¹)	τ_0/τ	τ_0	τ
0	1	136.77	136.77
8.96×10^{-8}	1.1945	136.77	114.5
3.17×10^{-7}	1.5287	136.77	89.47
K _{sv}	3.9×10^5		
K _q	4.64×10^2		

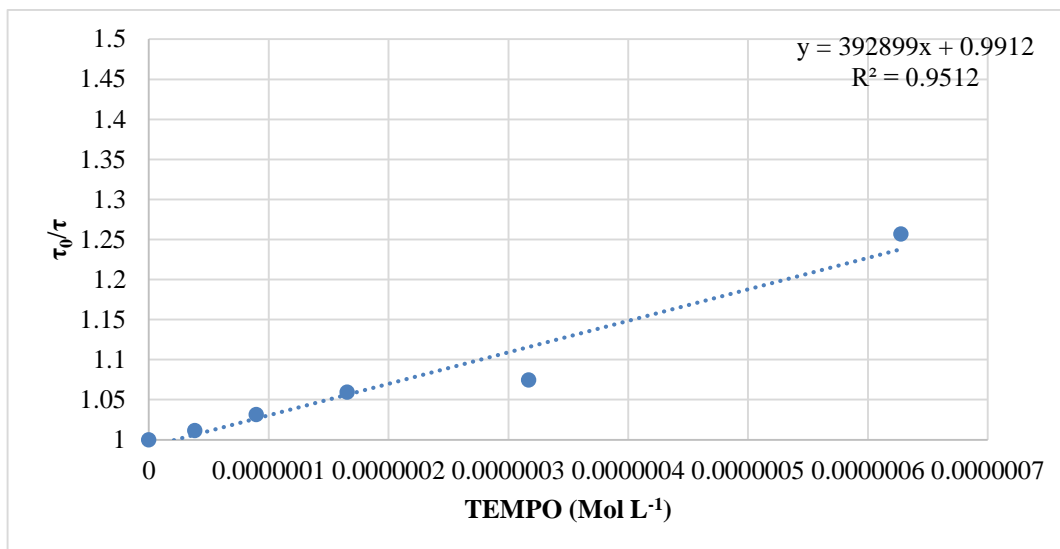


Figure 3.19 Variations of the lifetime ratio (τ_0/τ) PHACH₂ versus quencher (TEMPO) concentrations thin film form to pH 7.4 buffer in SDS media

Figures 3.16-3.18 reveals that the PHACH₂ dye also exhibited decreasing fluorescence lifetime based response which is the sign of dynamic quenching.

Table 3.11 Summary of the decay characteristics and chi square values of the studied composites in presence and absence of TEMPO for thin film form

TEMPO ($\mu\text{Mol L}^{-1}$)	τ_0 (μs)	τ_{TEMPO} (average)	χ^2	τ_0/τ	K_{sv} [TEMPO] $^{-1}$ (μM^{-1})	k_d ($\text{M}^{-1}\text{s}^{-1}$)
0	136.77 \pm 6.8 (31.26 %)	840.19	1.197	1	3.9×10^5	4.64×10^2
	1160.08 \pm 52.58(68.74 %)					
8.96×10^{-2}	114.49 \pm 5.14 (30.09 %)	811.72	1.107	1.53	3.9×10^5	4.64×10^2
	1111.8 \pm 42.76 (69.91 %)					
3.16×10^{-1}	89.47 \pm 3.90 (27.96 %)	686.97	1.240	1.52	3.9×10^5	4.64×10^2
	918.88 \pm 29.83 (72.04 %)					

Figures 3.20-3.23 reveals that the PHACH₂ dye also exhibited decreasing fluorescence lifetime based response which is the sign of dynamic quenching.

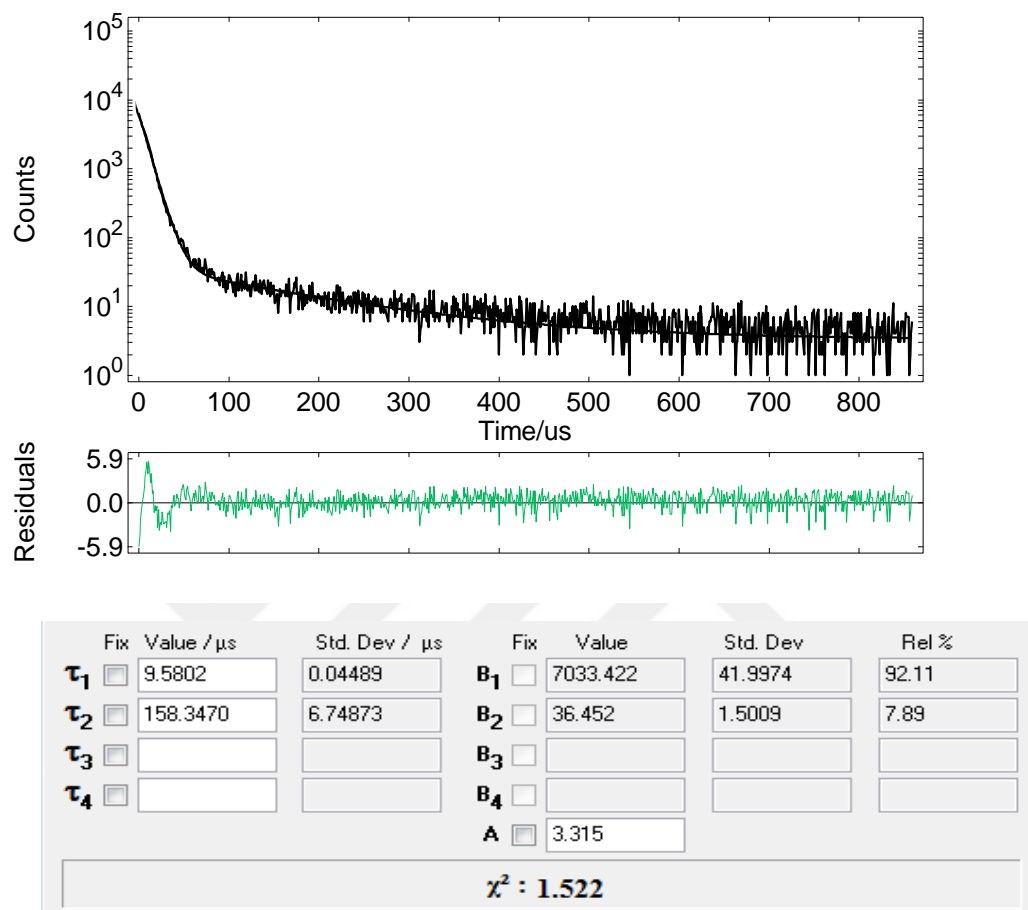
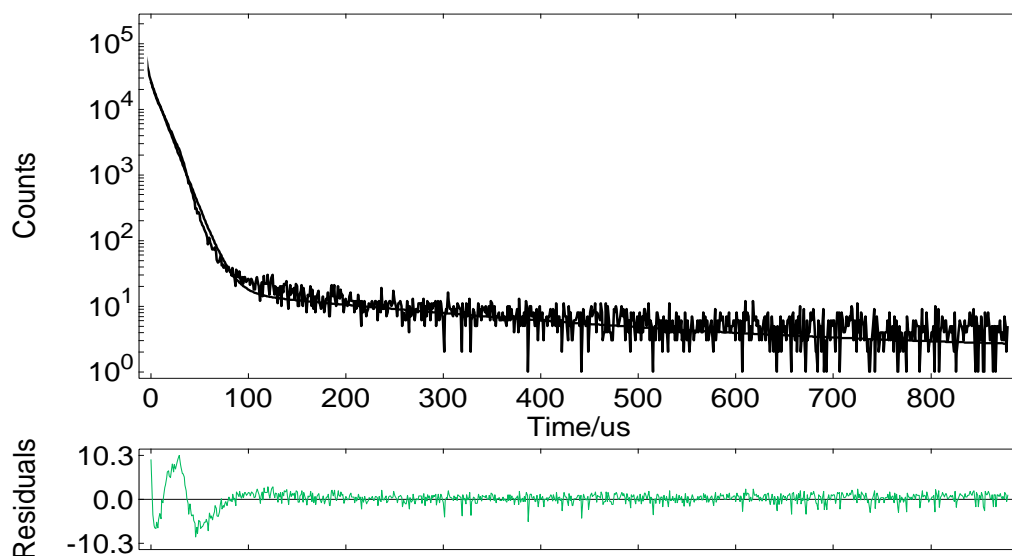
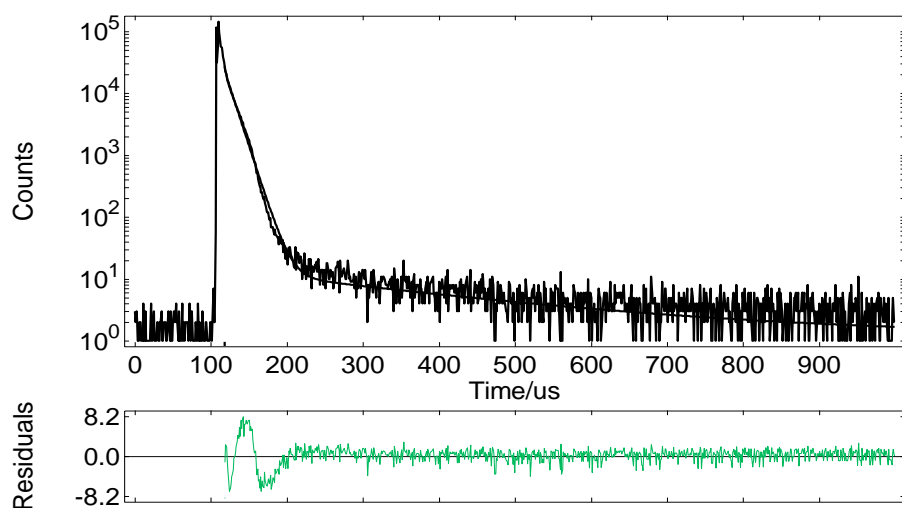


Figure 3.20 Decay response of PHACH₂ embedded PVC based nanofiber with in pH 7.4 buffer SDS media without TEMPO solution



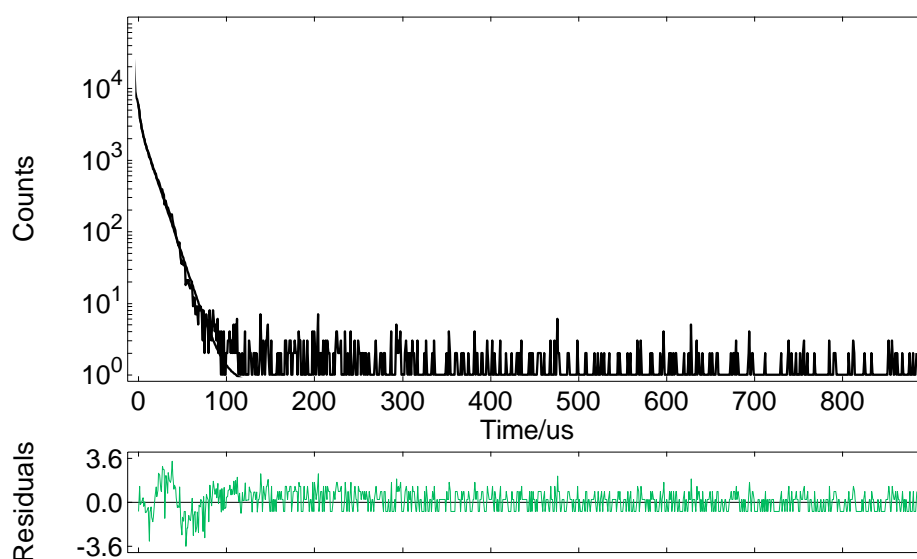
	Fix	Value / μs	Std. Dev / μs	Fix	Value	Std. Dev	Rel %
τ_1	<input type="checkbox"/>	11.2781	0.02132	B_1	28452.500	74.4429	98.52
τ_2	<input type="checkbox"/>	268.2813	23.29001	B_2	17.915	0.8936	1.48
τ_3	<input type="checkbox"/>			B_3			
τ_4	<input type="checkbox"/>			B_4			
				A	2.007		
$\chi^2 : 3.712$							

Figure 3.21 Decay response of PHACH₂ embedded PVC based nanofiber in the presence of 0.6 μl (7.68×10^{-9} Mol L⁻¹) TEMPO in pH 7.4 buffer in SDS media



	Fix	Value / μs	Std. Dev / μs	Fix	Value	Std. Dev	Rel %
τ_1	<input type="checkbox"/>	1.2272	0.10858	B_1	<input type="checkbox"/> 9951.665	864.3886	4.01
τ_2	<input type="checkbox"/>	11.4489	0.02836	B_2	<input type="checkbox"/> 25227.086	109.3742	94.87
τ_3	<input type="checkbox"/>	266.4168	26.58149	B_3	<input type="checkbox"/> 12.839	0.7744	1.12
τ_4	<input type="checkbox"/>			B_4	<input type="checkbox"/>		
				A	<input checked="" type="checkbox"/> 1.211		
$\chi^2 : 3.254$							

Figure 3.22 Decay response of PHACH₂ embedded PVC based nanofiber in the presence of 1 μl (1.28×10^{-8} Mol L⁻¹) TEMPO in pH 7.4 buffer in SDS media



	Fix	Value / μ s	Std. Dev / μ s	Fix	Value	Std. Dev	Rel %
τ_1	<input type="checkbox"/>	2.0240	0.10407	B_1	<input type="checkbox"/> 4430.665	172.9387	17.43
τ_2	<input type="checkbox"/>	11.6610	0.08503	B_2	<input type="checkbox"/> 3643.365	55.8093	82.57
τ_3	<input type="checkbox"/>			B_3	<input type="checkbox"/>		
τ_4	<input type="checkbox"/>			B_4	<input type="checkbox"/>		
				A	<input type="checkbox"/> 0.746		
$\chi^2 : 0.755$							

Figure 3.23 Decay response of PHACH₂ embedded PVC based nanofiber in the presence of 2.8 μ l (3.58×10^{-8} Mol L⁻¹) TEMPO in pH 7.4 buffer in SDS media

Table 3.12 shows the fluorescence lifetime and (τ_0/τ) values corresponding to TEMPO concentrations for nanofiber forms at pH 7.4 buffered SDS media.

Table 3.12 (τ_0/τ) values corresponding to TEMPO concentrations nanofiber form to pH 7.4 buffer SDS media TEMPO solution for PHACH₂ dye

Matrix: SDS			
Dye: PHACH ₂			
Concentration(Mol L ⁻¹)	τ_0/τ	τ_0	τ
0	1	21.31	21.31
7.68×10^{-9}	1.4131	21.31	15.08
1.28×10^{-8}	1.5342	21.31	13.89
3.58×10^{-8}	2.1353	21.31	9.98
K _{sv}	1.0×10^8		
K _q	4.7×10^6		

Figure 3.24 shows the variation of the lifetime ratio (τ_0/τ) of PHACH₂ versus quencher (TEMPO) concentrations in thin film form in pH 7.4 buffered SDS media.

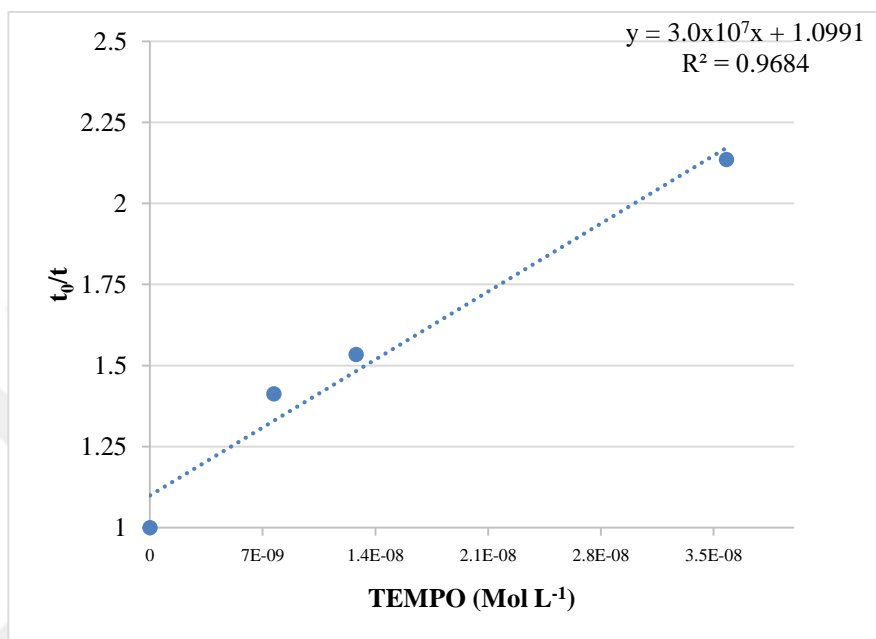
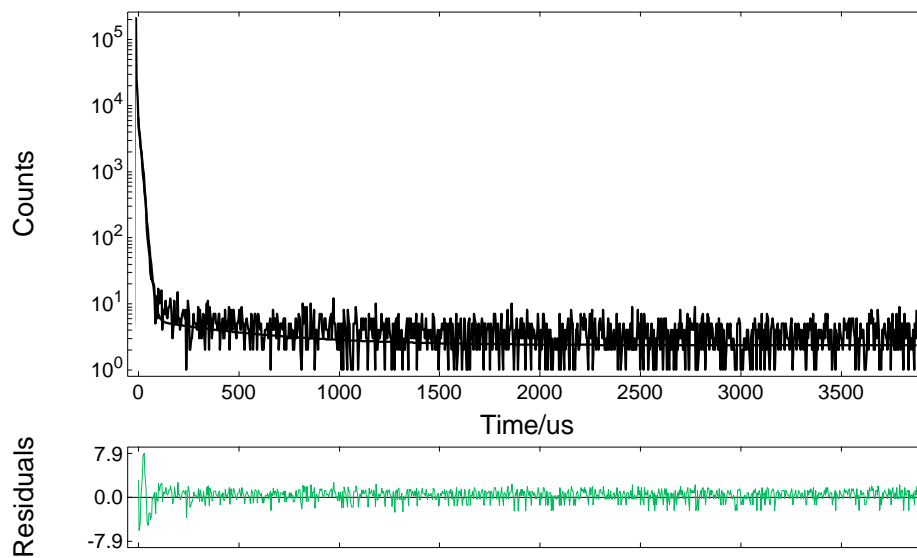


Figure 3.24 Variations of the lifetime ratio (τ_0/τ) PHACH₂ versus quencher (TEMPO) concentrations nano-fiber form to pH 7.4 buffer in SDS media

Table 3.13 shows the decay characteristics and chi square values of the studied composites to TEMPO for nanofiber forms.

Table 3.13 Summary of the decay characteristics and chi square values of the studied composites in presence and absence of TEMPO for nanofiber form

TEMPO ($\mu\text{Mol L}^{-1}$)	τ_0 , (μs)	τ_{TEMPO} (average)	χ^2	τ_0/τ	K_{sv} [TEMPO] $^{-1}$ (μM^{-1})	k_q ($\text{M}^{-1}\text{s}^{-1}$)
0	9.58 \pm 0.04 (92.11 %)	21.313	1.522	1	1.0×10^8	4.7×10^6
	158.35 \pm 6.75 (7.89 %)					
7.68×10^{-3}	11.27 \pm 0,02 (98.52 %)	15.081	3.712	1.41	1.0×10^8	4.7×10^6
	268.28 \pm 23.29 (1.48%)					
1.28×10^{-2}	1.22 \pm 0.10 (4.01 %)	13.894	3.254	1.53	1.0×10^8	4.7×10^6
	11.45 \pm 0.03 (94.87 %)					
	266.42 \pm 26.58 (1.12%)					
3.58×10^{-2}	2.02 \pm 0.10 (17.43 %)	9.981	0.755	2.13	1.0×10^8	4.7×10^6
	11.66 \pm 0.08 (82.57 %)					



	Fix	Value / μ s	Std. Dev / μ s	Fix	Value	Std. Dev	Rel %
τ_1	<input checked="" type="checkbox"/>	12.0841	0.08105	B_1	9191.861	92.7128	98.38
τ_2	<input checked="" type="checkbox"/>	500.0000	98.37791	B_2	3.659	0.5794	1.62
τ_3	<input type="checkbox"/>			B_3			
τ_4	<input type="checkbox"/>			B_4			
				A	2.339		
$\chi^2 : 1.484$							

Figure 3.25 Decay response of PHACH₂ embedded PVC based nanofiber in the presence of without in NH₃ media

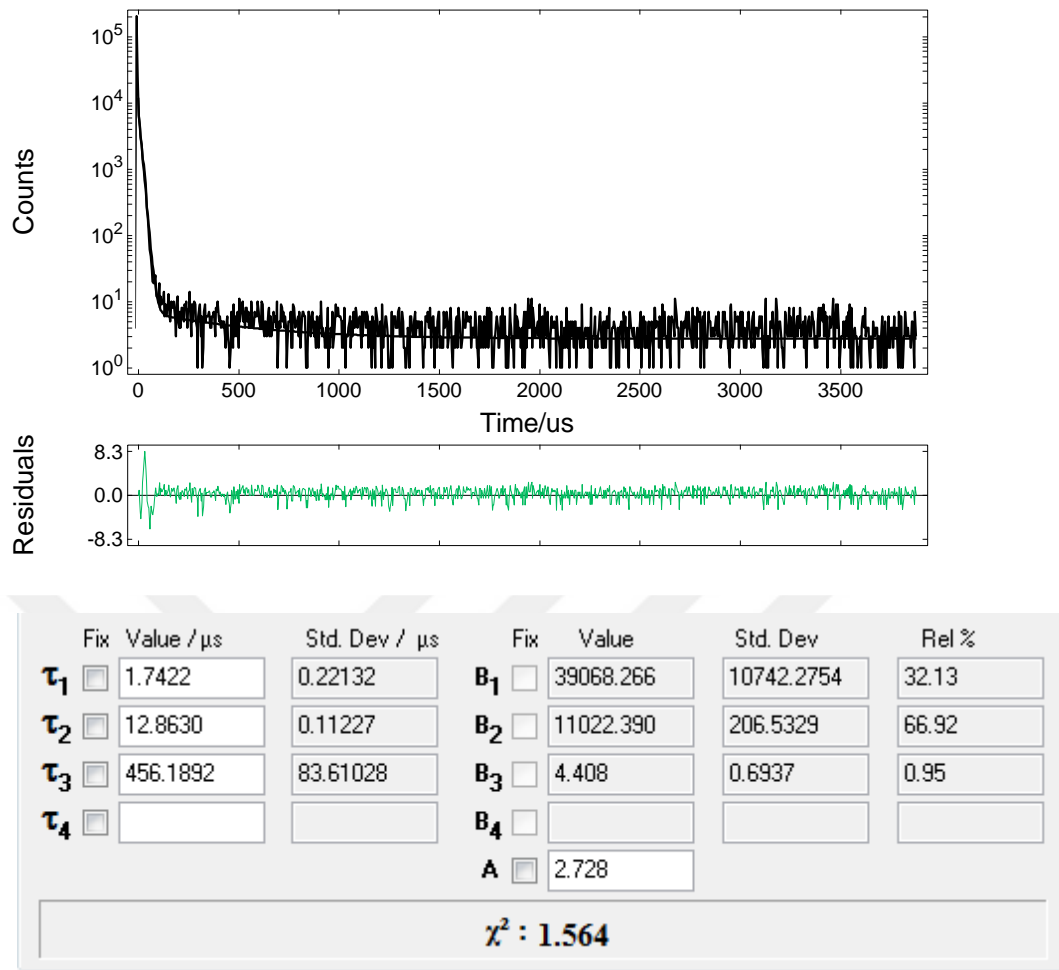
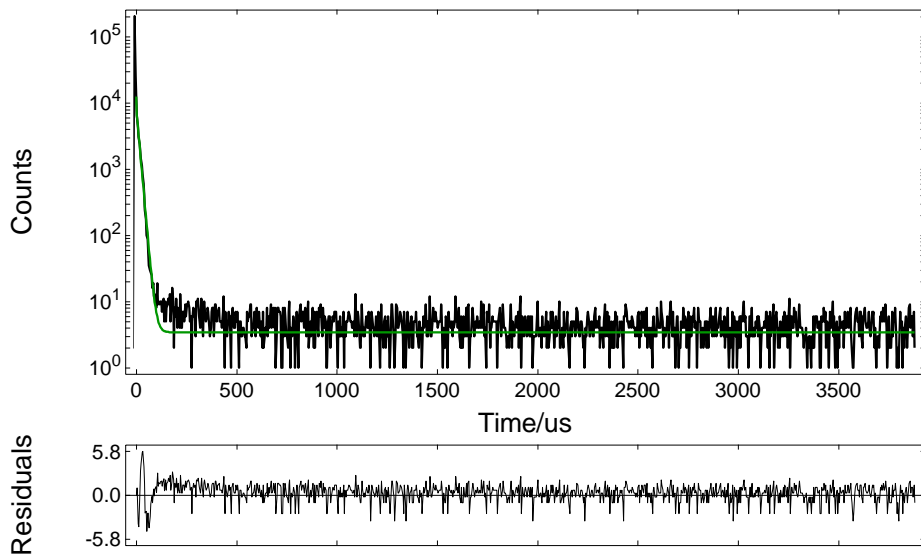
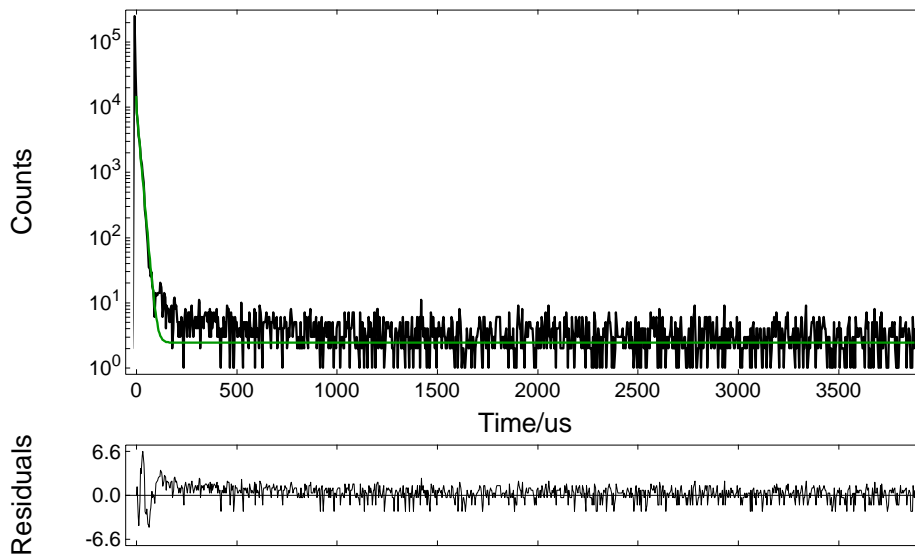


Figure 3.26 Decay response of PHACH₂ embedded PVC based nano fiber in presence of concentrated NH₃ medium exposed for 30 minutes



	Fix	Value / μ s	Std. Dev / μ s	Fix	Value	Std. Dev	Rel %
τ_1	<input checked="" type="checkbox"/>	1.6766	0.22077	B_1	44350.988	13431.4131	33.77
τ_2	<input checked="" type="checkbox"/>	12.8515	0.10518	B_2	11346.546	202.7252	66.23
τ_3	<input type="checkbox"/>			B_3			
τ_4	<input type="checkbox"/>			B_4			
				A	3.432		
$\chi^2 : 1.577$							

Figure 3.27 Decay response of PHACH₂ embedded PVC based nano fiber in presence of concentrated NH₃ medium exposed for 60 minutes



	Fix	Value / μ s	Std. Dev / μ s	Fix	Value	Std. Dev	Rel %
τ_1	<input type="checkbox"/>	1.9226	0.22403	B_1	<input type="checkbox"/>	36284.676	8365.1943
τ_2	<input type="checkbox"/>	12.4779	0.09571	B_2	<input type="checkbox"/>	14225.479	248.4590
τ_3	<input type="checkbox"/>			B_3	<input type="checkbox"/>		
τ_4	<input type="checkbox"/>			B_4	<input type="checkbox"/>		
				A	<input type="checkbox"/>	2.428	
$\chi^2 : 1.565$							

Figure 3.28 Decay response of PHACH₂ embedded PVC based nano fiber in presence of concentrated NH₃ medium exposed for 120 minutes

According to the data, the dye exhibited significant lifetime based response to NH₃ by time.

Table 3.14 shows the decay characteristics and chi square values of the studied composites in presence and absence of nano fiber forms.

Table 3.14 Summary of the decay characteristics and chi square values of the studied composites in presence and absence of nano fiber exposed to ammonia

Concentrated Ammonia steam media	τ_0 , (μs)	τ_{TEMPO} average	χ^2	τ_0/τ
0 min.	12.08±0.08 (98.38 %)	19.98	1.484	1
	500±98.38 (1.62%)			
30 min.	1.74±0.22 (32.13 %)	13.50	1.564	1.48
	12.86±0.11 (66.92 %)			
	456.19±83.61 (0.95 %)			
60 min.	1.68±0.22 (33.77 %)	9.08	1.577	2.20
	12.85±0.10 (66.23 %)			
120 min.	1.92±0.22 (28.21 %)	9.50	1.565	2.10
	12.48±0.1 (71.79 %)			

CHAPTER FOUR

ZnTPP (mesotetraphenylporphyrinato Zn(II)) BASED STUDIES

4.1 Introduction

The well-known ZnTPP dye along with THF has been utilized for optical chemical sensing of the nitric oxide. Structure of the ZnTPP dye were shown in Figure 4.1

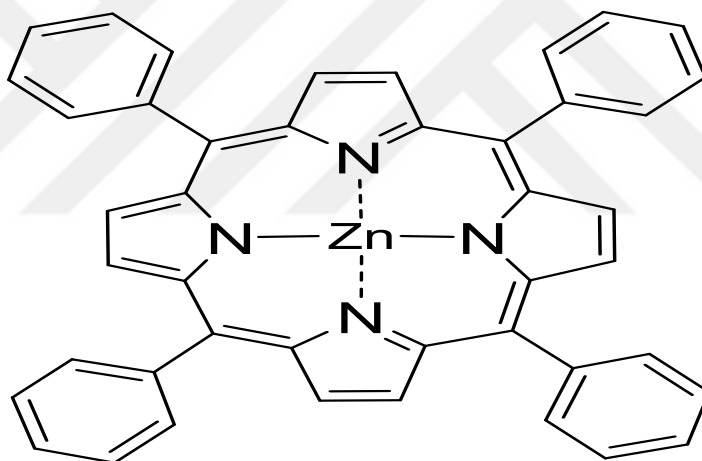


Figure 4.1 Structure of the ZnTPP dye

4.2 Spectral Characteristics of the ZnTPP Dye

Excitation and emission based spectral characteristics of the ZnTPP dye were recorded in THF solution in the absence of nitric oxide (Figure 4.2). When the ZnTPP dye was excited at 600 nm, it exhibited an emission spectrum in the wavelength range of 590-750 nm. There was seen emission maxima at 647 nm. The excitation spectrum was obtained for the emission wavelength of 650 nm. Two peak maxima were

observed at 550 and 590 nm. For further studies, 600 nm was chosen as excitation wavelength. The minimum Stoke's shift value was obtained as 60 nm. The absorption spectrum for ZnTPP dye in THF media was shown in Figure 4.3.

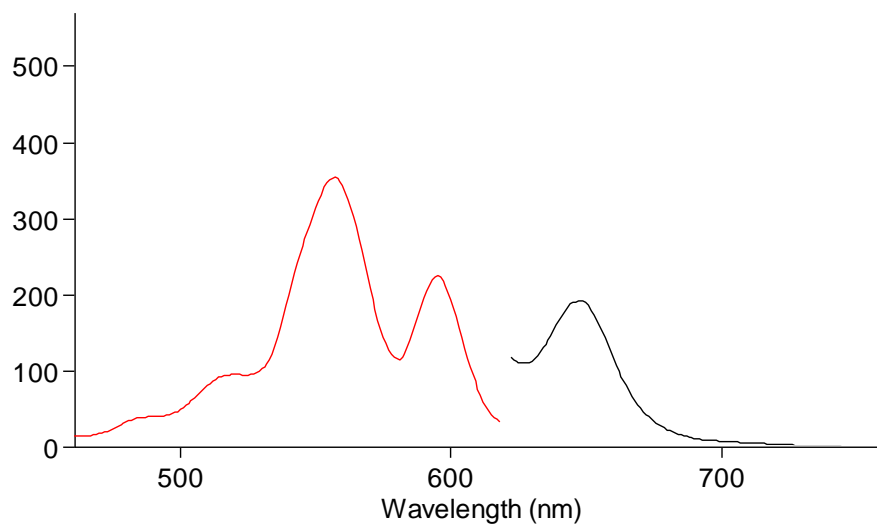


Figure 4.2 Excitation and emission spectral characteristics for ZnTPP dye in THF media

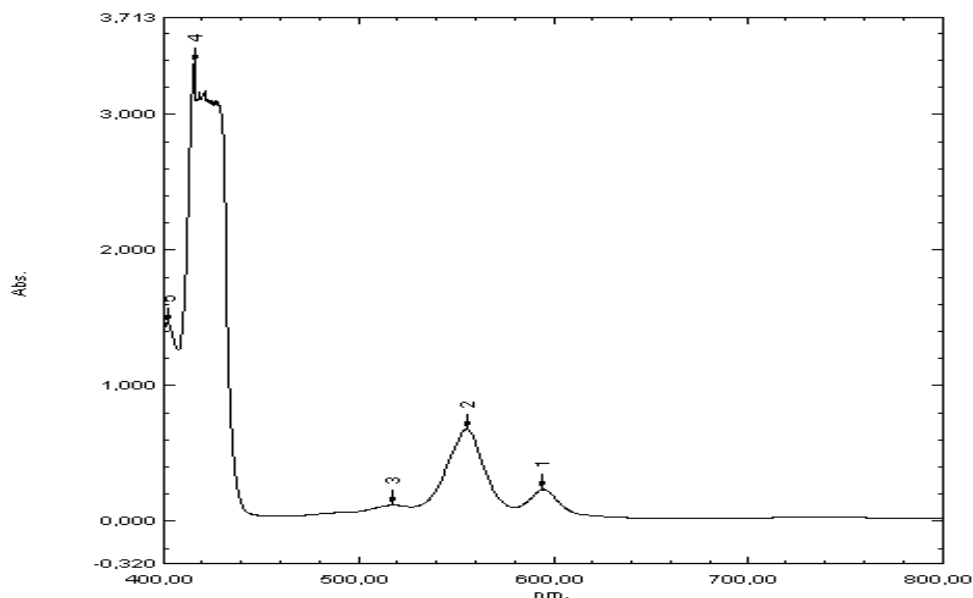


Figure 4.3 Absorption spectrum for the ZnTPP dye

4.3 Spectral Response of the ZnTPP Dye to TEMPO Radical

Emission based spectral response of the ZnTPP dye to TEMPO radical was investigated into detail.

Table 4.1 reveals spectral characteristics of the ZnTPP dye in THF media in presence and in absence of TEMPO radical. According to the data, no significant response was observed by the addition of TEMPO radical. The ZnTPP dye exhibited decreasing fluorescence intensity based response, while the concentrations of TEMPO radical was increased. The concerning data were shown in Table 4.2.

Table 4.1 Excitation and emission spectral characteristics of the ZnTPP dye

Dye	TEMPO (Mol L ⁻¹)	$\lambda_{\max}^{\text{ex}}$ (nm)	$\lambda_{\max}^{\text{em}}$ (nm)
ZnTPP in THF	-	550, 590	647
ZnTPP in THF	1.37×10^{-5}	580	645

Table 4.2 The fluorescence emission based data of ZnTPP dye to different TEMPO concentrations

Matrix: THF			
Dye: ZnTPP			
Concentration (Mol L ⁻¹)	I ₀ /I	I ₀	I
0	1	192.92	192.92
1.75×10 ⁻⁶	1.0243	192.92	188.35
4.08×10 ⁻⁶	1.0683	192.92	180.59
1.13×10 ⁻⁵	1.39152	192.92	138.64
1.37×10 ⁻⁵	1.5239	192.92	126.6

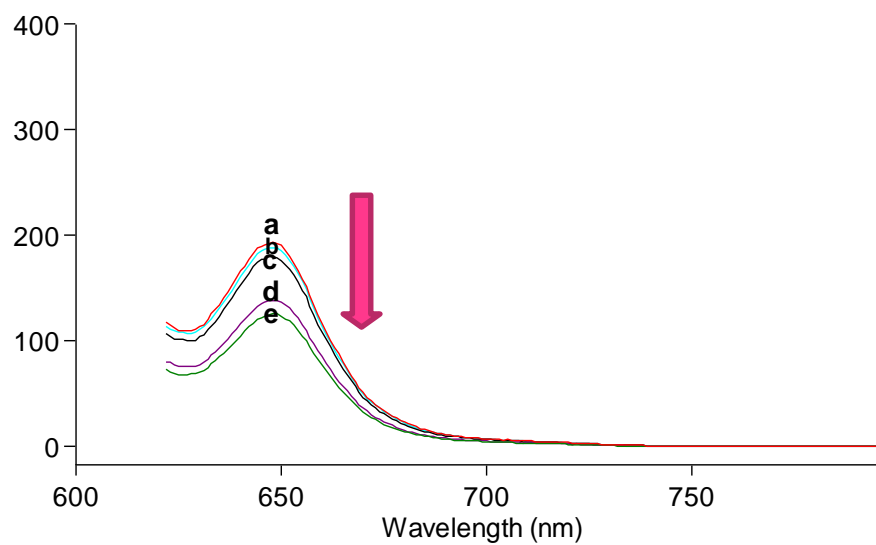


Figure 4.4 Fluorescence response of ZnTPP to different concentrations of TEMPO in THF media
 a) 0 Mol L⁻¹ b) 1.75×10⁻⁶ Mol L⁻¹ c) 4.08×10⁻⁶ Mol L⁻¹ d) 1.13×10⁻⁵ Mol L⁻¹ e) 1.37×10⁻⁵ Mol L⁻¹

Figure 4.4 also shows emission based response of ZnTPP to different concentrations of TEMPO in the range of 0-1.37×10⁻⁵ Mol L⁻¹.

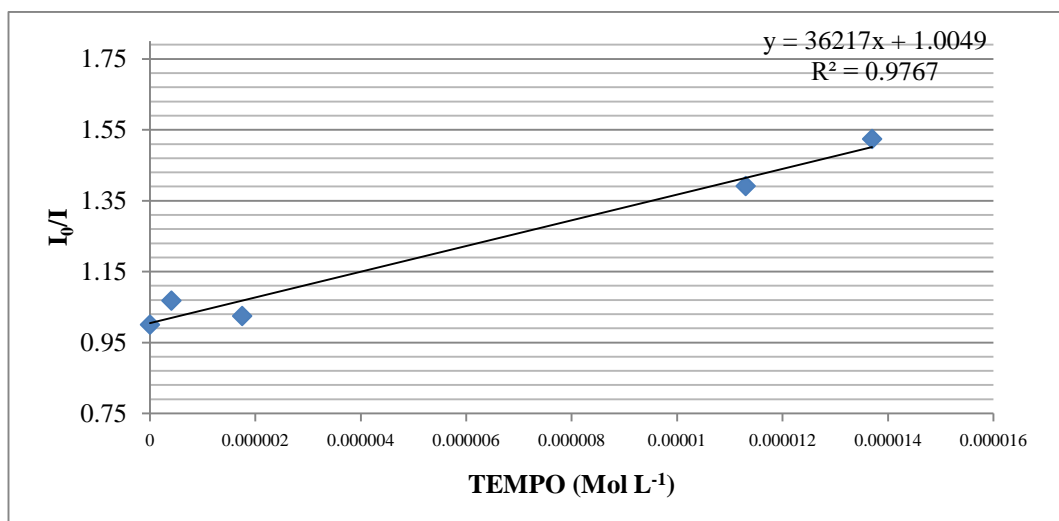
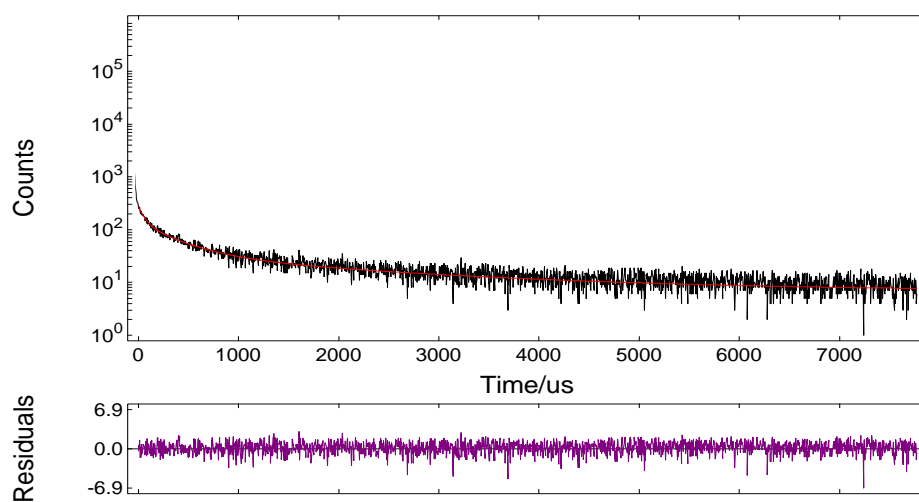


Figure 4.5 The calibration plot was drawn as I_0/I versus TEMPO concentrations for ZnTPP dye in THF solution

Figure 4.5 reveals the calibration plot (Stern Volmer plot) which was drawn as I_0/I versus TEMPO concentrations for ZnTPP dye in THF solution. The gathered equations of the Stern-Volmer plots(y) derived from the spectra, related regression coefficients and Stern-Volmer constants of all of the studied composites as well as THF media can be seen at Table 4.7.

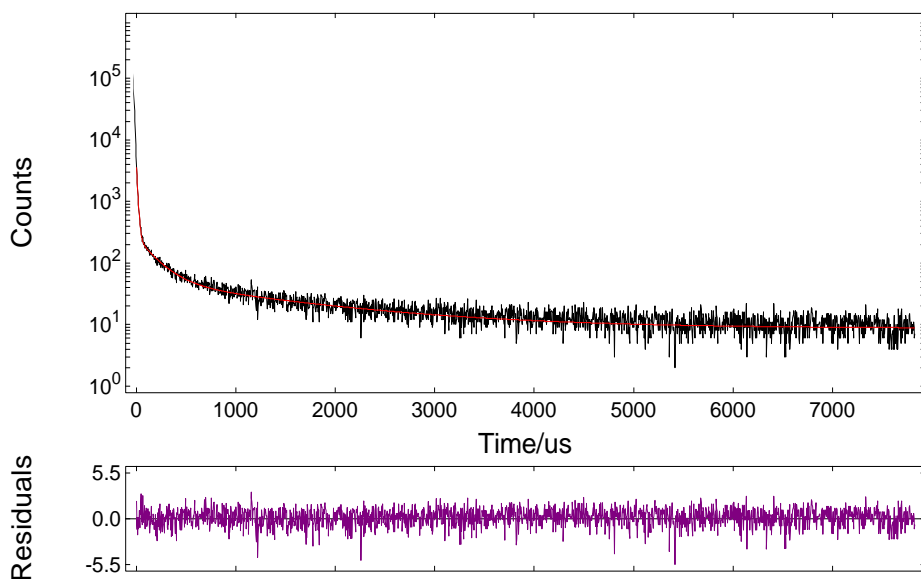
4.4 Lifetime Based Measurements in THF Media

The fluorescence lifetimes were recorded for the ZnTPP dye in THF media in absence and presence of different concentrations of TEMPO. The dye was excited with the microsecond flash lamp of the instrument at 600 nm. The excitation and emission slits were set to 5 nm. The figures 4.6 – 4.9 show the decay characteristics of the dye. Table 4.3 shows the variation of the lifetime ratio (τ_0/τ) in THF media. Table 4.4 gives a summary of the decay characteristics and chi square values of all studied concentrations. The Ksv constant was found as $3.6 \times 10^4 \mu\text{M}^{-1}$ and the quenching constant (k_q) was found as $25.5 \text{ M}^{-1} \text{ s}^{-1}$.



	Fix	Value / μs	Std. Dev / μs		Fix	Value	Std. Dev	Rel %
τ_1	<input type="checkbox"/>	60.6457	7.37400	B_1	<input type="checkbox"/>	143.261	9.5270	8.15
τ_2	<input type="checkbox"/>	357.6838	30.21757	B_2	<input type="checkbox"/>	99.450	6.8668	33.39
τ_3	<input type="checkbox"/>	2202.2449	207.83965	B_3	<input type="checkbox"/>	28.283	2.3645	58.46
τ_4	<input type="checkbox"/>			B_4	<input type="checkbox"/>			
				A	<input type="checkbox"/>	6.890		
$\chi^2 : 1.215$								

Figure 4.6 Decay response of ZnTPP in absence of TEMPO solution in THF media



	Fix	Value / μ s	Std. Dev / μ s	Fix	Value	Std. Dev	Rel %
τ_1	<input type="checkbox"/>	12.6995	0.20264	B_1	4545.721	76.8853	35.55
τ_2	<input type="checkbox"/>	184.7944	7.05975	B_2	214.230	6.8053	24.38
τ_3	<input type="checkbox"/>	1474.4325	57.61032	B_3	44.137	1.7871	40.07
τ_4	<input type="checkbox"/>			B_4			
				A	8.693		
$\chi^2 : 1.187$							

Figure 4.7 Decay response of ZnTPP in the presence of 2 μ l (2.56×10^{-8} Mol L⁻¹) TEMPO in THF media

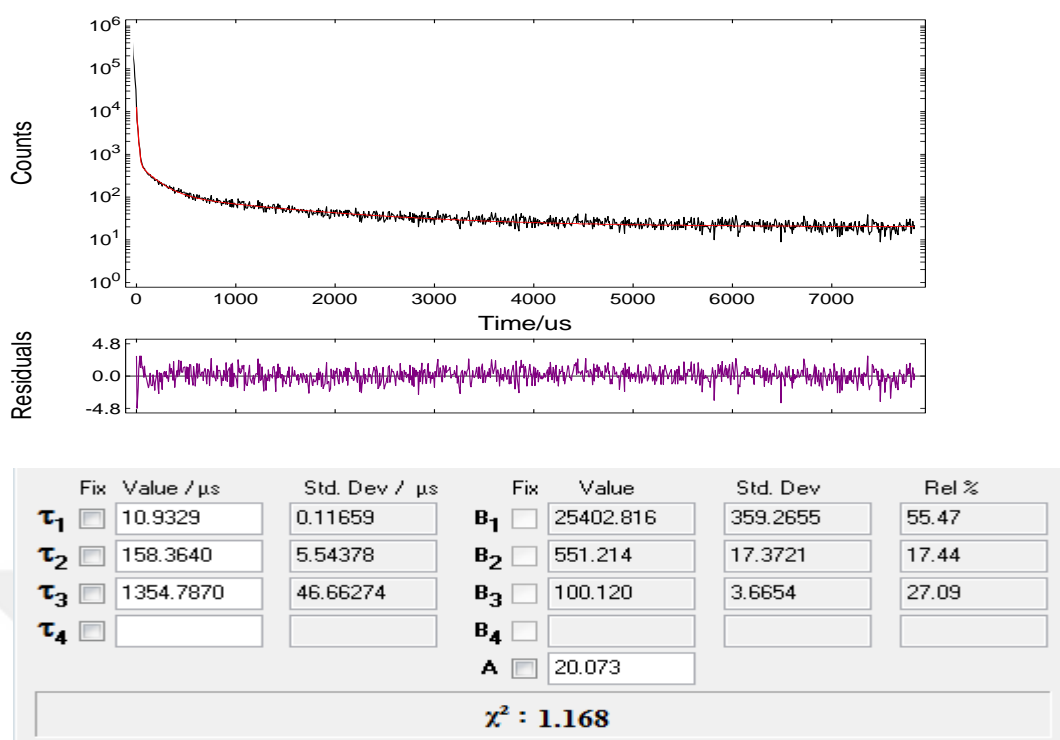


Figure 4.8 Decay response of ZnTPP in the presence of 6 μl ($7.68 \times 10^{-8} \text{ Mol L}^{-1}$) TEMPO in THF media

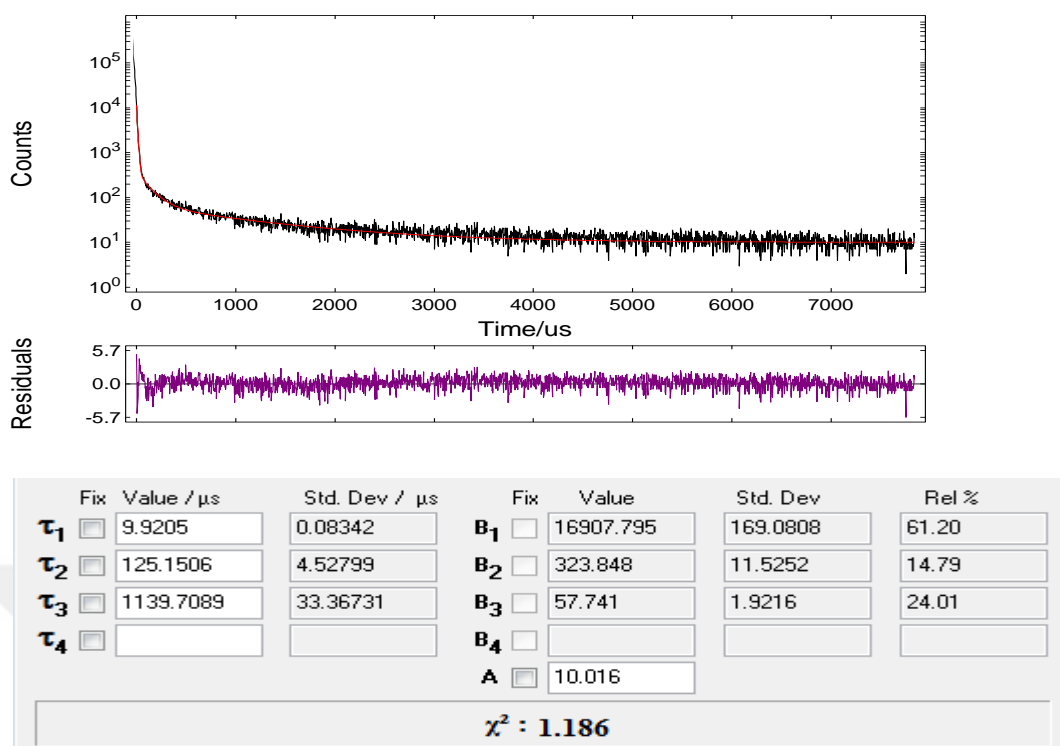


Figure 4.9 Decay response of ZnTPP in the presence of 12 μl (1.53×10^{-7} Mol L^{-1}) TEMPO in THF media

Table 4.3 The variation of the lifetime values for different TEMPO concentrations in THF

Matrix: THF			
Dye: ZnTPP			
Concentration (Mol L ⁻¹)	τ_0/τ	τ_0	τ
0	1	1412	1412
2.56×10^{-8}	2.2121	1412	638.32
7.68×10^{-8}	3.5397	1412	398.9
1.53×10^{-7}	4.7351	1412	298.2
K _{sv}	3.6×10^4		
K _q	25.5		

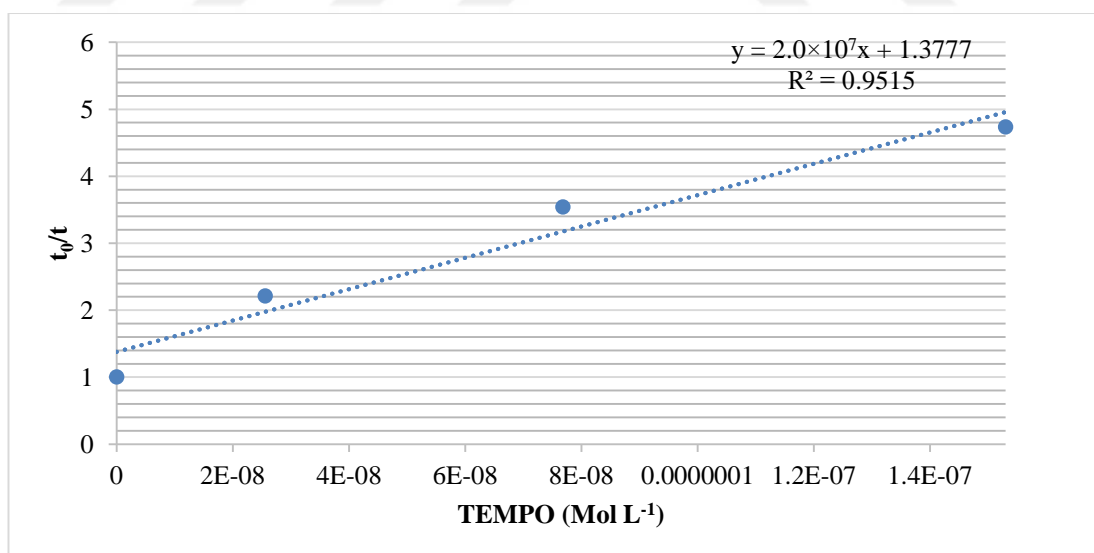


Figure 4.10 Variations of the lifetime ratio (τ_0/τ) of ZnTPP versus quencher (TEMPO) concentrations in THF media

Figures 4.6-4.9 reveals that the ZnTPP dye also exhibited decreasing fluorescence lifetime based response which is the sign of dynamic quenching.

Table 4.4 Summary of the decay characteristics and chi square values of the studied composites in presence and absence of TEMPO in THF media

TEMPO ($\mu\text{Mol L}^{-1}$)	τ_0 , (μs)	τ_{TEMPO} (average)	χ^2	τ_0/τ	K_{sv} [TEMPO] $^{-1}$ (μM^{-1})	k_q ($\text{M}^{-1}\text{s}^{-1}$)
0	60.64 \pm 7.37 (8.15 %)	1411.5	1.215	1	3.6 \times 10 ⁴	25.5
	357.68 \pm 30.21 (33.39 %)					
	2202.24 \pm 207.83(58.46%)					
2.56 \times 10 ⁻⁸	12.69 \pm 0.2 (35.55 %)	638.32	1.187	2.21	3.6 \times 10 ⁴	25.5
	184.79 \pm 7.05 (24.38 %)					
	1474.43 \pm 57.61(40.07%)					
7.68 \times 10 ⁻⁸	10.93 \pm 0.11 (55.47 %)	398.9	1.168	3.54	3.6 \times 10 ⁴	25.5
	158.36 \pm 5.54 (17.44 %)					
	1354.78 \pm 46.66(27.09%)					
1.53 \times 10 ⁻⁷	9.92 \pm 0.08 (61.2 %)	298.2	1.186	4.73	3.6 \times 10 ⁴	25.5
	125.15 \pm 4.52 (14.79 %)					
	1339.70 \pm 33.36(24.01%)					

4.5 Spectral Characteristics of the ZnTPP Dye in PVC matrix

The response of PVC encapsulated ZnTPP dye either in thin film form has been studied in SDS solution prepared in phosphate buffer at pH 7.4. The prepared cocktail composition containing the indicator and the additives was shown in Table 4.5

Table 4.5 Cocktail compositions for thin film sensing probes

	Matrix (PVC)	Plasticizer (DOP)	Dye Solution ZnTPP	Ionic Liquid [BMIM ⁺] [PF ₆ ⁻]	Solvent (SDS)
Thin film	120 mg	240 mg	50 μ L	-	2.5 mL

In all of the test moieties the ZnTPP dye exhibited two emission maxima around 658 and 720 nm. Table 4.6 reveals spectral characteristics of the embedded ZnTPP dye in SDS media at pH 7.4. The excitation has been performed at 350 nm. The Stoke's shift was calculated as 43 nm. Emission reduction wasn't observed when the emission-based response at 393 nm was exposed to increasing concentrations of TEMPO. Table 4.7 contains the gathered data of Stern-Volmer equations, regression coefficients and Stern-Volmer constants of all of the studied composites. The best Stern-Volmer constant for TEMPO was obtained for THF media.

Table 4.6 Excitation and emission spectral characteristics of the ZnTPP dye

Dye	Matrix	Thin Film	Solvent	$\lambda_{\max}^{\text{ex}}$ (nm)	$\lambda_{\max}^{\text{em}}$ (nm)	Stoke's Shift ($\Delta\lambda$) (nm)
ZnTPP	PVC	+	pH 7.4 buffer in SDS	350	393	43



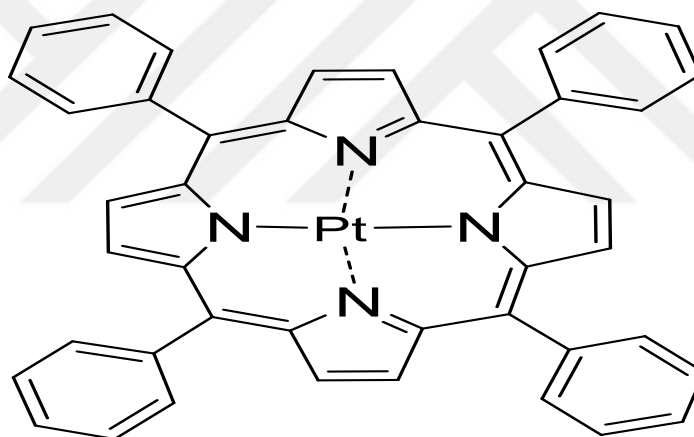
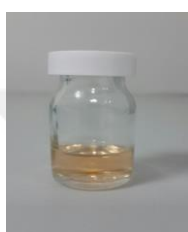
Table 4.7 The Stern-Volmer equations, regression coefficients and Stern-Volmer constants of all of the studied composites

Dye	Matrix	Thin Film	TEMPO	SOLVENT	Stern-Volmer Plots	Regression Coefficient
ZnTPP	THF	-	+	THF	$y = 36217x + 1.0049$	0.976
ZnTPP	PVC	TF	+	pH 7.4 Buffer in SDS	-	-

CHAPTER FIVE
TPPPt(II) (mesotetraphenylporphyrinato Pt(II))
BASED STUDIES

5.1 Introduction

The well-known TPPPt(II) dye along with THF has been utilized for optical chemical sensing of the nitric oxide. Structure of the TPPPt(II) dye were shown in Figure 5.1



peak maxima were observed at 420 and 510 nm. For further studies, 510 nm was chosen as excitation wavelength. The minimum Stoke's shift value was obtained as 140 nm. The absorption spectrum for TPPPt(II) dye in THF media was shown in Figure 5.3

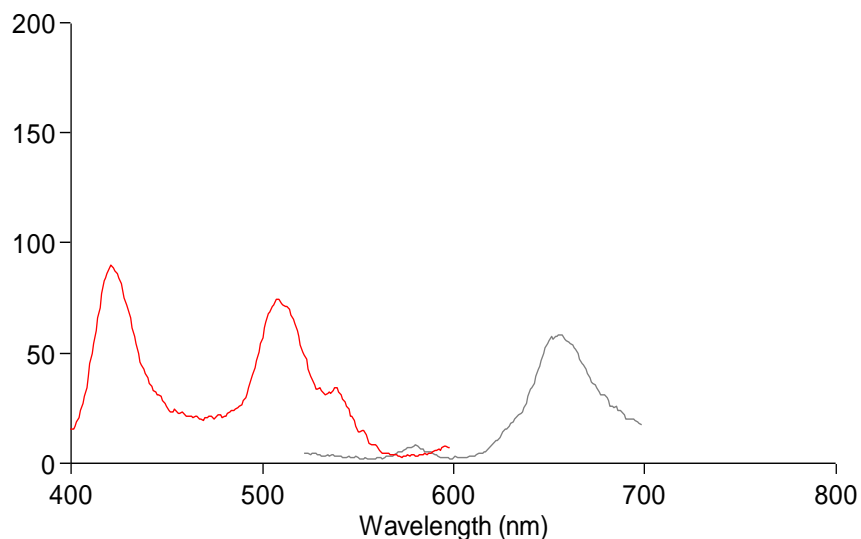


Figure 5.2 Excitation and emission spectral characteristics for TPPPt(II) dye in THF media

In all of the test moieties the TPPPt(II) dye exhibited excitation and emission maxima around 510 nm and 655 nm respectively. The average Stoke's shift was 155 nm.

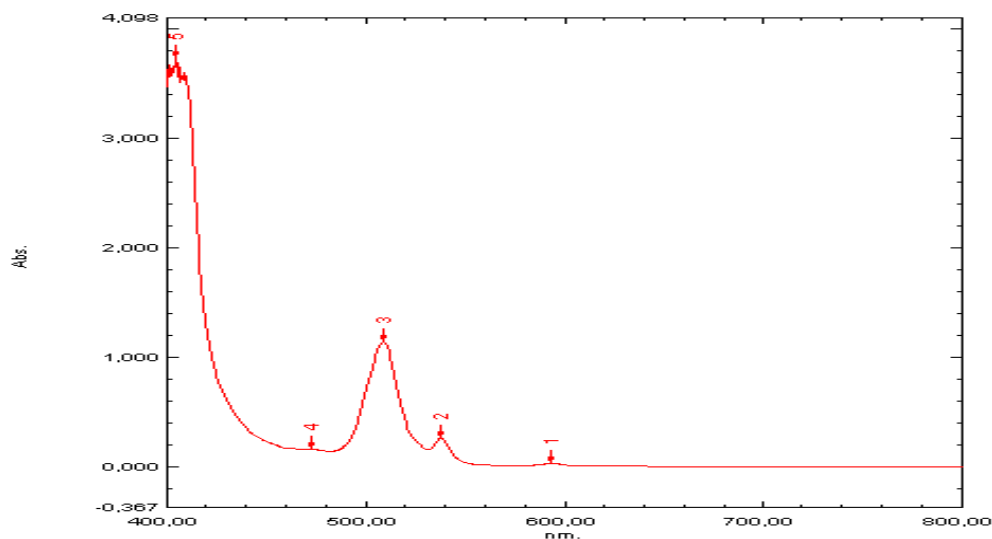


Figure 5.3 Absorption spectrum for TPPPt(II) dye in THF media

5.3 Spectral Response of the TPPPt(II) Dye to TEMPO Radical

Emission based spectral response of the TPPPt(II) dye to TEMPO radical was investigated into detail.

Table 5.1 reveals spectral characteristics of the TPPPt(II) dye in THF media in presence and in absence of TEMPO radical. According to the data, no significant response was observed by the addition of TEMPO radical. The TPPPt(II) dye wasn't exhibited decreasing fluorescence intensity based response, while the concentrations of TEMPO radical increased.

Table 5.1 Excitation and emission spectral characteristics of the TPPPt(II) dye

Dye	TEMPO (mol L ⁻¹)	$\lambda_{\max}^{\text{ex}}$ (nm)	$\lambda_{\max}^{\text{em}}$ (nm)
TPPPt(II) in THF	-	510	655
TPPPt(II) in THF	2.56×10^{-5}	505	650

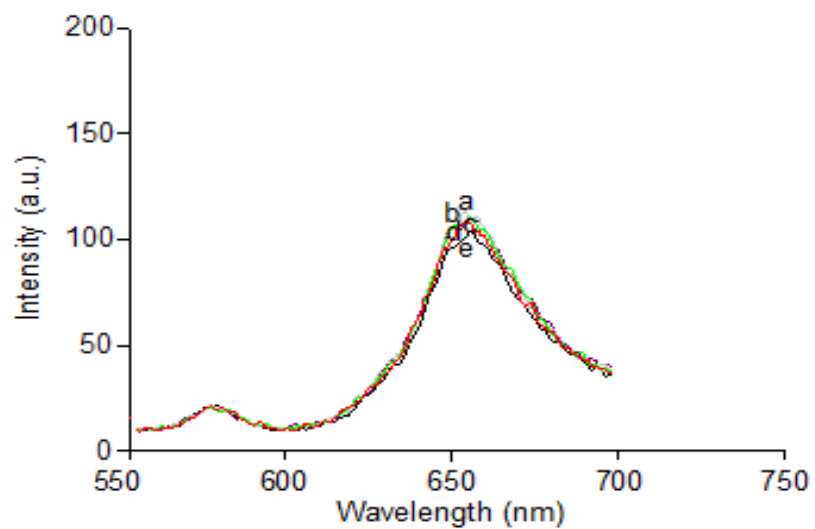


Figure 5.4 Fluorescence response of TPPPt(II) to different concentrations of TEMPO in THF media
 a) 0 Mol L⁻¹ b) 1.27×10^{-7} Mol L⁻¹ c) 2.54×10^{-7} Mol L⁻¹ d) 1.7×10^{-6} Mol L⁻¹ e) 2.56×10^{-5} Mol L⁻¹

Figure 5.4 also shows emission based response of TPPPt(II) to different concentrations of TEMPO in the range of 0- 2.56×10^{-5} mol L⁻¹. The Stern Volmer plot plotted as I_0/I versus TEMPO concentrations for TPPPt(II) dye in THF solution did not reach the desired result.

5.4 Lifetime Based Measurements in THF Media

The fluorescence lifetimes were recorded for the TPPPt(II) dye in THF media in absence and presence of different concentrations of TEMPO. The dye was excited with the microsecond flash lamp of the instrument at 510 nm. The excitation and emission slits were set to 5 nm. The figures 5.5 – 5.8 show the decay characteristics of the dye. Table 5.2 shows the variation of the lifetime ratio (τ_0/τ) in THF media. Table 5.3 gives a summary of the decay characteristics and chi square values of all studied concentrations. The Ksv constant was found as 5.79×10^5 and the quenching constant (k_q) was found as $8.47 \times 10^2 \text{ M}^{-1} \text{ s}^{-1}$

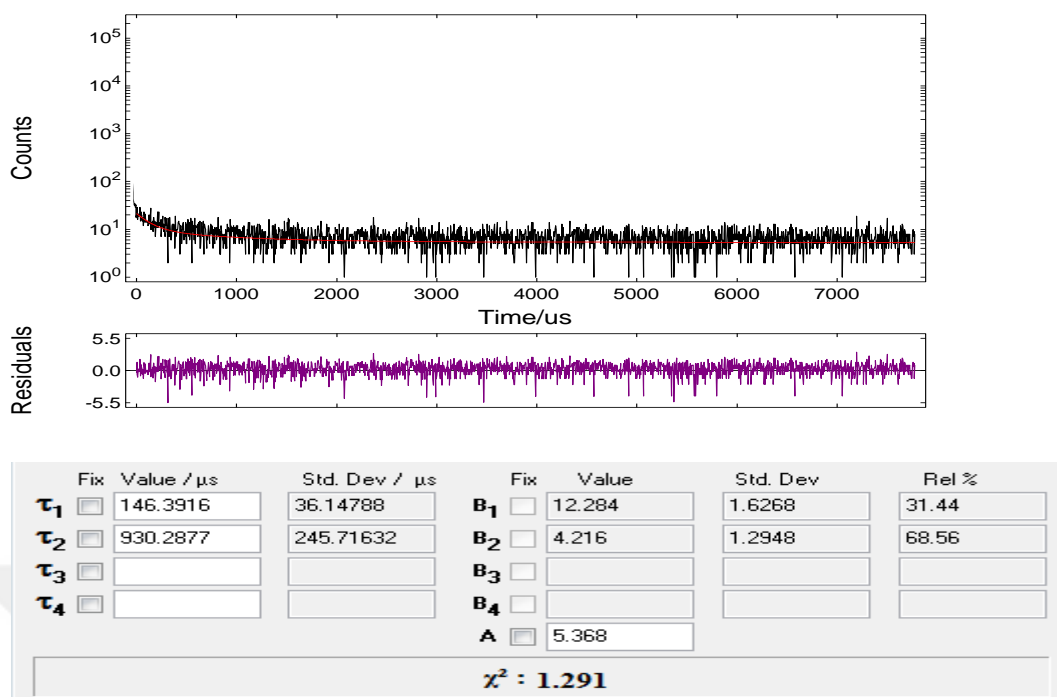
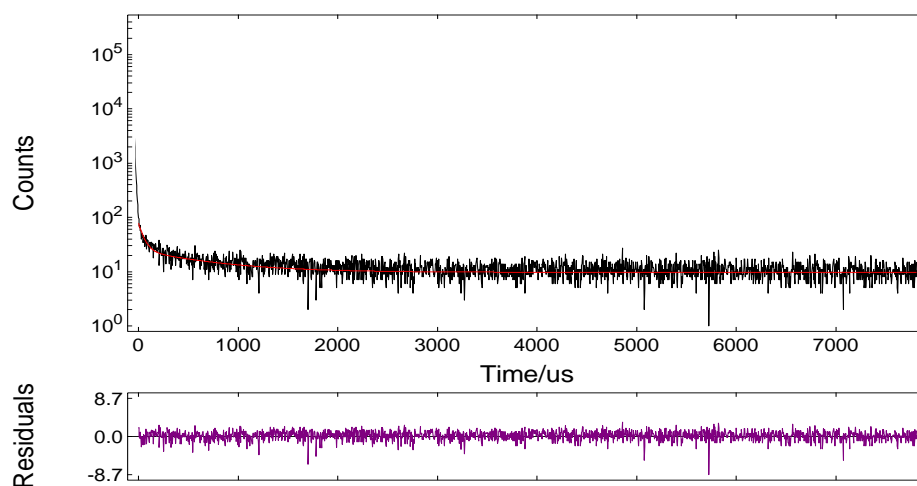
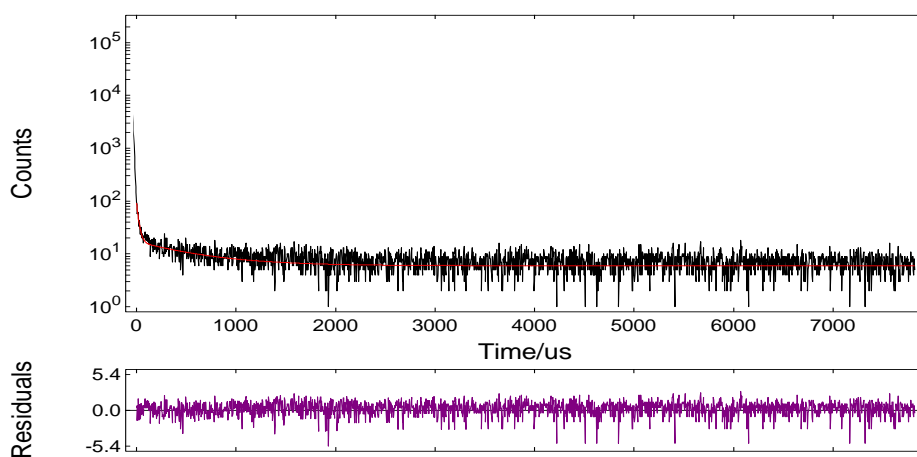


Figure 5.5 Decay response of TPPPt(II) in absence of TEMPO solution in THF media



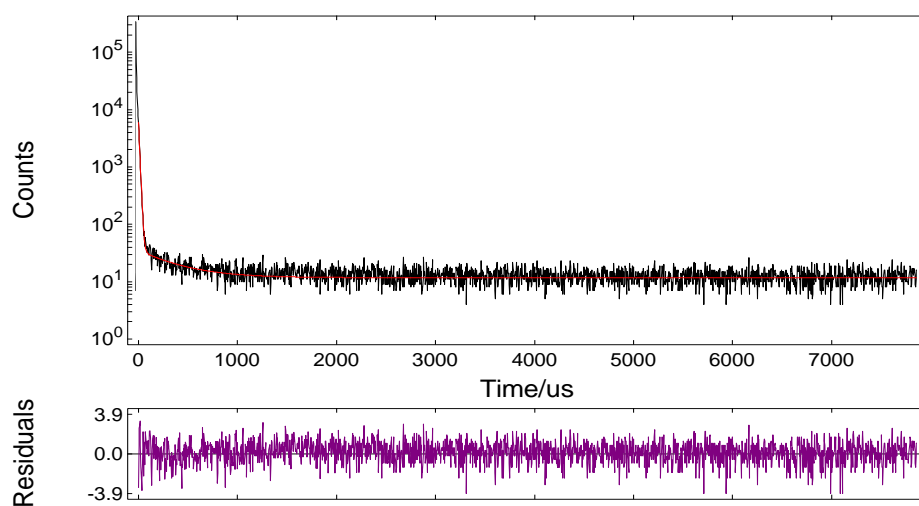
	Fix	Value / μs	Std. Dev / μs	Fix	Value	Std. Dev	Rel %
τ_1	<input type="checkbox"/>	52.0747	6.42203	B_1	<input type="checkbox"/> 57.408	5.0484	21.93
τ_2	<input type="checkbox"/>	702.1494	57.11784	B_2	<input type="checkbox"/> 15.153	1.1888	78.07
τ_3	<input type="checkbox"/>			B_3	<input type="checkbox"/>		
τ_4	<input type="checkbox"/>			B_4	<input type="checkbox"/>		
				A	<input type="checkbox"/> 9.701		
$\chi^2 : 1.199$							

Figure 5.6 Decay response of TPPPt(II) in presence of 10 μl (1.27×10^{-7} Mol L⁻¹) TEMPO in THF media



	Fix	Value / μs	Std. Dev / μs	Fix	Value	Std. Dev	Rel %
τ_1	<input type="checkbox"/>	21.5205	2.17345	B_1	<input type="checkbox"/>	90.215	22.67
τ_2	<input type="checkbox"/>	585.0499	47.53305	B_2	<input type="checkbox"/>	11.323	77.33
τ_3	<input type="checkbox"/>			B_3	<input type="checkbox"/>		
τ_4	<input type="checkbox"/>			B_4	<input type="checkbox"/>		
				A	<input type="checkbox"/>	5.967	
$\chi^2 : 1.226$							

Figure 5.7 Decay response of TPPPt(II) in presence of 20 μl (2.54×10⁻⁷ Mol L⁻¹) TEMPO in THF media



	Fix	Value / μ s	Std. Dev / μ s	Fix	Value	Std. Dev	Rel %
τ_1	<input type="checkbox"/>	10.8447	0.08905	B_1	8603.179	100.9672	91.26
τ_2	<input type="checkbox"/>	376.2350	25.01211	B_2	23.736	1.5010	8.74
τ_3	<input type="checkbox"/>			B_3			
τ_4	<input type="checkbox"/>			B_4			
				A	11.734		
$\chi^2 : 1.183$							

Figure 5.8 Decay response of TPPPt(II) in presence of 1000 μ l (2.56×10^{-5} Mol L⁻¹) TEMPO in THF media

Table 5.2 The variation of the lifetime values for different TEMPO concentrations in THF

Matrix: THF			
Dye: TPPPt(II)			
Concentration (Mol L ⁻¹)	τ_0/τ	τ_0	τ
0	1	683.83	683.83
1.27×10^{-7}	1.2220	683.83	559.59
2.54×10^{-7}	1.4954	683.83	457.3
2.56×10^{-5}	15.9885	683.83	42.77
K _{sv}	5.79×10^5		
K _q	8.47×10^2		

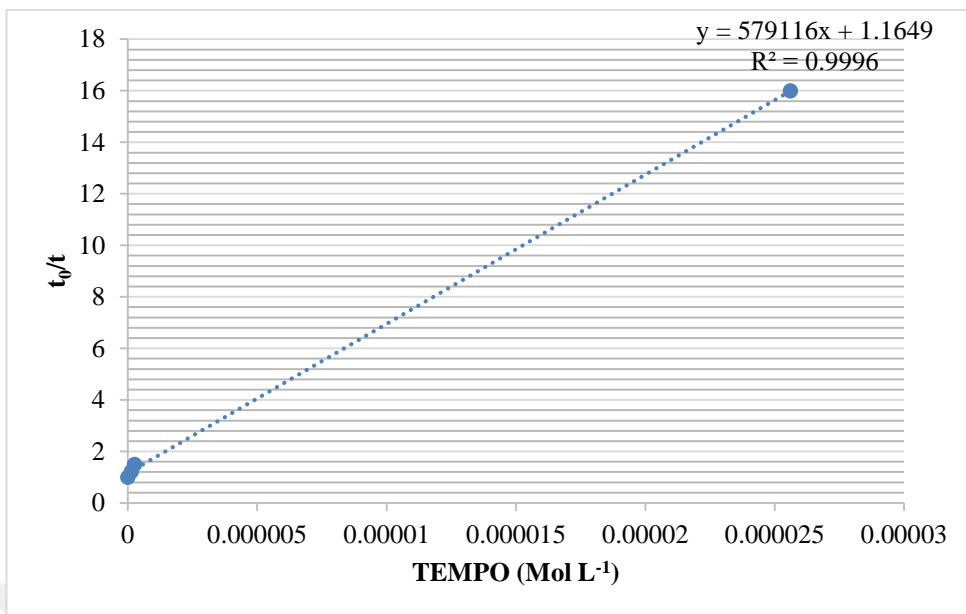


Figure 5.9 Variations of the lifetime ratio (τ_0/τ) of TPPPt(II) versus quencher (TEMPO) concentrations in THF media

Figures 5.5-5.8 reveals that the TPPPt(II) dye also exhibited decreasing fluorescence lifetime based response which is the sign of dynamic quenching.

Table 5.3 Summary of the decay characteristics and chi square values of the studied composites in presence and absence of TEMPO in THF media

TEMPO ($\mu\text{Mol L}^{-1}$)	τ_0 , (μs)	τ_{TEMPO} average	χ^2	τ_0/τ	K_{sv} [TEMPO] $^{-1}$ (μM^{-1})	k_q ($\text{M}^{-1}\text{s}^{-1}$)
0	146.39 \pm 36.14 (31.44 %)	683.83	1.291	1	5.79×10^5	8.47×10^2
	930.28 \pm 245.71 (68.56%)					
1.27×10^{-1}	52.07 \pm 6.42 (21.93 %)	559.59	1.199	1.22	5.79×10^5	8.47×10^2
	702.14 \pm 57.11 (78.07 %)					
2.54×10^{-1}	21.52 \pm 2.17 (22.67 %)	457.3	1.226	1.49	5.79×10^5	8.47×10^2
	585.04 \pm 47.53 (77.33 %)					
25.6	10.84 \pm 0.08 (91.26 %)	42.77	1.183	15.98	5.79×10^5	8.47×10^2
	376.23 \pm 25.01 (8.74 %)					

5.5 Spectral Characteristics of the TPPPt(II) Dye in PVC Matrix

The response of PVC encapsulated TPPPt(II) dye either in thin film and in nano-fiber form has been studied in SDS solution prepared in phosphate buffer at pH 7.4. The prepared cocktail composition containing the indicator and the additives was shown in Table 5.4

Table 5.4 Cocktail compositions for thin film and nano-fiber sensing probes

	Matrix (PVC)	Plasticizer (DOP)	Dye Solution ZnTPP	Ionic Liquid [BMIM ⁺] [PF ₆ ⁻]	Solvent (SDS)
Thin film / nano-fiber	120 mg	240 mg	50 μ L	-	2.5 mL

In all of the test moieties the TPPPt(II) dye exhibited emission maxima around 658 and 740 nm. Table 5.5 reveals spectral characteristics of the embedded TPPPt(II) dye in SDS media at pH 7.4. The excitation has been performed at 404 nm. The Stoke's shift was calculated as 254 nm. Emission based response at 658 nm decreased upon exposure to the increasing concentrations of the TEMPO. Table 3.7 contains the fluorescence intensities for nanofiber forms in pH 7.4 buffered SDS media at different TEMPO concentrations.

Table 5.5 Excitation and emission spectral characteristics of the TPPPt(II) dye

Dye	Matrix	Thin Film/ Nano fiber	Solvent	$\lambda_{\max}^{\text{ex}}$ (nm)	$\lambda_{\max}^{\text{em}}$ (nm)	Stoke's Shift ($\Delta\lambda$) (nm)
TPPPt(II)	PVC	+/+	Ph 7.4 buffer in SDS	404	658	254

It was seen that a linear graph could not be created in Stern Volmer studies of the thin films performed in pH 7.4 buffered SDS in the studied TEMPO concentration range. This can be attributed to the inefficient diffusion of TEMPO through PVC membrane which is obtained by manual knife coating method.

In the case of nano-fibers, the dye exhibited a decrease in signal intensity at 658 nm when exposed to TEMPO. In Figure 5.10 emission based response of TPPPt(II) to different concentrations of TEMPO in the range of 0- 3.79×10^{-7} Mol L⁻¹ was shown. In Figure 5.11, the calibration plot and related equation were also shown.

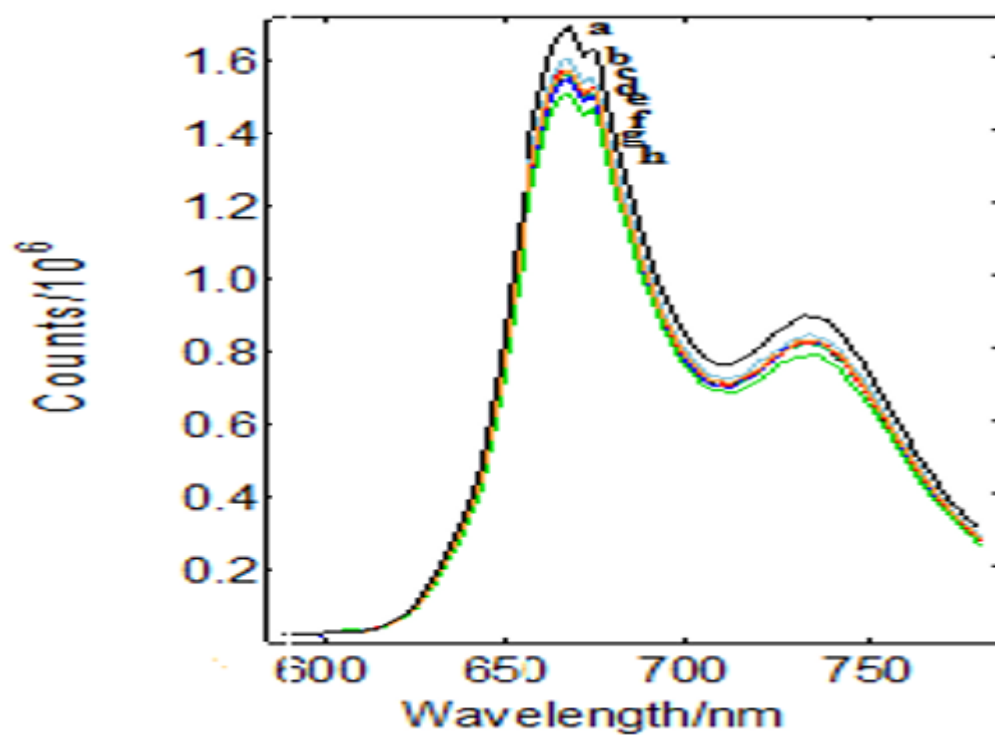


Figure 5.10 Fluorescence intensity based response of TPPPt(II) in nanofiber form to TEMPO concentrations in pH 7.4 buffered SDS media a) 0 Mol L⁻¹ b) 5.12×10^{-9} Mol L⁻¹ c) 1.02×10^{-9} Mol L⁻¹ d) 1.54×10^{-8} Mol L⁻¹ e) 2.56×10^{-8} Mol L⁻¹ f) 5.12×10^{-8} Mol L⁻¹ g) 1.27×10^{-7} Mol L⁻¹ h) 3.79×10^{-7} Mol L⁻¹

Table 5.6 The fluorescence intensities for nanofiber forms in pH 7.4 buffered SDS media at different TEMPO concentrations

Matrix: SDS			
Dye: TPPPt(II)			
Concentration (Mol L ⁻¹)	I ₀ /I	I ₀	I
0	1.0000	1.69×10 ⁶	1.69×10 ⁶
1.02×10 ⁻⁸	1.0563	1.69×10 ⁶	1.60×10 ⁶
1.54×10 ⁻⁸	1.1267	1.69×10 ⁶	1.50×10 ⁶

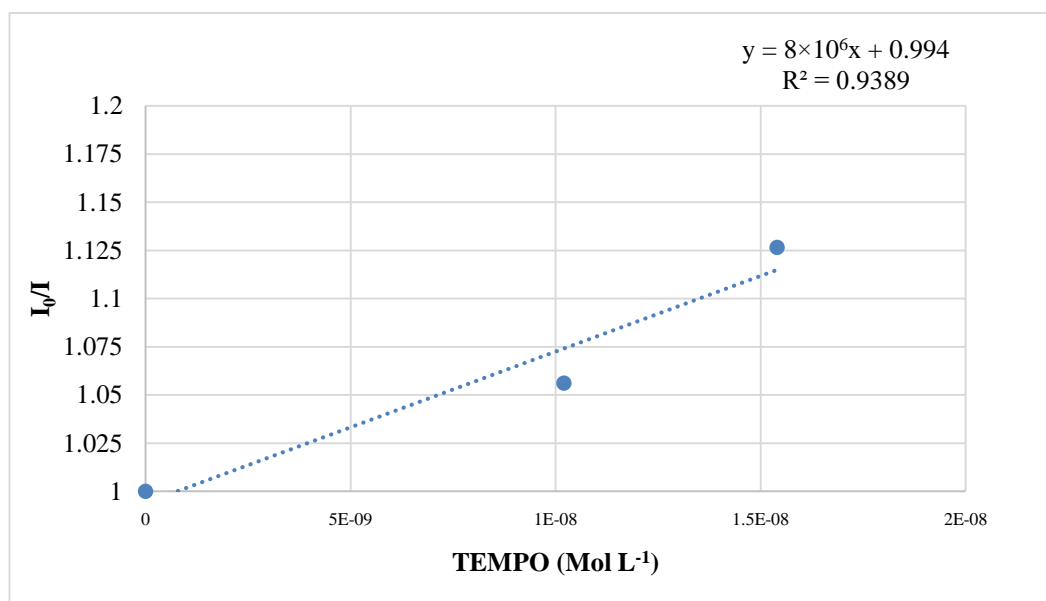


Figure 5.11 The calibration plot for TPPPt(II) nanofiber form in pH 7.4 buffered SDS media

Table 5.7 The Stern-Volmer plots, regression coefficients and Stern-Volmer constants of all of the studied composites

Dye	Matrix	Thin Film/ Nano fiber	TEMPO	SOLVENT	Stern-Volmer plots	Regression Coefficient
TPPPt (II)	THF	-	+	THF	-	-
TPPPt (II)	PVC	Thin film	+	Ph 7.4 Buffer in SDS	-	-
TPPPt (II)	PVC	Nano fiber	+	Ph 7.4 Buffer in SDS	$y = 8 \times 10^6 x + 0.994$	0.9389

5.6 Lifetime Based Measurements of Embedded Forms

The fluorescence lifetimes were recorded for PVC forms of the TPPPt(II) dye. The Figures between 5.12 – 5.14 show decay characteristics of the encapsulated dyes in buffered solutions in the absence and presence of the TEMPO. Table 5.8 show the variation of the lifetime ratio (τ_0/τ) of TPPPt(II) versus quencher (TEMPO) concentration in pH 7.4 buffer media. Table 5.9 gives a summary of the decay characteristics and chi square values of the studied composites



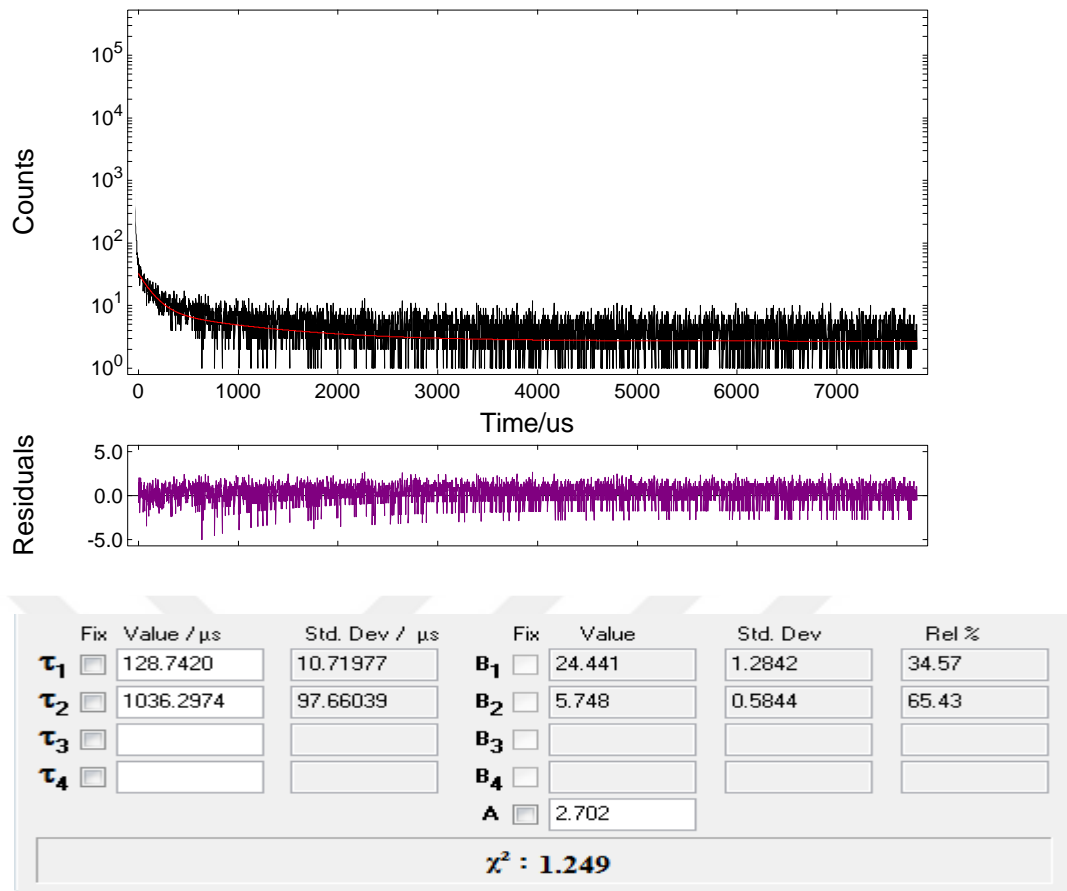


Figure 5.12 Decay response of TPPPt(II) embedded PVC based thin film with in pH 7.4 buffer SDS media without TEMPO solution

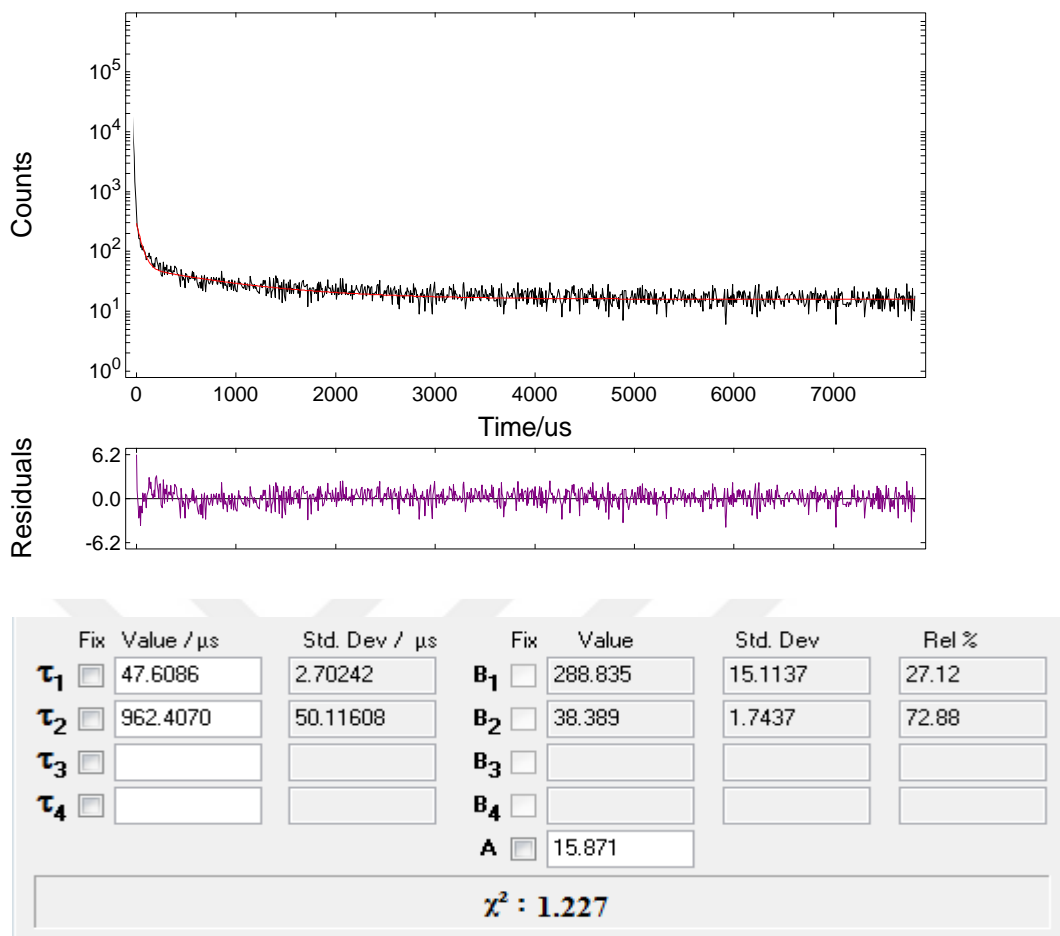
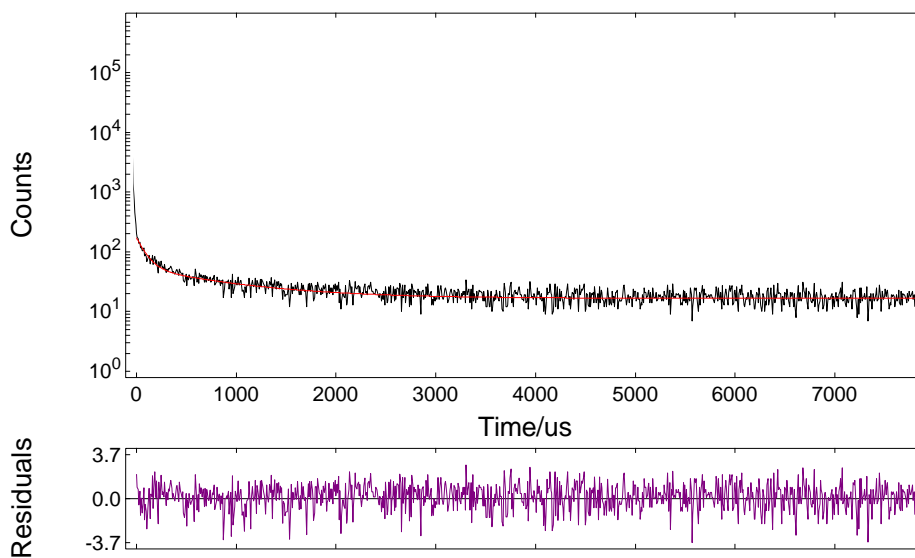


Figure 5.13 Decay response of TPPPt(II) embedded PVC based thin film in the presence of 3 μl ($3.84 \times 10^{-8} \text{Mol L}^{-1}$) TEMPO in pH 7.4 buffer in SDS media



	Fix	Value / μ s	Std. Dev / μ s	Fix	Value	Std. Dev	Rel %	
τ_1	<input type="checkbox"/>	91.8072	8.18060	B_1	<input type="checkbox"/>	129.922	7.8120	25.50
τ_2	<input type="checkbox"/>	908.8336	58.89028	B_2	<input type="checkbox"/>	38.339	2.5860	74.50
τ_3	<input type="checkbox"/>			B_3	<input type="checkbox"/>			
τ_4	<input type="checkbox"/>			B_4	<input type="checkbox"/>			
				A	<input type="checkbox"/>	16.600		
$\chi^2 : 1.203$								

Figure 5.14 Decay response of TPPPt(II) embedded PVC based thin film in the presence of 7 μ l ($8.96 \times 10^{-8} \text{Mol L}^{-1}$) TEMPO in pH 7.4 buffer in SDS media

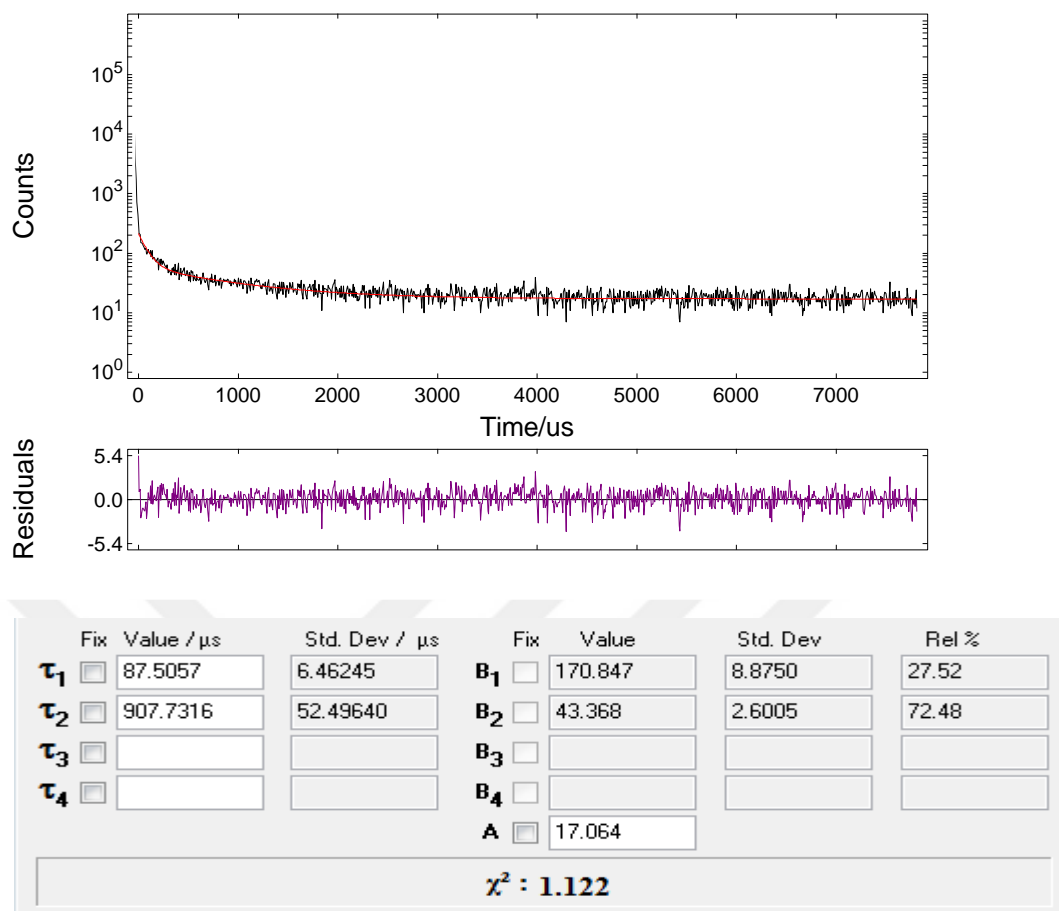


Figure 5.15 Decay response of TPPPt(II) embedded PVC based thin film in the presence of 13 μl ($1.66 \times 10^{-7} \text{Mol L}^{-1}$) TEMPO in pH 7.4 buffer in SDS media

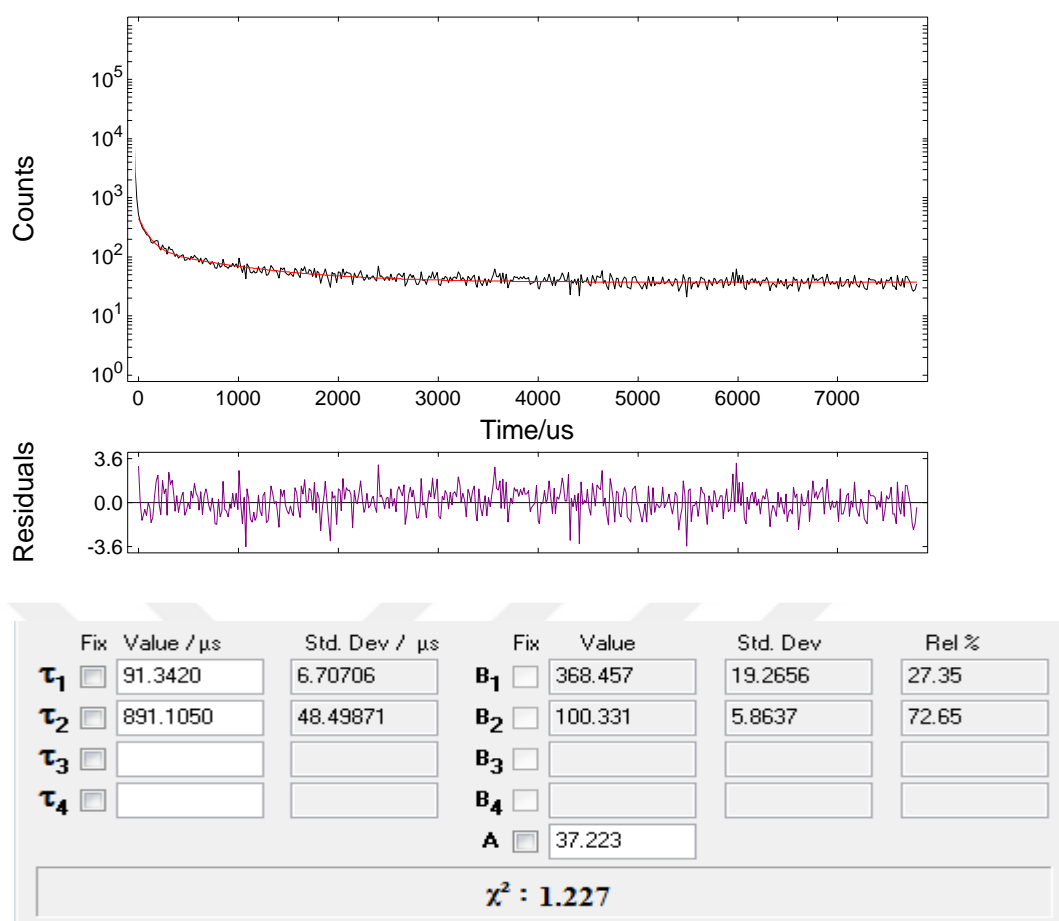


Figure 5.16 Decay response of TPPPt(II) embedded PVC based thin film in the presence of 25 μl ($3.17 \times 10^{-7} \text{ Mol L}^{-1}$) TEMPO in pH 7.4 buffer in SDS media

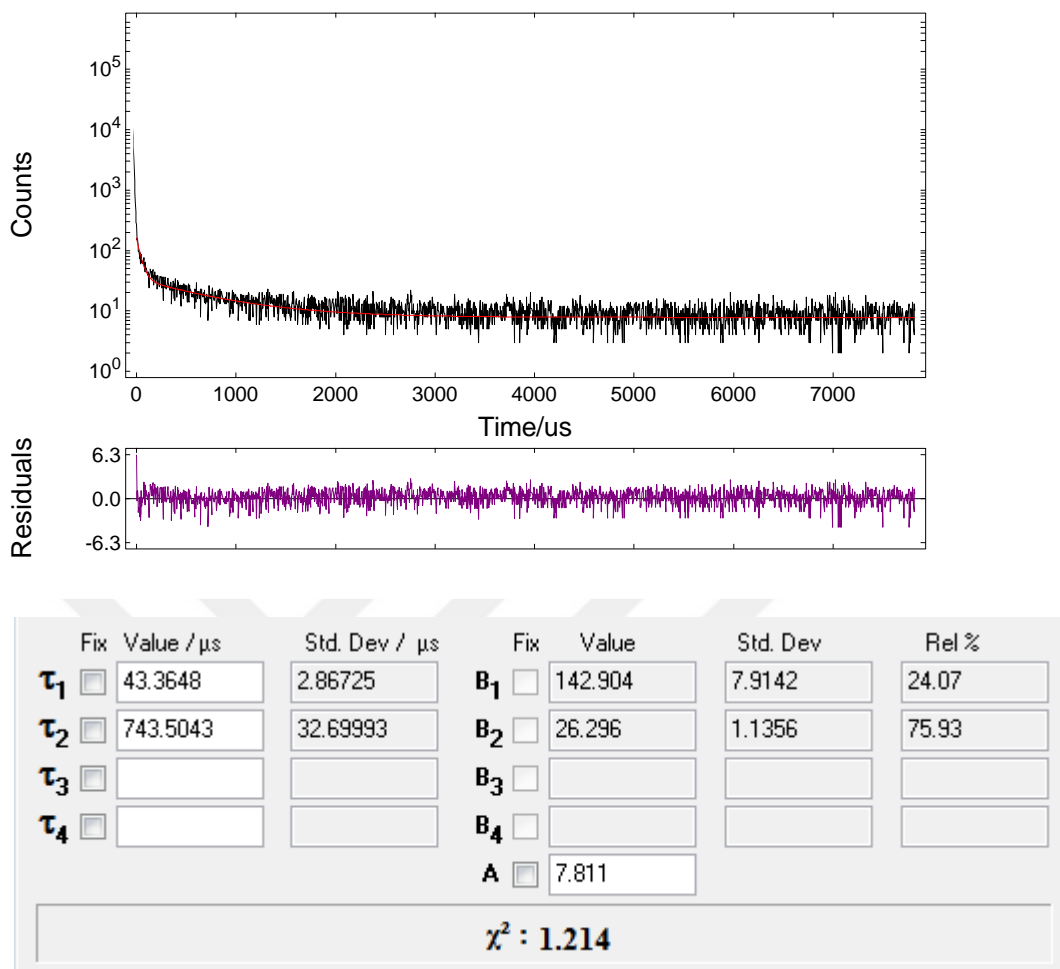


Figure 5.17 Decay response of TPPPt(II) embedded PVC based thin film in the presence of 50 μ l ($6.28 \times 10^{-7} \text{Mol L}^{-1}$) TEMPO in pH 7.4 buffer in SDS media

Table 5.8 (τ_0/τ) values corresponding to TEMPO concentrations thin film form to pH 7.4 buffer SDS media TEMPO solution for TPPPt(II) dye

Matrix: SDS			
Dye: TPPPt(II)			
Concentration (Mol L ⁻¹)	τ_0/τ	τ_0	τ
0	1	722.54	722.54
3.84×10^{-8}	1.0115	722.54	714.31
8.96×10^{-8}	1.0315	722.54	700.48
1.66×10^{-7}	1.05944	722.54	682
3.17×10^{-7}	1.0746	722.54	672.36
6.28×10^{-7}	1.2566	722.54	574.98
K _{sv}	3.93×10^5		
K _q	5.44×10^2		

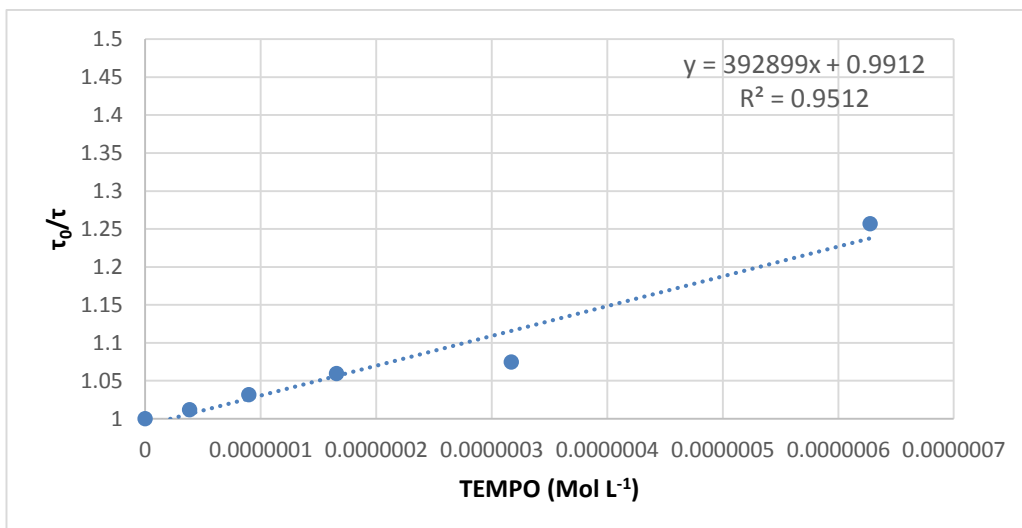


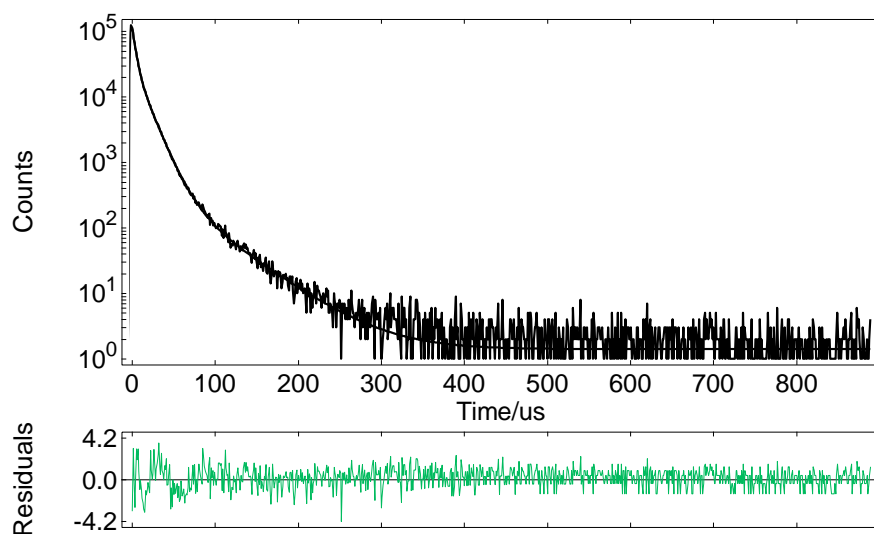
Figure 5.18 Variations of the lifetime ratio (τ_0/τ) TPPPt(II) versus quencher (TEMPO) concentrations thin film form to pH 7.4 buffer in SDS media

Figures 5.12-5.17 reveals that the TPPPt(II) dye also exhibited decreasing fluorescence lifetime based response which is the sign of dynamic quenching.

Table 5.9 Summary of the decay characteristics and chi square values of the studied composites in presence and absence of TEMPO for thin film form

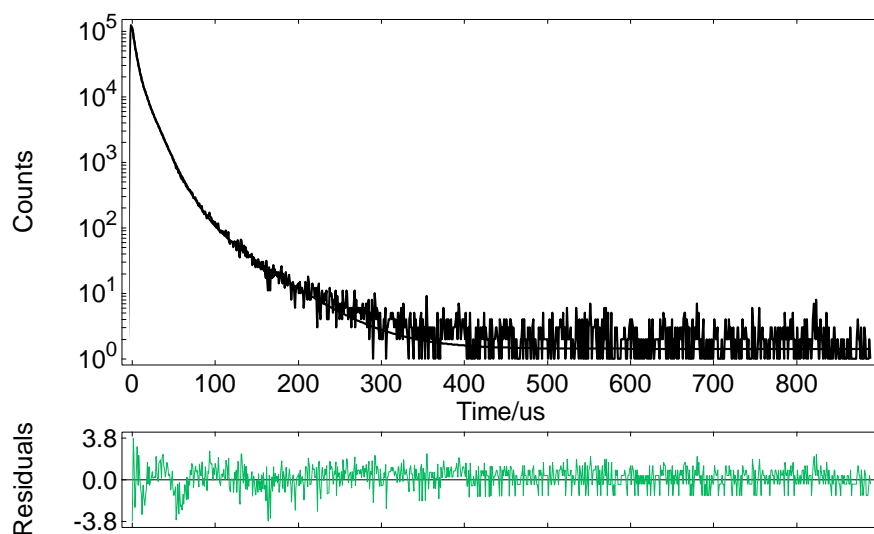
TEMPO ($\mu\text{Mol L}^{-1}$)	τ_0 , (μs)	τ_{TEMPO} average	χ^2	τ_0/τ	K_{sv} [TEMPO] $^{-1}$ (μM^{-1})	k_q ($\text{M}^{-1}\text{s}^{-1}$)
0	128.74 \pm 10.71 (34.57 %)	722.54	1.249	1	3.93×10^5	5.44×10^2
	1036.29 \pm 97.66 (65.43 %)					
3.84×10^{-2}	47.60 \pm 2.70 (27.12 %)	714.31	1.227	1.01	3.93×10^5	5.44×10^2
	962.40 \pm 50.11 (72.88 %)					
8.96×10^{-2}	91.80 \pm 8.18 (25.5 %)	700.48	1.203	1.03	3.93×10^5	5.44×10^2
	908.83 \pm 58.89 (74.5 %)					
1.65×10^{-1}	87.50 \pm 6.46 (27.52 %)	682.00	1.122	1.05	3.93×10^5	5.44×10^2
	907.73 \pm 52.49 (72.8 %)					
3.16×10^{-1}	91.34 \pm 6.70 (27.35 %)	672.36	1.227	1.07	3.93×10^5	5.44×10^2
	891.10 \pm 48.49 (72.65 %)					
6.27×10^{-1}	43.36 \pm 2.86 (24.07 %)	574.98	1.214	1.25	3.93×10^5	5.44×10^2
	743.50 \pm 32.69 (75.93 %)					

Figures 5.19-5.26 reveals that the TPPPt(II) dye also exhibited decreasing fluorescence lifetime based response which is the sign of dynamic quenching.



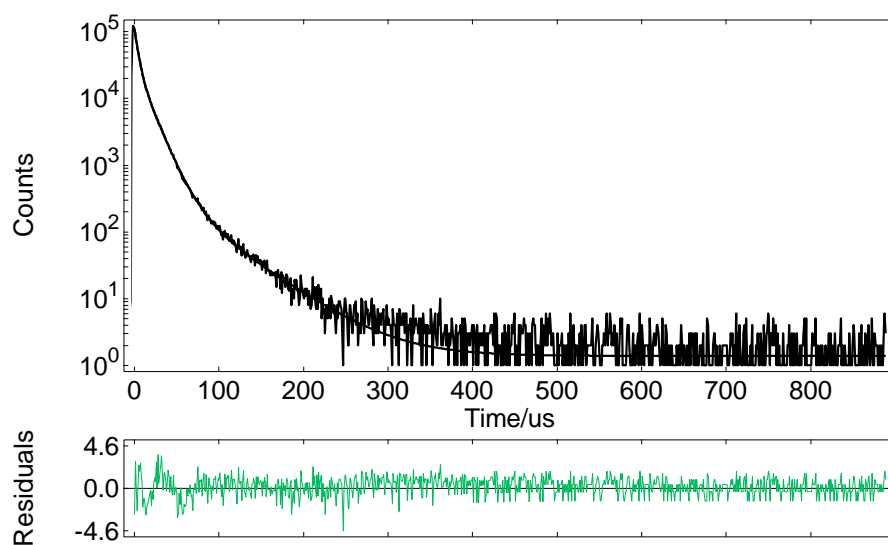
	Fix	Value / μ s	Std. Dev / μ s	Fix	Value	Std. Dev	Rel %
τ_1	<input type="checkbox"/>	4.0883	0.02842	B_1	<input type="checkbox"/> 107386.039	467.8704	47.00
τ_2	<input type="checkbox"/>	13.7609	0.09861	B_2	<input type="checkbox"/> 33600.805	455.7259	49.50
τ_3	<input type="checkbox"/>	49.0027	0.95489	B_3	<input type="checkbox"/> 665.534	39.3533	3.49
τ_4	<input type="checkbox"/>			B_4	<input type="checkbox"/>		
				A	<input type="checkbox"/> 1.400		
$\chi^2 : 1.120$							

Figure 5.19 Decay response of TPPPt(II) embedded PVC based nanofiber with in pH 7.4 buffer SDS media without TEMPO solution



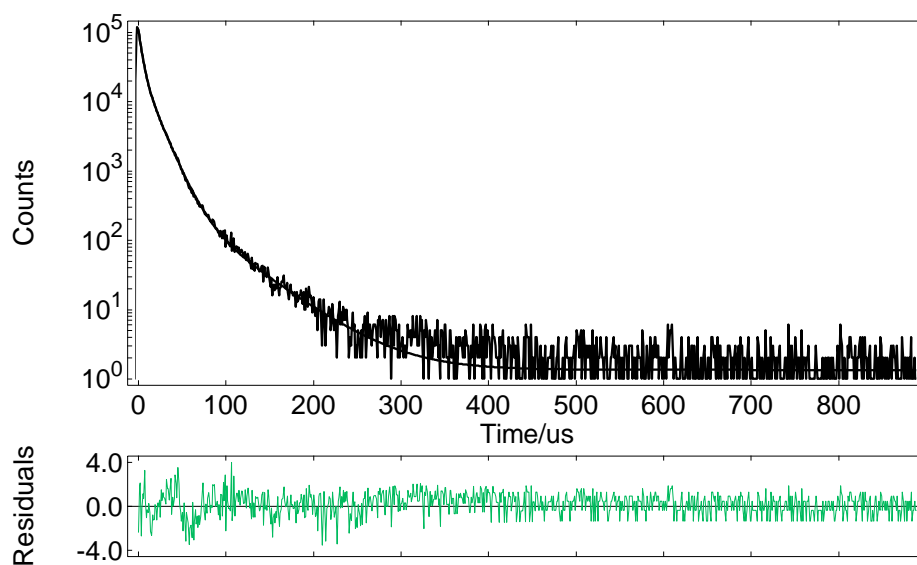
	Fix	Value / μs	Std. Dev / μs	Fix	Value	Std. Dev	Rel %
τ_1	<input type="checkbox"/>	4.0864	0.02784	B_1	106884.539	453.1921	47.18
τ_2	<input type="checkbox"/>	14.0311	0.10066	B_2	32631.408	429.6115	49.45
τ_3	<input type="checkbox"/>	48.9158	1.02916	B_3	637.769	41.1232	3.37
τ_4	<input type="checkbox"/>			B_4			
				A	1.418		
$\chi^2 : 1.101$							

Figure 5.20 Decay response of TPPPt(II) embedded PVC based nanofiber in the presence of 0.4 μl (5.12×10^{-9} Mol L⁻¹) TEMPO in pH 7.4 buffer in SDS media



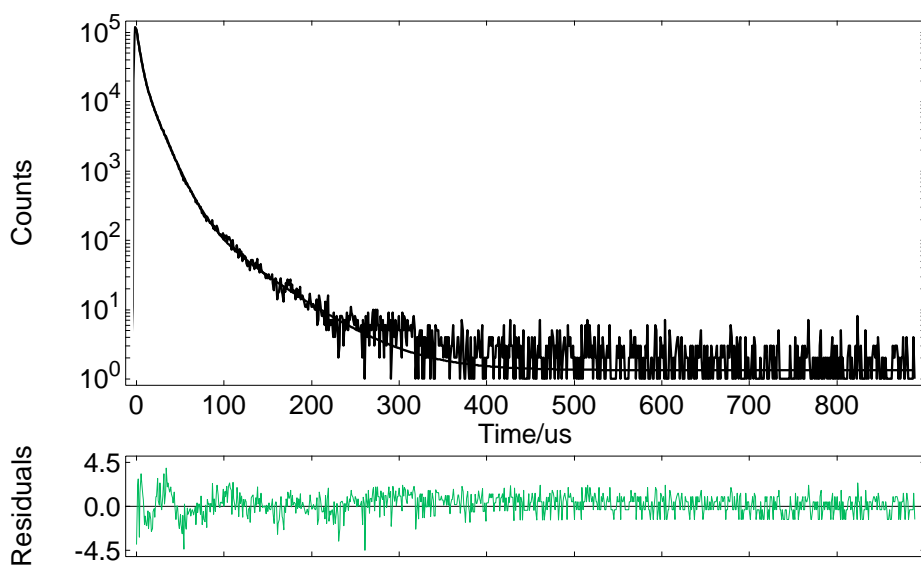
	Fix	Value / μ s	Std. Dev / μ s	Fix	Value	Std. Dev	Rel %
τ_1	<input type="checkbox"/>	4.1220	0.02897	B_1	104472.930	460.4932	46.83
τ_2	<input type="checkbox"/>	13.8665	0.09949	B_2	32978.766	448.9830	49.73
τ_3	<input type="checkbox"/>	49.4410	0.97445	B_3	639.144	38.3114	3.44
τ_4	<input type="checkbox"/>			B_4			
				A	1.383		
$\chi^2 : 1.111$							

Figure 5.21 Decay response of TPPPt(II) embedded PVC based nanofiber in the presence of 0.8 μ l (1.02×10^{-8} Mol L⁻¹) TEMPO in pH 7.4 buffer in SDS media



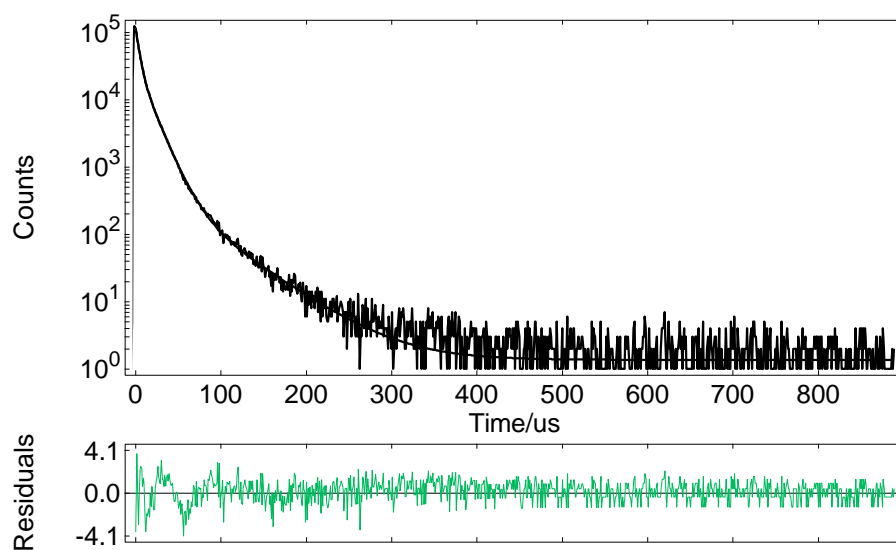
	Fix	Value / μs	Std. Dev / μs	Fix	Value	Std. Dev	Rel %
τ_1	<input type="checkbox"/>	4.0558	0.02879	B_1	<input type="checkbox"/> 101290.383	447.6977	46.55
τ_2	<input type="checkbox"/>	13.8986	0.10127	B_2	<input type="checkbox"/> 31784.289	426.1823	50.06
τ_3	<input type="checkbox"/>	48.2474	1.01052	B_3	<input type="checkbox"/> 620.686	40.3128	3.39
τ_4	<input type="checkbox"/>			B_4	<input type="checkbox"/>		
				A	<input type="checkbox"/> 1.341		
$\chi^2 : 1.131$							

Figure 5.22 Decay response of TPPPt(II) embedded PVC based nanofiber in the presence of 1.2 μl ($1.54 \times 10^{-8} \text{ Mol L}^{-1}$) TEMPO in pH 7.4 buffer in SDS media



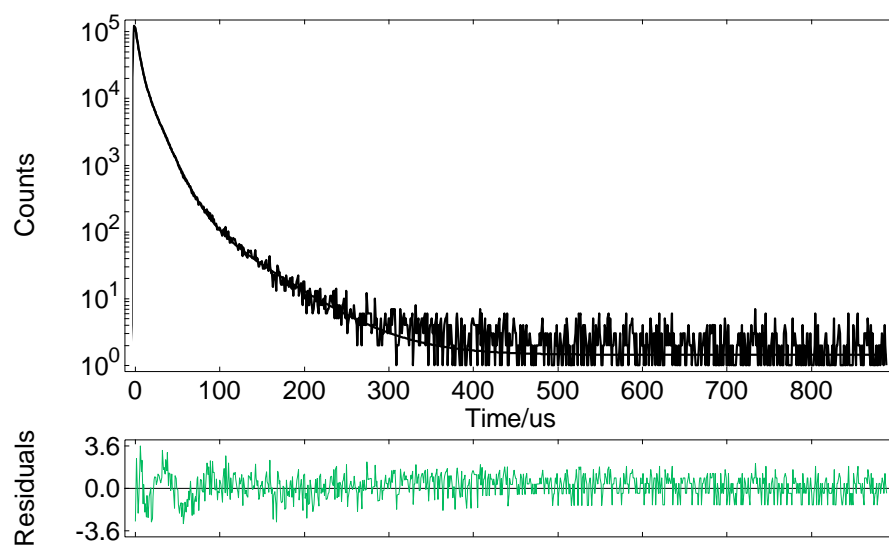
	Fix	Value / μs	Std. Dev / μs	Fix	Value	Std. Dev	Rel %
τ_1	<input type="checkbox"/>	4.1735	0.02895	B_1	102763.438	447.0570	47.54
τ_2	<input type="checkbox"/>	14.0739	0.10195	B_2	31546.256	433.0022	49.22
τ_3	<input type="checkbox"/>	50.1237	1.05044	B_3	582.713	37.1487	3.24
τ_4	<input type="checkbox"/>			B_4			
				A	1.326		
$\chi^2 : 1.166$							

Figure 5.23 Decay response of TPPPt(II) embedded PVC based nanofiber in the presence of 2 μl ($2.56 \times 10^{-8} \text{ Mol L}^{-1}$) TEMPO in pH 7.4 buffer in SDS media



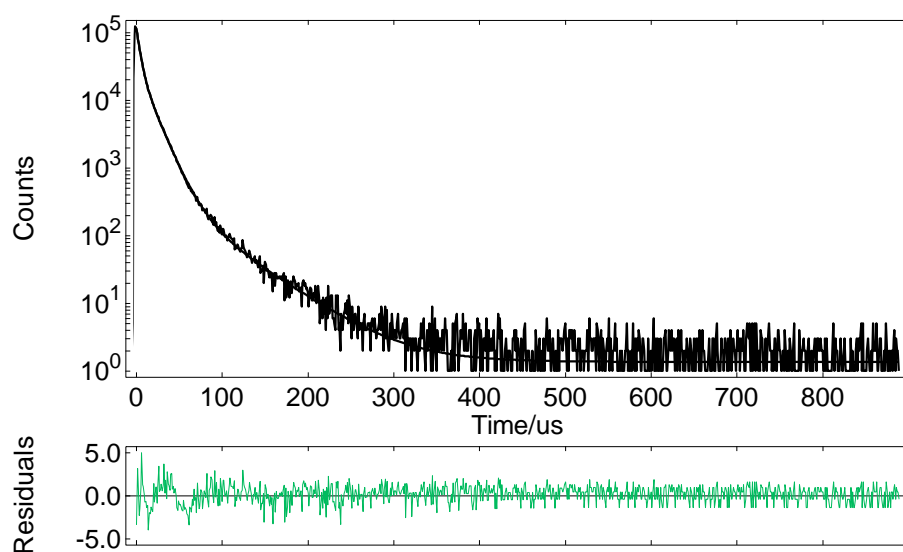
	Fix	Value / μ s	Std. Dev / μ s	Fix	Value	Std. Dev	Rel %
τ_1	<input type="checkbox"/>	4.1911	0.02918	B_1	106233.172	468.9510	47.50
τ_2	<input type="checkbox"/>	13.8642	0.10032	B_2	33236.480	464.8712	49.16
τ_3	<input type="checkbox"/>	49.9307	0.99261	B_3	628.180	37.7220	3.35
τ_4	<input type="checkbox"/>			B_4			
				A	1.360		
$\chi^2 : 1.135$							

Figure 5.24 Decay response of TPPPt(II) embedded PVC based nanofiber in the presence of 4 μ l (5.12×10^{-8} Mol L⁻¹) TEMPO in pH 7.4 buffer in SDS media



	Fix	Value / μs	Std. Dev / μs	Fix	Value	Std. Dev	Rel %
τ_1	<input type="checkbox"/>	4.2332	0.02829	B_1	<input type="checkbox"/> 106837.242	448.2782	48.25
τ_2	<input type="checkbox"/>	14.2335	0.10047	B_2	<input type="checkbox"/> 32034.061	434.1920	48.65
τ_3	<input type="checkbox"/>	51.5489	1.07573	B_3	<input type="checkbox"/> 564.327	35.2998	3.10
τ_4	<input type="checkbox"/>			B_4	<input type="checkbox"/>		
				A	<input type="checkbox"/> 1.427		
$\chi^2 : 1.090$							

Figure 5.25 Decay response of TPPPt(II) embedded PVC based nanofiber in the presence of 10 μl ($1.27 \times 10^{-7} \text{ Mol L}^{-1}$) TEMPO in pH 7.4 buffer in SDS media



	Fix	Value / μs	Std. Dev / μs	Fix	Value	Std. Dev	Rel %
τ_1	<input type="checkbox"/>	4.1676	0.02871	B_1	<input type="checkbox"/> 106579.133	461.8225	47.28
τ_2	<input type="checkbox"/>	13.9712	0.09959	B_2	<input type="checkbox"/> 33191.828	451.0621	49.36
τ_3	<input type="checkbox"/>	50.0524	0.99572	B_3	<input type="checkbox"/> 630.731	37.9378	3.36
τ_4	<input type="checkbox"/>			B_4	<input type="checkbox"/>		
				A	<input type="checkbox"/> 1.359		
$\chi^2 : 1.140$							

Figure 5.26 Decay response of TPPPt(II) embedded PVC based nanofiber in the presence of 30 μl ($3.79 \times 10^{-7} \text{ Mol L}^{-1}$) TEMPO in pH 7.4 buffer in SDS media

Table 5.10 Summary of the decay characteristics and chi square values of the studied composites in presence and absence of TEMPO for nanofiber form

TEMPO ($\mu\text{Mol L}^{-1}$)	τ_0 , (μs)	τ_{TEMPO} average	χ^2	τ_0/τ	K_{sv} [TEMPO] $^{-1}$ (μM^{-1})	k_q $\text{M}^{-1}\text{s}^{-1}$
0	4.09 \pm 0.03 (47 %)	10.44	1.120	1	8×10^6	7.7×10^5
	13.76 \pm 0.1 (49.5 %)					
	49.00 \pm 0.95 (3.49 %)					
5.12×10^{-3}	4.09 \pm 0.03 (47.18 %)	10.52	1.101	0.992	8×10^6	7.7×10^5
	14.03 \pm 0.1 (49.45 %)					
	48.91 \pm 1.03 (3.37 %)					
1.02×10^{-2}	4.12 \pm 0.03 (46.83 %)	10.53	1.111	0.991	8×10^6	7.7×10^5
	13.87 \pm 0.1 (49.73 %)					
	49.44 \pm 0.97 (3.44 %)					
1.54×10^{-2}	4.05 \pm 0.03 (46.55 %)	10.47	1.131	0.997	8×10^6	7.7×10^5
	13.9 \pm 0.1 (50.06 %)					
	48.25 \pm 1.01 (3.39 %)					
2.56×10^{-2}	4.17 \pm 0.03 (47.54 %)	10.52	1.166	0.992	8×10^6	7.7×10^5
	14.07 \pm 0.10 (49.22 %)					
	50.12 \pm 1.05 (3.24 %)					
5.12×10^{-2}	4.19 \pm 0.03 (47.5 %)	10.47	1.135	0.997	8×10^6	7.7×10^5
	13.86 \pm 0.10 (49.16 %)					
	49.93 \pm 0.99 (3.35 %)					
1.27×10^{-1}	4.23 \pm 0.03 (48.25 %)	10.56	1.090	0.989	8×10^6	7.7×10^5
	14.23 \pm 0.10 (48.65 %)					
	51.55 \pm 1.07 (3.10 %)					
3.79×10^{-1}	4.17 \pm 0.03 (47.28 %)	10.54	1.140	0.990	8×10^6	7.7×10^5
	13.97 \pm 0.10 (49.36 %)					
	50.05 \pm 0.1 (3.36 %)					

CHAPTER SIX

CONCLUSIONS

In this thesis we utilized PHACH₂, ZnTPP, TPPPt(II) dyes as NO sensitive molecular probes in embedded form.

Nitrogen oxides are one of the major pollutants in the atmosphere which cause acid rains, photochemical smog and ozone accumulation. Therefore real-time sensor development studies for nitric oxide attract great attention. This study is largely concerned with the development of optical chemical sensor for nitric oxide radical that can be applied for quantification studies in aqueous environments.

We fabricated thin films and electrospun fibers to prepare the sensing agents. The dyes used showed an emission-based response to radical NO to decrease signal intensity. The reaction of the dyes used was controlled in THF media, in SDS matrix embedded in PVC and in nanofiber form. All the PHACH₂, ZnTPP, TPPPt(II) dyes exhibited emission based response to radicalic NO in direction of decrease in signal intensity. The spectral response of each dye in the prepared media was tested and evaluated for Stern-Volmer plots and Stern-Volmer constants (K_{sv}), which are indicative of the sensitivity of the fluorescent dye to the analyte.

Matrix material of PVC (polyvinyl chloride) were chosen due to excellent compatibility with the indicator dyes, resistant characteristics to water and harsh conditions providing an appropriate micro environment for them.

Spectral response of the PVC embedded dye to TEMPO in buffered solutions and SDS micelles were also recorded. The performances of the potential sensing agents were tested by steady state fluorescence and decay time measurements. Among them the PHACH₂ dye exhibited the highest response for radicalic nitric oxide. The best spectral response of PVC embedded PHACH₂ dye to TEMPO was attained in the solution of THF and buffered SDS solution for nano fiber forms.

The relative signal change of 27% was attained for the concentration range of 0.0-11.2 μM TEMPO in THF media. Limit of detection (LOD) for NO was defined as the concentration at which the signal is equal to the blank signal plus 3σ and found to be 0.04 μM . Limit of quantification (LOQ) is the smallest NO concentration measured experimentally and was found as 0.13 μM for PHACH₂ in THF media.

The relative signal change of 99% was attained for the concentration range of 0.0-0.04 μM TEMPO for nanofiber form in pH 7.4 buffered SDS media. Limit of detection (LOD) for nanofiber form was found to be 8.54×10^{-4} μM . Limit of quantification (LOQ) was found as 2.56×10^{-3} μM for PHACH₂ in nanofiber form.



REFERENCES

- Allen, W. M. (2010). *Measurement of fluorescence quantum yields*. Retrieved October 27, 2012, from <http://www.thermofisher.com/au/Uploads/file/ENewsAU/Technical-Note-Measurement-of-Fluorescence-QuantumYields.PDF>
- Bright, F. V., & Munson, C. A. (2003). Time-resolved fluorescence spectroscopy for illuminating complex systems. *Analytica Chimica Acta*, 500, 71–104.
- Cao, N. W., Shakin, C. M., & Sun, W. D. (1992). Quasiparticle properties of the quarks of the Nambu–Jona-Lasinio model. *Physical Review, C*, 46, 2535 – 2546.
- Chemistry Libretexts (2017). *Fluorescence and Phosphorescence*. Retrieved May 1, 2017, from https://chem.libretexts.org/Core/Physical_and_Theoretical_Chemistry/Spectroscopy/Electronic_Spectroscopy/Fluorescence_and_Phosphorescence#Jablonski_Diagrams
- FLS920 Series. (2011). Retrieved July, 18, 2014, from <http://www.edinburghphotonics.com/files/file/brochures/FLS920-Brochure.pdf>
- Frohne, H. (2004). *Doping of hole conducting polymers utilized to enhance polymer electronics*. Retrieved October 27, 2012, from <http://kups.ub.uni-koeln.de/1096/>.
- Galster, H. (1991). *pH Measurements: fundamentals, methods, applications, instrumentation*. Germany: Weinhein
- Itoh, Y., Ma, F.H., Hoshi, H., Oka, M., Noda, K., Ukai, Y., et al. (2000). Determination and bioimaging method for nitric oxide in biological specimens by diaminofluoresce in fluorometry. *Analytical Biochemistry*, 287, 203-209

Kacmaz, S., Ertekin, K., Oter, O., Hizliates, C.G., Ergun, Y., Celik, E. (2015). Manipulation of pH induced sensitivity of a fluorescent probe in presence of silver nanoparticles. *Journal of Luminescence*, 168, 228–235

Kaçmaz, S., (2012). *Design of optical chemical nanosensors for determination of some selected cations and anions in aqueous samples and evaluation of the interference effects*. Phd Thesis, Dokuz Eylül University, İzmir.

Lakowicz, J. R. (1983). *Principles of fluorescence spectroscopy*, (1st ed.). New York and London: Plenum Press.

Moncada, S., & Bolanos, J.P., (2006). Nitric oxide, cell bioenergetics sand neurodegeneration. *Journal of Neurochemistry*, 97, 1676–1689.

Ongun, M. Z., (2013). *Development of nano material based sensors for determination of some-cation/anion in groundwater and complementary usage of ion chromatography*. Phd Thesis, Dokuz Eylül University, İzmir.

Parker, C. A. (1968). *Photoluminescence of solutions*. Amsterdam: Elsevier.

Schmidt, W. (1994). *Optische Spektroskopie*. Weinheim: VCH Verlagsgesellschaft.

Sheffield Hallam University, Bioscience Department, (n.d.). Retrieved May 1, 2017 from <http://teaching.shu.ac.uk/hwb/chemistry/tutorials/molspec/lumin1.htm>

Sigma-Aldrich, Tempo (2017). *Tempo*. Retrieved March 17, 2017, from <http://www.sigmaaldrich.com/catalog/product/aldrich/214000?lang=en®ion=TR>

Solomon, S. D., Bahadory, M., Jeyarajasingam, A. V., Rutkowsky, S. A., & Boritz, C. (2007). Synthesis and study of silver nanoparticles. *Journal of Chemical Education*, 84 (2), 322.